

Final Design Review:  
Helicopter Payload Stabilization Project

Team Jury

Giacomo Fratus, Sidharth Subbarao, Hieu Nguyen  
Seong Hong, Jeremy Wong, Jake Smith, Chiraag Hebbar  
June 10, 2021

# Table of Contents

<b>Introduction and Overview (Sidharth, Chiraag)</b>	<b>4</b>
<b>Problem Statement (Sidharth)</b>	<b>4</b>
<b>Preliminary Analysis (Jeremy, Chiraag, Jake)</b>	<b>11</b>
Objective Tree Analysis	11
Performance Specification Method	14
Quality Function Deployment Method	14
Function Analysis – Transparent Box Model	16
Morphological Chart	21
Weighted Objective Method	22
<b>Design Specifications (All)</b>	<b>24</b>
Mechanical System:	24
Electrical System:	26
Control Algorithm:	29
<b>System Design (All)</b>	<b>33</b>
System Dynamics	33
Mechanical Subsystem	39
Electrical Subsystem	48
Software Architecture	51
Algorithm	52
<b>Analysis (All)</b>	<b>56</b>
Formulation of Test Scenarios	56
Numerical Simulation	57
Mechanical Simulation	60
<b>Design Outcome Versus Requirements (Hieu, Jeremy, Chiraag)</b>	<b>93</b>
<b>Conclusion and Discussion (Jeremy, Chiraag)</b>	<b>94</b>
<b>Appendix 1 - Technical Drawings</b>	<b>95</b>
Part Drawings	95
Assembly Drawings	101
<b>Appendix 2 - Bills of Materials</b>	<b>103</b>
<b>Appendix 3 - Comprehensive &amp; Elevator Pitch Presentation Slides</b>	<b>106</b>
<b>Appendix 4 - GANTT Chart</b>	<b>106</b>

**Appendix 5 - Collaboration Task Matrix** **112**

**Appendix 6 - Peer Review Assessment** **113**

# Introduction and Overview (Sidharth, Chiraag)

In this report, we present our MAE 162E/ECE183E senior design capstone project in the form of a Final Design Review (CDR). Our goal over the winter and spring quarters was to find and solve a problem of importance using the engineering frameworks given to us by the professors. We aim to design a helicopter evacuation stabilization device that prevents the spin of a litter during hoist operations due to external winds and downwash.

In the following sections, we will first explicate the problem and determine the requirements necessary to solve it. This will make use of various design and analysis methods to determine our primary objectives and restrictions. From this, we will present design specifications for the mechanical, electrical, and controls subsystems. We will then compile these into an integrated system design. Finally, we will present our analyses that validate the effectiveness of our design in satisfying its capabilities.

## Problem Statement (Sidharth)

### Explication of Problem

A common occurrence during helicopter rescue missions are helicopter hoisting operations (HHOs). During a HHO, a stationary helicopter at a fixed elevation is positioned directly above the load, which is oftentimes a person in a stretcher. The load is connected to the helicopter through a cable, which is then used to hoist up the load so that it can be stored in the helicopter. During HHOs, downwash, which is defined as the change in direction of air by the aerodynamic action of the helicopter rotor blades, can cause the load to spin out of control<sup>1</sup>. This spinning has the potential to damage the helicopter, hoisting cable, and load itself, which might result in monetary damages and loss of life. Team Jury's proposed solution to this problem would be to build a stabilization device that can prevent spin when a stationary helicopter is hoisting up a load, specifically a stretcher. Below is a picture of the downwash caused by a helicopter during a HHO:



Downwash caused by helicopter during hoisting operation<sup>2</sup>

---

<sup>1</sup> <https://en.wikipedia.org/wiki/Downwash>

<sup>2</sup> U.S. Navy photo by Photographer's Mate Airman Sarah E. Ard

### **Problem Positioning and Justification:**

The context regarding helicopter hoisting operations (HHOs) is as follows. HHOs occur in rescue scenarios where patients need to be quickly transported to hospitals in order to receive first aid. Scenarios that utilize HHOs are where patients suffer a car accident or critical work related injury, and as a result, would need to be transported to a hospital within 15 minutes in order to save their lives. HHOs can also occur when people who are trapped in remote wilderness locations need to be rescued. Examples of this include having to rescue people on a stranded ship, or having to rescue injured hikers on the side of a mountain<sup>3</sup>. During HHOs involving rescuing people, it is imperative that the person being hoisted does not spin due to downwash. Excessive spin of the load during a HHO can cause nausea, which can lead to drowning if the patient is strapped to a stretcher and cannot control their airways. Furthermore, spin of the load during a HHO can result in a severed hoisting cable, ejection of the patient from the stretcher, or collision of the patient with an external object, all of which are life threatening<sup>4</sup>. Spin of the load during a HHO can cause damage to the load, cable, and helicopter itself, which is why it is imperative to stop load spin during HHOs.

The design and computation aspects of the solution to the described problem are as follows. The solution to this problem requires the design of a device that is capable of exerting a counter torque on the load, or stretcher, in order to prevent it from spinning. The device we chose was ducted fans. The design aspect of this problem would focus on deciding the type, placement, and other electrical and mechanical structures needed to make the ducted fan counter-torque device work as specified. The computational aspects of the problem would include deriving an algorithm to control the selected actuators in order to reduce spin of the load, or stretcher. We decided to use a PID control algorithm for this project. This algorithm would then be tested and refined using analytical and physics based simulations.

The solvability of the problem is described as follows. The scope of the problem is limited to designing a device with an algorithm that is capable of controlling one degree of freedom (spin), on a defined load (stretcher), attached to a stationary helicopter with variable wind conditions. By placing these limitations on the problem, the problem should be solvable within the remaining time we have left.

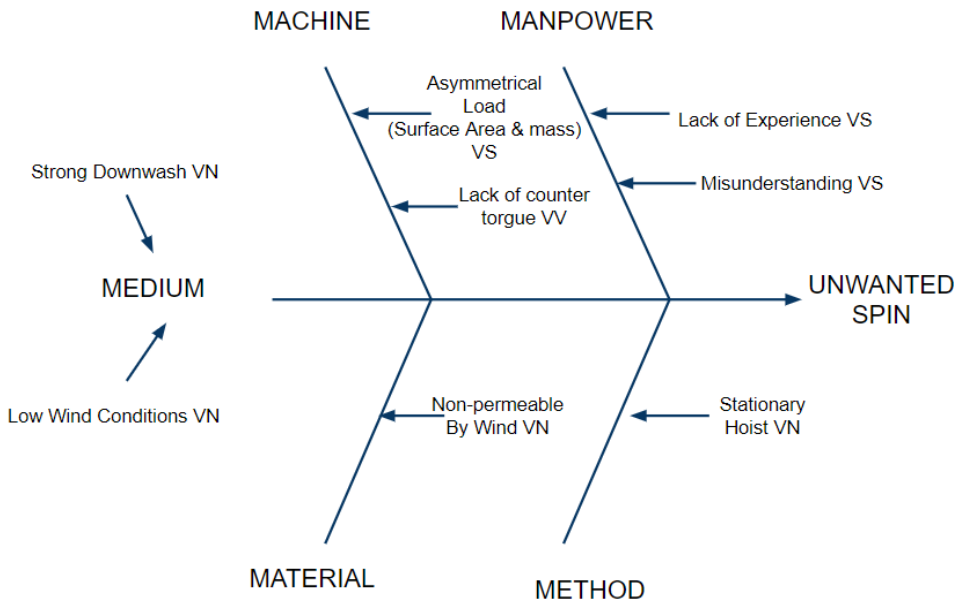
### **Root Cause Analysis:**

Below is a Fishbone Diagram detailing the root cause of the problem, that being unwanted spin of the load during helicopter hoisting operations (HHOs):

---

<sup>3</sup> [https://link.springer.com/chapter/10.1007%2F978-3-642-69262-8\\_80](https://link.springer.com/chapter/10.1007%2F978-3-642-69262-8_80)

<sup>4</sup> <https://www.airmedandrescue.com/latest/long-read/spinning-avoidance>



The physical reasons for spin are the downwash caused by the helicopter in low wind conditions. The problem is worsened when the load is surrounded by non-permeable material, which adds to the surface area that wind can act on. On the human side, lack of experience and misunderstanding of how to properly mount the load can cause spin of the load. Therefore, the solution to this problem should be a machine that is able to deal with an asymmetrical load and exerting counter torque on the load in order to prevent spin.

#### **Define Resources:**

Parties that have experienced the problem of unwanted spin during helicopter hoisting operations (HHOs) involve helicopter pilots and rescue workers. Rescue workers include winchmen who are manually deployed in order to prevent spin on the helicopter load, as well as other staff who are responsible for placing the patient in a stretcher and mounting it to the helicopter hoisting cable. Furthermore, the most affected party in this situation is the patient itself, whose safety is predicated on the stretcher not spinning during the HHO.

Examining the literature regarding this problem shows that the most common way to solve the issue of spinning load during HHO is through non-technical solutions. The United States Department of Transportation Federal Aviation Administration released a Safety Alert for Operators, specifying techniques to reduce spin of load during HHO. Furthermore, the Air Med and Rescue magazine aimed at helicopter rescue operators go over specific techniques for preventing spin of load during HHO. The links to the following two sources are posted below:

[https://www.faa.gov/other\\_visit/aviation\\_industry/airline\\_operators/airline\\_safety/safo/all\\_safo/media/2013/safo13010.pdf](https://www.faa.gov/other_visit/aviation_industry/airline_operators/airline_safety/safo/all_safo/media/2013/safo13010.pdf)

<https://www.airmedandrescue.com/latest/long-read/spinning-avoidance>

Recently, a private company Vita Inclinata has come up with automated solutions to preventing load spin during HHOs. Vita Inclinata has developed devices that reduce swing, sway, and vertical pitch of the load during HHOs. Below is a link to the company website, which contains details regarding their various products:

<https://vitatech.co/products/>

## Define Strategies and Methods:

The problem of load spin during helicopter hoisting operations (HHOs) has been addressed in the Air and Med Rescue magazine as well as the private company Vita Inclinata Technologies. The Air and Med Rescue magazine explains to helicopter operators on things that they can personally do to reduce spin on loads during HHOs. Vita Inclinata technologies is a private company which has devised technical solutions to reduce spin and other unwanted motion during HHOs.

The Air and Med Rescue magazine covers various non-technical solutions regarding preventing spin of load during HHOs. One such technique is to manually deploy a winchman to supervise the hoisting operation and manually reduce spin. Another technique specified by the magazine is to travel in the forward direction at a speed of 10 to 15 knots<sup>5</sup>. Travelling at this speed would eliminate downwash, causing the load to stop spinning. The other techniques specified by the Air and Med Rescue magazine involve altering the load so that the center of mass is in line with the hoisting cable, altering the stretcher so that there is less surface area, or hoisting the load in a stretcher with vertical rather than horizontal orientation<sup>6</sup>. While these non-technical solutions are effective in reducing spin in HHO operations, not all of these solutions can be implemented during rescue operations due to external circumstances. In situations where the helicopter must be stationary, where no winchman is available, where the patient needs to be hoisted horizontally, and where no netted stretcher is available, it will be difficult to utilize the aforementioned non-technical solutions to prevent spin due to downwash.

The private company Vita Inclinata has come up with two relevant technical solutions that reduce unnecessary motion of the load during HHO operations. The first solution is the LSS-HR hoist rescue device. This device is autonomous, wirelessly operable, and controls 3 degrees of freedom, being spin, sway, and other oscillatory motion. The LSS-HR hoist rescue device is meant to be easily attachable to any hoisting cable, not stretcher. The LSS-HR hoist rescue device is capable of handling loads up to 750 lbs, controls at a rate of 1.5 periods per swing, and has a control range of around 1000 feet<sup>7</sup>. Below is a picture of the LSS-HR Hoist Rescue device, and a link to the system specification sheet of this device provided by Vita Inclinata:



<https://vitatech.co/wp-content/uploads/2020/05/vita-lss-hr-data-sheet-0520.pdf>

This product differs from our proposed solution in a number of key areas. The LSS-HR hoist rescue device is meant to be attached to a hoisting cable, while our proposed solution involves attaching a device to a stretcher. From the datasheet provided by Vita Inclinata, even while the device is autonomous, a winchman is still required to make sure the load, or patient, is properly stabilized<sup>8</sup>. Our solution seeks to eliminate the need for a winchman entirely. While the

<sup>5</sup> <https://www.airmedandrescue.com/latest/long-read/spinning-avoidance>

<sup>6</sup> <https://www.airmedandrescue.com/latest/long-read/spinning-avoidance>

<sup>7</sup> <https://vitatech.co/wp-content/uploads/2020/05/vita-lss-hr-data-sheet-0520.pdf>

<sup>8</sup> <https://vitatech.co/wp-content/uploads/2020/05/vita-lss-hr-data-sheet-0520.pdf>

LSS-HR hoist rescue device is capable of loads up to 750 lbs, our proposed solution only needs to be capable of loads up to 250 lbs, which would be the approximate maximum weight of a person being hoisted in a stretcher. Furthermore, the LSSR-HR hoist rescue device is wirelessly operable, however; as seen in later parts of the PDR, our proposed solution will likely not utilize wireless communication. Most importantly, the LSS-HR device is capable of controlling three degrees of freedom, while our solution at the time being is only concentrated on controlling one degree of freedom, that being spin<sup>9</sup>. Similarities with our proposed solution and Vita Inclinata's proposed solution include the stability specification of being able to handle wind and down wash conditions of around 60 knots, and being lightweight, around 35 lbs<sup>10</sup>.

The second technical solution devised by Vita Inclinata is the LSS-LA-litter attachment device. Similar to the LSS-HR hoist rescue device, the LSS-LA litter attachment device is autonomous, wirelessly operable, and controls three degrees of freedom, being spin, sway, and oscillatory motion. The LSS-LA litter attachment device is in the form of a netted stretcher with ducted fans placed underneath. These fans are meant to provide actuation that stabilizes the stretcher. The LSS-LA litter attachment device is capable of handling loads up to 750 lbs, controls at a rate of 1.5 periods per swing, and has a control range of around 1000 feet<sup>11</sup>. Below is a picture of the LSS-LA litter attachment device, alongside link to the system specification sheet provided by Vita Inclinata:



---

<https://vitatech.co/wp-content/uploads/2020/05/vita-lss-la-data-sheet-0520.pdf>

This product is similar to our proposed solution as seen later in the PDR report. Our proposed solution is structurally similar to the LSS-LA litter attachment, and seeks to provide actuation in the same way, using ducted fans. Furthermore, as seen from the product description from Vita Inclinata, the LSS-LA litter attachment device does not require a winchman, which is similar to our proposed solution as well. Our proposed solution also seeks to achieve similar stability parameters to the LSS-LA litter attachment, which is capable of stabilizing loads in winds up to 60 knots<sup>12</sup>. Our proposed solution differs from the LSS-LA litter attachment due to the fact that we seek to create a device that can attach to pre-existing stretchers, while the LSS-LA litter attachment product is itself a stretcher with actuators already attached to it<sup>13</sup>. While the LSS-LA litter attachment device is capable of loads up to 750 lbs, our proposed solution only needs to be capable of loads up to 250 lbs, which would be the approximate maximum weight of a person being hoisted in a stretcher. Furthermore, the LSS-LA

---

<sup>9</sup> <https://vitatech.co/wp-content/uploads/2020/05/vita-lss-hr-data-sheet-0520.pdf>

<sup>10</sup> <https://vitatech.co/wp-content/uploads/2020/05/vita-lss-hr-data-sheet-0520.pdf>

<sup>11</sup> <https://vitatech.co/wp-content/uploads/2020/05/vita-lss-la-data-sheet-0520.pdf>

<sup>12</sup> <https://vitatech.co/wp-content/uploads/2020/05/vita-lss-la-data-sheet-0520.pdf>

<sup>13</sup> <https://vitatech.co/wp-content/uploads/2020/05/vita-lss-la-data-sheet-0520.pdf>

litter attachment device is wirelessly operable, however; as seen in later parts of the PDR, our proposed solution will likely not utilize wireless communication. Most importantly, the LSS-LA litter attachment device is capable of controlling three degrees of freedom, while our solution at the time being is only concentrated on controlling one degree of freedom, that being spin<sup>14</sup>.

### Background / Related Work / References:

In order to understand the problem and solution, knowledge is required about the forces and torques involved on the load during helicopter hoisting operations, and knowledge for controls and stabilization is required for the design algorithm. Previous work on this issue is covered in the Define Strategies and Methods section. This work includes non-technical solutions to prevent spin on loads as stated in the Air Med and Rescue magazine, or the technical solutions proposed by Vita Inclinata. Below is a link describing the physics behind downwash related spin on loads. There is also a link to a report by NASA about how parameters on ducted fans such as diameter, duct length, number of blades, and motor choice all affect the resultant thrust and lift. Our group will reference these links, alongside other resources in order to come up with the mathematical formulation and algorithm to solve the problem:

<https://www.intechopen.com/books/flight-physics-models-techniques-and-technologies/helicopter-flight-physics>

[https://rotorcraft.arc.nasa.gov/Publications/files/Abrego2\\_AHS02.pdf](https://rotorcraft.arc.nasa.gov/Publications/files/Abrego2_AHS02.pdf)

Since our solution involves spin control, or applying opposite torque to the load, other relevant research would be on anti-torque systems found on helicopter rotors. Various anti-torque systems such as tipped blades at variable pitch, or “fan in tail” systems help minimize excessive torque on helicopter rotors<sup>15</sup>. While these solutions regarding helicopter rotors may not be directly applicable to our design, some of the techniques described can be used on the blades of the ducted fans used as actuators for stabilization. Below are pictures demonstrating helicopter rotor stabilization systems, and links regarding sources



<https://www.flight-mechanic.com/helicopter-structures-and-airfoils-anti-torque-systems/>

<https://www.hindawi.com/journals/ijae/2016/5396876/>

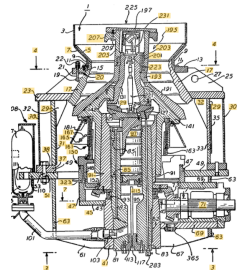
Anti-spin systems have been applied elsewhere as seen in a gyratory crusher system. The picture below shows the design for a mechanism, which through the use of uni-directional valves prevents the spin of the mantle of a crusher unless a certain force is exceeded<sup>16</sup>. While the context of this problem is different from helicopter rescue operations, it is interesting to see a

<sup>14</sup> <https://vitatech.co/wp-content/uploads/2020/05/vita-lss-la-data-sheet-0520.pdf>

<sup>15</sup> <https://www.flight-mechanic.com/helicopter-structures-and-airfoils-anti-torque-systems/>

<sup>16</sup> <https://patents.google.com/patent/US4206881A/en>

purely mechanical approach to solving issues regarding spin. Below is a link to the patent description of said device:

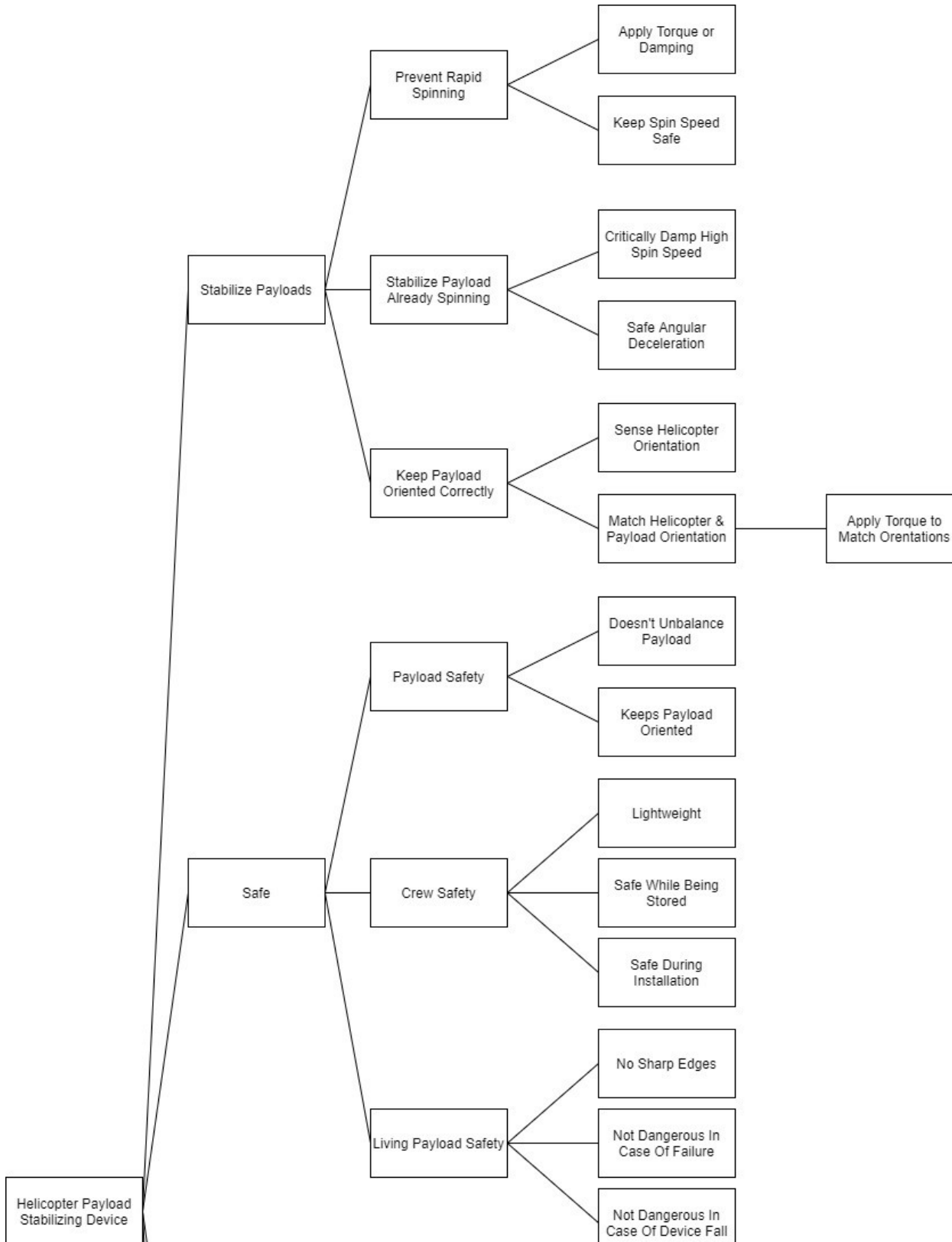


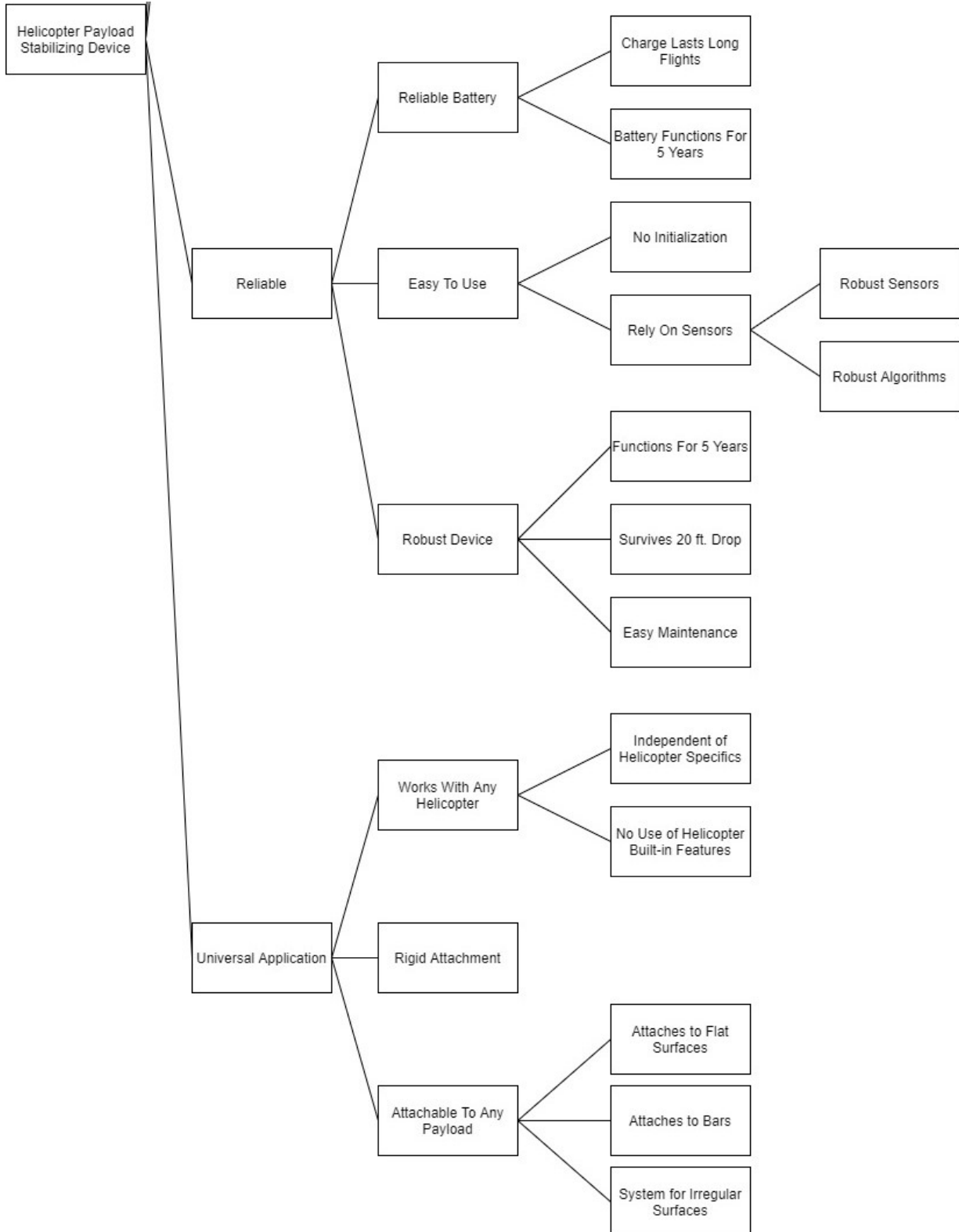
solving this sub problem is to build a modular device capable of attaching to existing stretchers to allow for spin stabilization during HHOs. Our group plans on testing our solution using simulation software such as Solidworks, Webots, and analytical simulations. Using Solidworks, it is possible to conduct structural tests on our device, and perform aerodynamic flow analysis. Through modelling the problem as a controls problem, it is possible to use metrics such as step tracking error, sinusoid tracking error, max overshoot, peak time, and other controls parameters to quantitatively measure the performance of the device. These metrics could be attained through Webots and analytical simulations.

## Preliminary Analysis (Jeremy, Chiraag, Jake)

### Objective Tree Analysis

The first method of analysis used was the objectives tree. The objectives tree is a way of visualizing what we want a project to be able to do, by ranking the objectives. As the tree gets more branched out, the blocks gradually go from nebulous objectives to actionable design parameters. This way, the whole problem is thought through to ensure the stabilizer does everything it needs to. There are four basic objectives for this project. It should stabilize payloads, be safe, be reliable, and have a universal application.





## Performance Specification Method

The second method of analysis used was the performance specification method. The purpose of the performance specification method is to list performance attributes and weight them so that designs can be compared. Because the solution must fit a problem correctly and not the other way around, we considered different options besides actuators that induce torque via force generation from the side of a payload. Among alternatives considered were landing the helicopter first to remove the need for an HHO, using multiple cables to keep a payload in line, or even foregoing airlifts and using conventional ground transport. All of these alternatives are lacking in some way, and none can compete with the versatility and agility of HHO's. The next step was to determine actuators. The team considered a flywheel whose axis was tipped, passive damping, thrusters, rotors, and turbines.

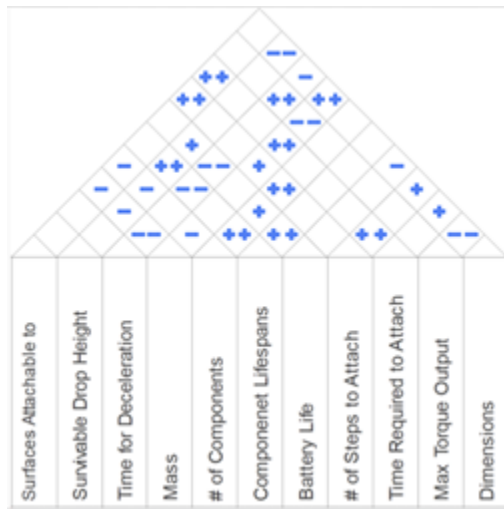
It was determined that the angular payload should not be allowed angular velocity greater than 15 rpm, and a maximum angular acceleration of 30 rpm<sup>2</sup>. All assembly and parts must have a factor of safety of 2.5 or higher to keep in line with industry standards, and the device must be effective on a payload of 300 lbs. or more.

## Quality Function Deployment Method

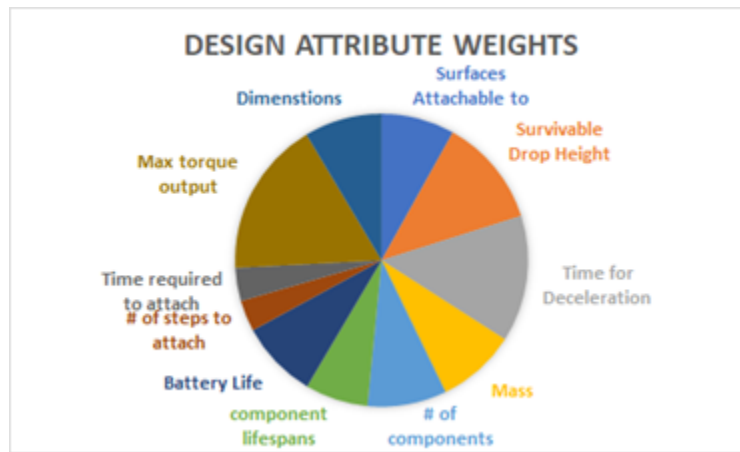
The last method of analysis used was the quality function deployment method, also known as the house of quality. This method uses a complex weighting system to determine what design attributes are the most important to design for.

	Surfaces Attachable to	Survivable Drop Height	Time for Deceleration	Mass	# of components	Component Lifespans	Battery Life	# of Steps to attach	Time Required to Attach	Max torque output	Dimensions
	↑	↑	↓	↓	↓	↑	↑	↓	↓	↑	↓
	Weight (1-10)	% Weight									
Stabilize Payload	8	0.296296296									
Safe	9	0.333333333	●	●	●	●	●		●	●	●
Reliable	6	0.222222222	●	●	●	●	●	●	●	●	●
Easy to Use	4	0.148148148	●	●	●	●	●	●	●	●	●
Imputed importance	4	5	6	4	4	3	4	2	2	8	3.9
Units	#	m	s	kg	#	hr	hr	#	s	Nm	m <sup>3</sup>
Design % Weight	8	12	14	9	9	7	9	3	4	17	8.6

The “roof” on the house of quality is used to visually understand how changing an aspect can affect others.



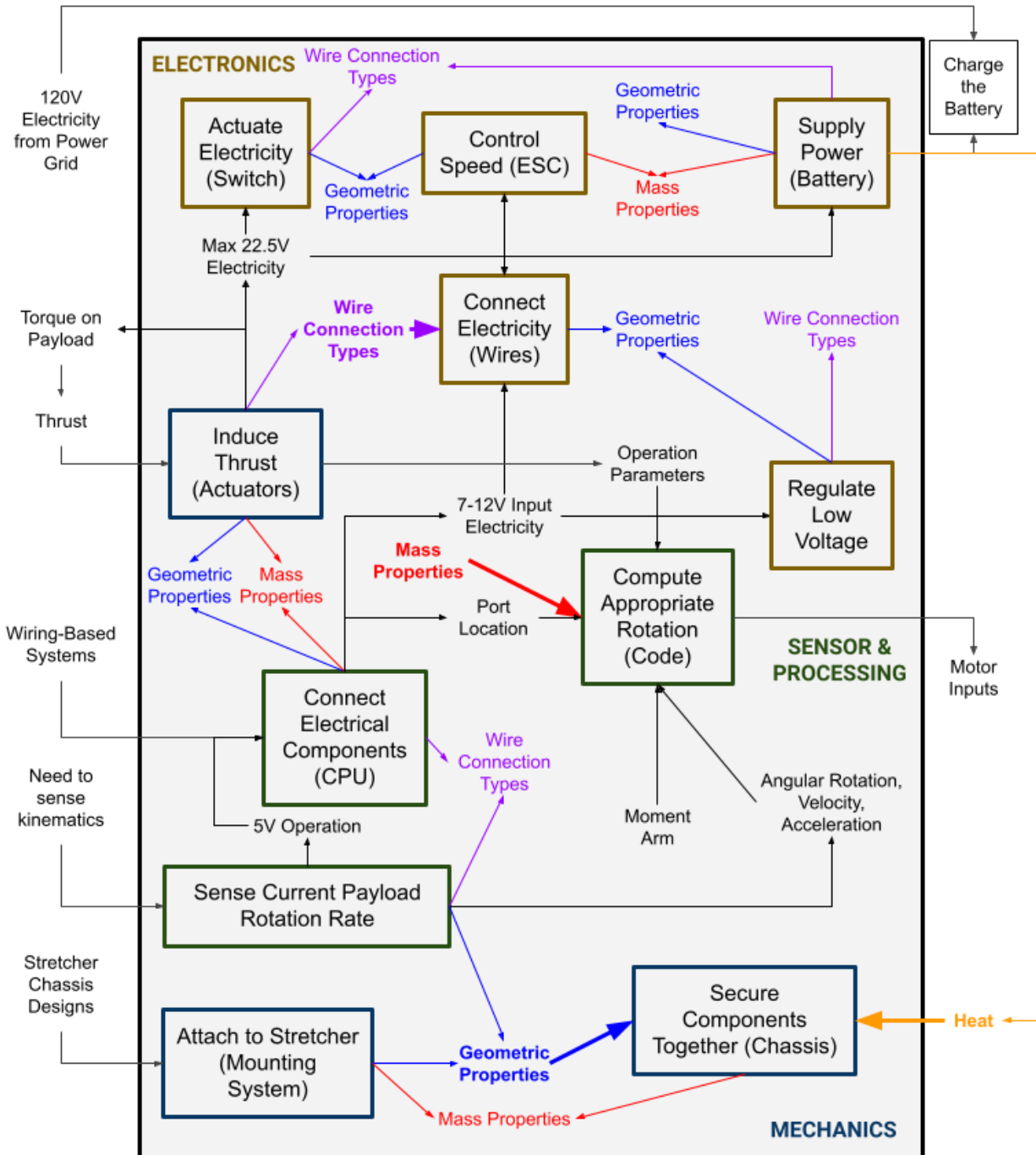
The end result of performing a quality function deployment method analysis is a series of design weights that tell the designers what the most important attributes to design for are.



As is evident in the above figure, maximum torque output is the most important parameter, and the time for deceleration is second most important.

## **Function Analysis – Transparent Box Model**

As was the case in the PDR, the block diagram is defined such that the design decisions that must go into each subsystem and subproblem result in the completion of these specifications to ensure overall project success. The solutions to these design decisions affect the design parameters of the blocks that each subproblem points to, not what parameter is affected by the previous in its function. Some properties do not have arrows pointing to the subproblem specified; in these cases, ‘teleport’ to the bolded property with the bolded arrow. For example, the geometric properties specified by the “Actuate Electricity (Switch)” show that design decisions about the switch design dictate how components are secured together in the chassis.



There are three types of components given by different colors in the diagram above: electronics (given in gold), sensor and processing (given in green), and mechanics (given in dark blue). Additionally, information each component produces or is dependent on is described below. Three pieces of information (the geometric properties, the wire connections, and the mass properties) have colors associated with them. These components and information in the diagram are discussed in detail below.

## Components: Electronics

### Supply Power (Battery)

The rechargeable battery supplies 22.2V electricity to each actuator as well as the CPU. The electricity is sent to these devices through wires and regulated through a voltage regulator. The geometric properties of the power supply will be taken into account such that the chassis can hold the battery and prevent movement throughout actuation. Currently, we will need five batteries per actuators, (the number of actuators needed is discussed in Part V). The mass of each battery will also be taken into account when calculating the required thrust. Heat will be produced by the battery and accurate ventilation will be designed to prevent overheating of other elements.

### Connect Electricity (Wires)

The wires distribute electricity from the battery throughout the module. The chassis must be designed such that the wires are able to reach the devices they need to supply power. Except for the LED, chassis, and the mounting system, all components use wires to route electricity back and forth; thus, the wire selection is dependent on the connection mechanisms of each device. Additionally, the wires are dependent on the voltage of the electricity that is run through them.

### Actuate Electricity (Switch)

The switch will receive an on/off orientation. When on, it will distribute electricity to the voltage regulator. We assume that the mass of the switch is negligible, but include its geometric properties in the design of the chassis. Only one switch is needed, and this switch is located on the main module.

### Regulate Voltage (Low)

The voltage regulator receives electricity from the wires from the battery and adjusts the voltage to the correct amount so as not to overheat the electrical components. The sensors and CPU will operate at 7.5V while the actuators, switch, battery will operate at around 22.2V. One type of voltage regulator is needed and is located with the CPU to adequately distribute the adjusted power. The chassis must be designed to ensure that the voltage regulators are held secure.

## Components: Sensors and Processing

### Central Processing Unit (CPU)

The CPU's purpose is to receive and distribute information such as the moment arm, angular kinematics, and motor inputs to the appropriate devices. Only one CPU is required for this system. The CPU will house the code that computes the appropriate rotation. The types of wires used must be able to connect to the CPU. The CPU determines the electricity we will use throughout the system, which is 7.5V. The chassis must be designed to ensure the safety of the CPU, and its mass properties will be taken into account in the rotation calculation. The appropriate port locations must be taken into account from the Arduino guide.<sup>19</sup>

---

<sup>19</sup> <https://store.arduino.cc/usa/arduino-uno-rev3>

### Compute Appropriate Rotation (Code)

The code's purpose is to calculate the appropriate amount of thrust for the actuators in motor inputs based on the mass properties of each component and the angular kinematics gathered from the sensors and distributed by the CPU. The code is the only component without a mass, inertial, or geometric property under consideration in this module. The code will be uploaded into the CPU before the CPU is installed. The code must be compatible with the CPU's programming language.<sup>20</sup>

### Sense Current Payload Rotation Rate

These sensors determine the current rotation rate of the payload and determine the payload's current angular rotation, velocity, and acceleration. This information is sent to the code via the CPU. The current payload rotation rate is also based on the torque previously applied by the actuators in a negative feedback loop. The sensor locations correspond to the location of the actuators. The mass of the sensors must be taken into account and their geometric properties must be considered in the design of the chassis. The wires connecting the sensors must have adequate connections and the sensors must be able to run 5V electricity.

## **Components: Mechanics**

### Secure Components Together (Chassis)

The chassis's purpose is to secure all devices. It must ensure that adequate ventilation is met for devices that produce heat. It must consider the geometric properties of all components except the code. The chassis will be designed into multiple parts, one part for each actuator. Its mass must be considered when calculating the appropriate thrust.

### Induce Acceleration (Actuators)

The actuators receive electricity from the power supply via the wires and PWM inputs to produce the appropriate thrust determined by the code in the CPU. The thrust creates a torque on the payload. The electricity we will use is 22.2V based on the 70mm fan we are considering.

Depending on the type of actuator, it will also produce sound that must not exceed the noise level requirements given by the National Institute for Occupational Safety and Health. It is recommended that the sound generation be below 85 dB<sup>21</sup>, but we do not anticipate the actuators we use to exceed 60 dB. More on actuators is discussed in Part V, including the type and quantity of each actuator. The chassis must be designed to ensure the proper operation of the actuator, and its mass properties will be taken into account in the rotation calculation.

### Attach to Stretcher (Mounting System)

The attachments to the stretcher secure the actuators and CPU to the stretcher such that a force created by the actuators will not cause actuators to fall off. The attachments are designed based on the stretcher chassis designs we will clamp the device to. Ideally, the modules would be able to attach to any stretcher regardless of design. The number of attachment mechanisms correspond to the number of modules needed. These attachments

---

<sup>20</sup> <https://www.arduino.cc/en/guide/introduction>

<sup>21</sup> <https://www.cdc.gov/niosh/topics/noise/infographic-noiselevels.html>

must be designed to fit the chassis and its mass properties will be taken into account in the rotation calculation.

## Information

### Heat

Some heat is generated through the CPU and the sensors, but most heat in our system is generated through the batteries. The chassis must be adequately designed such that the heat is appropriately ventilated away from the device to be sure to not melt any critical components.

### Geometric Properties

These properties are required of all physical components so that the chassis can be designed to fit them.

### Mass Properties

These properties are required of all non-negligible physical components so that the appropriate values can be calculated for the thrust. The heavier the actuators, the more thrust the actuators must be able to provide. We assume that the weight of the payload is about 95kg and the mass of the system is expected to be around 35-40lbs (18kg). Maximum load is 250 lbs (113kg). The code uses the mass to calculate the inertial properties of the system.

### Wire Connection Types

The wires will have different connection types depending on the device it is connecting to. The wires will be designed depending on these device connections.

### Electricity (22.2V, 7.5V, 5V, 120V AC from Power Grid)

The only source of energy used in our design is from our battery. The battery will output electricity for each component through wires. Electricity will be used exclusively to power our system, from the actuators and sensors to the central processing unit (CPU) itself. The electricity will undergo conversion to the appropriate voltage to be sure to power each device appropriately and not blow anything up. The electricity will be distributed through wires from the power supply, which is charged with electricity through a charging port and wire from the electrical grid before use in a helicopter.

### Angular Rotation, Velocity, Acceleration

Different angular kinematics are output depending on the type of sensor. The code must be adjusted to convert and manipulate these values into usable quantities.

### Moment Arm

We hardcode the value of the moment arm, fed to the code via the PCB and are used along with the mass of the actuators to calculate the appropriate torque on the payload.

## Port Location

The code must be compatible with the CPU's ports such that the right signals are sent to the right places using the right commands. The code must be adjusted if a change in CPU or CPU orientation occurs.

## Thrust

Thrust is generated from electricity in the actuators that propels the stretcher. Ideally, the thrust will come from two actuators equally at a certain distance apart such that a torque is created on the stretcher with a net force of zero, preventing additional sway from the stretcher.

## **Morphological Chart**

The morphological chart is a rational design method in which we create design blocks that present many alternatives for a given feature of the solution. By comparing many possible design decisions, we can explore different combinations of design features and determine which best satisfies the design requirements. Below is our morphological chart, with most viable options listed in bold.

Design Block	Option 1	Option 2	Option 3	Option 4
Actuation	Flywheel	Turbine	<b>Rotor</b>	Twisting Cable (powered)
Number of Actuators	1	<b>2</b>	3	<b>4+</b>
Power	<b>Electric</b>	Gas	Hybrid	
Device Location	Edge of payload	<b>Under Payload</b>	Center of mass	Hoist cable replacement
Shape	Basket/Bed	<b>Box attached to payload</b>	Cable	
Sensors	IMU	Compass		
Modular vs. Combined	<b>Modular</b>	Combined		

For actuation, we found that having a turbine or rotor to enact forces in various directions would be the most simple and reliable way to stabilize the payload system. Rotating flywheels require large power input and complex actuation, and focusing actuation on the cable would only solve anti-spin stabilization and ignore the possibility of anti-sway. In terms of the number of actuators, two actuators is the minimum number needed to counteract spin, and four is the minimum to counteract sway; similarly, an even number of actuators is preferred to maintain

symmetry. Finally, we determined that a modular approach is advantageous because it minimizes weight and allows for versatility with existing stretcher models.

### Weighted Objective Method

The weighted objectives chart is the second of the rational design methods for this project. This chart is derived from the weighted objective tree, where we assign a weight to each objective at a given layer. This weight is scaled similar to a rank, and is normalized to a factor such that the combined weights at a given layer add up to one. The result is a relative ranking of objectives which we are to address in our design. Below is an example of the calculations involved in the top layer of the objective tree.

Objective	Weight (scaled)	Weight (fraction)	Weight (normalized/sum of 1)
Safety	3	3/10	0.3
Universal Application	1	1/10	0.1
Reliability	2	2/10	0.2
Payload Stabilization	4	4/10	0.4

Under each node, its children are similarly weighted and normalized to a sum of one. The total weight of a given node is the multiplication of its weight and that of its parent nodes. We repeat this process for each node in the tree until the third and bottom layer, when we can compare the final weight of each objective and determine which design criteria are the most important to consider. The weight and normalization is based on the total number of sibling nodes. Below is the final weighted objectives chart, with local and total weights shown for each node.

Layer 1	Layer 2	Layer 3
Payload Stabilization (0.4)	Prevent Spinning (0.4x0.5)=0.2	Apply Torque/Damping (0.2x0.5)=0.1
		Safe Spin Speed (0.2x0.5)=0.1
	Stabilize Payload already spinning (0.4x0.333)=0.13	Damp high spin speed (0.13x0.5)=0.065
		Safe deceleration (0.13x0.5)=0.065

	Keep Payload Oriented Correctly $(0.4 \times 0.167) = \mathbf{0.07}$	Sense Helicopter Orientation $(0.07 \times 0.33) = \mathbf{0.023}$ Match Orientations $(0.07 \times 0.66) = \mathbf{0.046}$
Safety (0.3)	Payload Safety $(0.3 \times 0.167) = \mathbf{0.05}$	Doesn't unbalance payload $(0.05 \times 0.66) = \mathbf{0.033}$ Maintain orientation $(0.05 \times 0.33) = \mathbf{0.017}$
	Crew Safety $(0.3 \times 0.333) = \mathbf{0.1}$	Portable $(0.1 \times 0.33) = \mathbf{0.033}$ Safe in Storage $(0.1 \times 0.17) = \mathbf{0.017}$ Safe in Installation $(0.1 \times 0.5) = \mathbf{0.05}$
	Living Payload Safety $(0.3 \times 0.5) = \mathbf{0.15}$	Safe in use $(0.15 \times 0.5) = \mathbf{0.075}$ Safe in structural failure $(0.15 \times 0.33) = \mathbf{0.05}$ Safe when device fails $(0.15 \times 0.17) = \mathbf{0.025}$
Reliability (0.2)	Reliable Battery $(0.2 \times 0.5) = \mathbf{0.1}$	Lasts long flights $(0.01 \times 0.66) = \mathbf{0.066}$ 5 Year reliability $(0.01 \times 0.33) = \mathbf{0.033}$
	Easy to Use $(0.2 \times 0.333) = \mathbf{0.07}$	No Initialization $(0.07 \times 0.33) = \mathbf{0.023}$ Reliable Sensors $(0.07 \times 0.66) = \mathbf{0.046}$
	Robust Device $(0.2 \times 0.167) = \mathbf{0.03}$	5 Year functionality $(0.03 \times 0.167) = \mathbf{0.005}$ Survives 20 ft. drop $(0.03 \times 0.5) = \mathbf{0.015}$ Minimal Maintenance $(0.03 \times 0.33) = \mathbf{0.01}$

Universal Application (0.1)	Works with Any Helicopter (0.1x0.5)= <b>0.07</b>	Independent of Helicopter specifics (0.07x0.5)= <b>0.035</b>
		No use of Helicopter features (0.07x0.5)= <b>0.035</b>
	Rigid Attachment (0.1x0.167)= <b>0.0167</b>	N/A <b>(.0167)</b>
	Attachable to any payload (0.1x0.333)= <b>0.033</b>	Attach to flat surface (0.033x0.33)= <b>0.01</b>
		Attach to Bars (0.033x0.5)= <b>0.0165</b>
		System for irregular surfaces (0.033x0.17)= <b>0.006</b>

As we can see from the weighted objectives chart, objectives that have a higher parent such as payload stabilization and safety tend to have higher final weights. In addition, throughout the final layer we see that objectives related to the hoisting/rescue operation and the safety of the patient involved are of higher priority than those relating to long-term reliability or general compatibility. As such, in our design process our priority is to create a product that solves the problem statement by safely stabilizing the system, and compatibility and convenience is an important but secondary objective.

## Design Specifications (All)

Using the morphological chart and weighted objective method, we determined the best actuators to use are four ducted fans powered by electricity. We also determined that we should place the modules on the sides of the stretcher, and connect them via communication wires. Finally, we determined that a single IMU and CPU placed in one module would be sufficient for closed loop control.

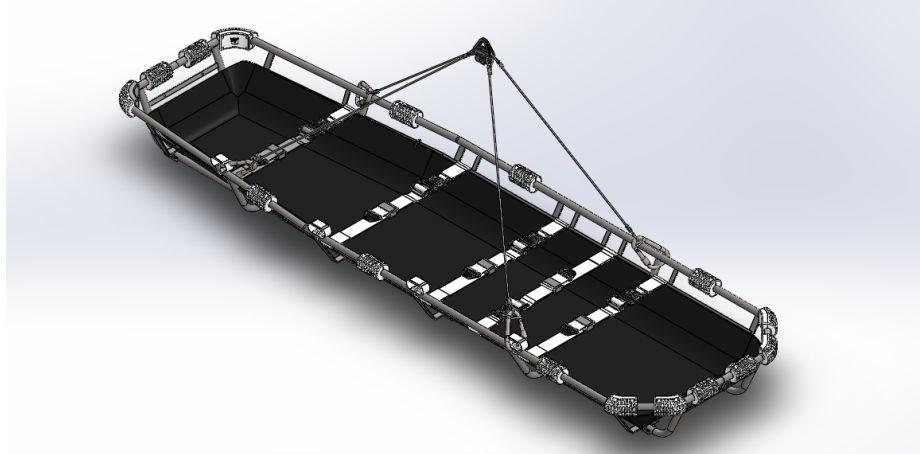
### Mechanical System:

The mechanical system consists of the stretcher litter, device chassis, mounting hardware, and the connective components such as screws, etc. These must also be compatible with our electrical system components.

#### Stretcher

The primary stretcher litter that we are designing around is the Lifesaving Systems Corp 404 Medevac Stainless Steel Rigid Litter, which is the most common litter used in helicopter

rescues<sup>22</sup>. This features a steel frame with a top bar diameter of  $\frac{3}{4}$ " and secondary support bars of diameter  $\frac{1}{2}$ ", which are the primary points of contact for our device. We contacted LSC for a model of their litter for our design process, which they were kind enough to provide. Below is the CAD model of the 404 Medevac Litter.



In order to satisfy our requirement of being compatible with more than one stretcher model, we also found 3 other stretcher models that span the majority of available litter from manufacturers. These are the Junkin JSA-300 Basket Stretcher<sup>23</sup>, the CMCPRO Stainless Steel Rescue Litter,<sup>24</sup> and the Cascade Rescue Professional Series Litter.<sup>25</sup> We contacted these companies as well but were unable to obtain CAD models. However, we were able to gather common features in all four of our stretchers. All stretchers had at least 1 foot of bar at the head and tail of the litter with a top bar diameter of either  $\frac{3}{4}$ " or 1", and a slightly varied support bar system. We determined that if we could design our device such that it is compatible with either bar diameter and had a mounting system robust enough to secure despite support bar locations, then our device will be compatible with all these stretchers.

### Mounting Hardware

The mount to the horizontal pipes on the stretcher is meant to be rigid and with zero degrees of freedom. It is important that it can accommodate different diameters of pipe. The maximum diameter pipe we found on various stretchers was one inch. For this reason, the maximum allowable pipe diameter on the horizontal mounting hardware is one inch as well. The mount to the “vertical pipes” is meant to fasten onto pipes on the stretcher that are most likely not vertical at all, but for the purpose of this document they are referred to as “vertical pipes”.

The horizontal mounts have three requirements. They must be able to mount securely to different diameter pipes (with a maximum diameter of one inch), they must be able to be taken off without opening any parts of the chassis, and they must operate at or preferably above a factor of safety of 2.5 during normal operation of the stabilization device.

<sup>22</sup> <https://lifesavingsystems.com/product/medevac-ii-rigid-litter-stainless-steel-with-flotation-kit>

<sup>23</sup> <https://www.junkinsafety.com/stretchers>

<sup>24</sup> [https://www.cmcpo.com/equipment/stainless-steel-rescue-litter/#learn\\_more](https://www.cmcpo.com/equipment/stainless-steel-rescue-litter/#learn_more)

<sup>25</sup> <https://cascade-rescue.com/cascade-rescue-professional-series-stainless-litters/>

The vertical mounts have four requirements. Like the horizontal mounts, they must be able to mount securely to different diameter pipes (with a maximum diameter of one inch), and they must operate at or preferably above a factor of safety of 2.5 during normal operation of the stabilization device. In addition, they must be able to support the weight of the chassis to prevent tipping down, and they must be able to attach to the vertical pipes that are in an unknown position and orientation (each stretcher model is different).

### Chassis

The simplest method to manufacture our chassis involves using plastic injection molding with polycarbonate. Since there is no tapping required on the screws, a mold can be designed to hold the actuators, batteries, and CPU. The latter two components must be separated from the actuators so that dirt, water, or oils do not get into the chassis. These components will also require vents such that heat dissipation occurs. The chassis is designed in two main parts, top and bottom, such that easy installation and swapping of inner components is achieved, with adhesive present for loose components. Socket head screws are used to ensure minimal interference with the smoothness of the chassis.

### **Electrical System:**

The electrical system consists of the ducted fans (actuators), electronic speed controllers (ESC), central processing unit (CPU), inertial measurement unit (IMU), batteries, voltage regulator, and various wires/connectors. All parts must be compatible and meet our design requirements.

### Actuators

Given a moment arm of 1.1m (half length of stretcher), our actuators must produce at least 5.5N each to counteract the 12Nm of external torque seen in the spinning stretcher video. The more thrust our actuators can produce, the better we can counteract external torque. However, increasing actuator power reduces battery life.

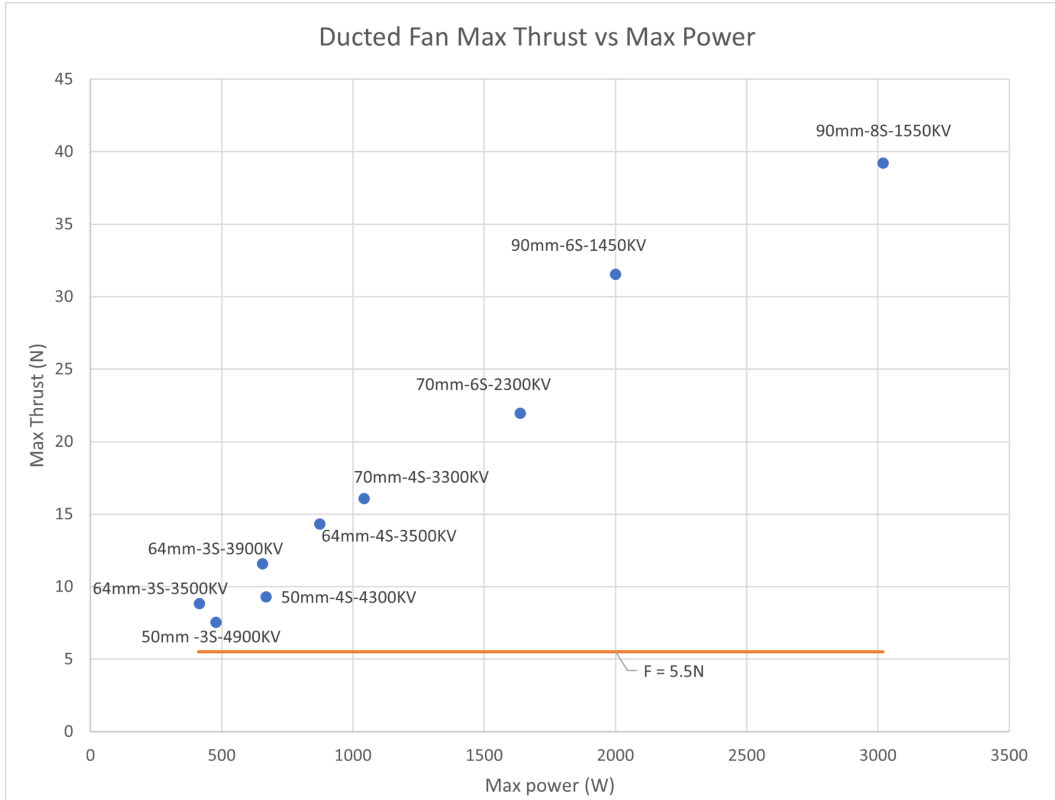


Figure: Actuator power vs thrust comparison

As seen in the figure above, all actuators above 50mm meet the minimum safety requirement of 5.5N. Since we want the maximum actuator thrust to be considerably higher than the minimum thrust requirement, we narrowed the choice to 70mm rotors or greater. Rotors of 90mm have good thrust, but consume over 2000W at max thrust, meaning the device could only operate for a short period. Our final choice is the 70mm-6s-2300KV ducted fans, since they deliver over 4 times the minimum thrust requirement while operating under 2000W.

### Electronic speed controllers (ESC)

To keep things simple, we chose the ESCs that were recommended by the ducted fan manufacturers. These are the Skywalker Hobbywing 80A ESCs.

### Central processing unit (CPU)

We chose Arduino Uno Rev 3 due to multiple reasons. Arduino IDE is simple to code, there are many code libraries that are available to use, which will be sufficient for our project. This board has 20 I/O pins, and 6 of them are PWM output pins<sup>26</sup>, which are enough to command 4 actuators in our project and communicate with the IMU sensor. This board has 3.3V and 5V pins, which can act as voltage supplies for many kinds of sensor.

<sup>26</sup> <https://store.arduino.cc/usa/arduino-uno-rev3>

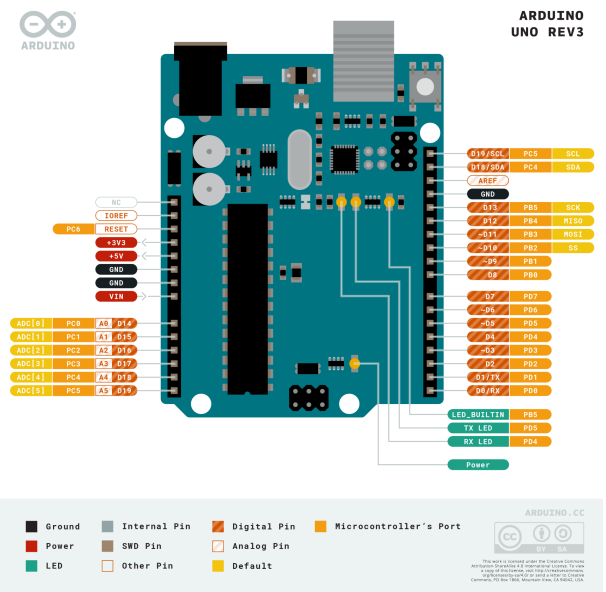


Figure: Arduino Uno Rev3 pin diagram

### Inertial measurement unit (IMU)

The IMU that we desired for this project was required to be compatible with our Arduino and had to be capable of measuring angular velocity at a reasonable resolution. The 6 DOF Adafruit ISM330DH CX IMU was the device we chose to use for this project. This IMU is capable of measuring angular velocity at a resolution of 4000 degrees per second at a sample frequency of 6.75kHz<sup>27</sup>. The high resolution and measuring frequency coupled with a low noise margin of 2% error on angular velocity makes this an ideal IMU for this project. Furthermore, this IMU operates on both 3 volt or 5 volt pin from the Arduino, and comes at a relatively cheap price point of \$14.95<sup>28</sup>.

### Batteries

To power the ducted fans, the manufacturer recommends 22.2V/6S - 35C batteries. Given that HHOs typically take at most 13 minutes<sup>29</sup>, we wanted our system to last for multiple rescues on one battery charge. Using 10 batteries per model, we can achieve 30 minutes at maximum thrust, which allows us to make 2 consecutive rescues in the worst case scenario. While this is the worst case scenario, the actuators are unlikely to remain at maximum thrust during the entire HHO. For prolonged battery health, we will try to keep the batteries between 20% and 80% charge. We will use a 10A lipo charger to recharge and balance the battery packs, resulting in a 3.5 hour charge time.

The batteries will emit enough heat such that ventilation is required. However, the batteries must also be insulated such that no water, dirt, or oils interfere with the battery. Thus, we concluded that a material that is waterproof, has high thermal conductivity, and prevents electrical breakdown will be sufficient for our purposes.

<sup>27</sup> <https://www.st.com/resource/en/datasheet/ism330dhcx.pdf>

<sup>28</sup> <https://www.st.com/resource/en/datasheet/ism330dhcx.pdf>

<sup>29</sup> <https://www.sciencedirect.com/science/article/pii/S1080603219301140>

## Voltage regulator

Since our CPU runs on 7-12V, we require a step down regulator to reduce the 22.2V power supply. We also would like to limit the amount of back EMF entering the CPU. Thus, we chose a Pololu 7.5V step down regulator to achieve both these requirements.

## Wires, connectors, and battery charging

All wire gauges and connectors are detailed in our electrical schematic. The battery charging input must handle 10A, so we will use an XT60 connector. The Battery output to ESCs must handle 130A (65A per motor), so we will use 1 AWG wire. Power from batteries to CPU will be routed via 12 AWG (low current requirement). Finally, all communication (I2C) will be routed with 22 AWG.

## **Control Algorithm:**

The goal of the control algorithm is to drive the stretcher angular velocity to zero. While this goal is our number one priority, we have certain safety and comfort criteria that our system must meet. For the safety requirements, we want to limit the acceleration experienced by the patient. For comfort, we will attempt to reduce the jerk experienced by the patient.

## Safety Derivation

Below is a chart going over the variables that will be used in the safety measures derivation:

Parameter	Definition	Units
$t$	Time	Seconds
$r$	Distance of patient's head to center of rotation	Meters
$\theta(t)$	Angle of stretcher with respect to original position, function of time	Radians
$\omega(t) = \frac{d\theta(t)}{dt}$	Angular Velocity of stretcher, function of time	Radians/Second
$\alpha(t) = \frac{d\omega(t)}{dt}$	Angular Acceleration of stretcher, function of time	Radians/(Seconds^2)
$x(t)$	Position vector of patient's head with respect to standard (non – rotating) reference frame.	Meters
$v(t) = \frac{dx(t)}{dt}$	Velocity vector of patient's head with respect to standard (non-rotating) reference frame.	Meters/Second
$a(t) = \frac{dv(t)}{dt}$	Acceleration vector of patient's head with respect to standard (non-rotating) reference frame.	Meters/(Second^2)
$J(t) = \frac{da(t)}{dt}$	Jerk vector of patient's head with respect to standard (non-rotating) reference frame.	Meters/(Second^3)
$u_R(t)$	Radial Direction vector in current alignment with stretcher	N/A
$u_T(t)$	Tangential direction vector in alignment with current tangential direction of the stretcher	N/A
$v_T(t) = \langle u_T(t), v(t) \rangle$	Tangential linear velocity of the patient's head	Meters/Second
$a_T(t) = \langle u_T(t), a(t) \rangle$	Tangential linear acceleration of the patient's head	Meters/(Second^2)
$a_R(t) = \langle u_R(t), a(t) \rangle$	Radial linear acceleration of the patient's head	Meters/(Second^2)

The position of the patient's head is modeled by the vector  $x(t)$ :

$$x(t) = r * \begin{pmatrix} \cos(\theta(t)) \\ \sin(\theta(t)) \end{pmatrix}$$

The velocity of the patient's head is obtained by taking the derivative with respect to time of  $x(t)$ :

$$v(t) = r * \begin{pmatrix} -\omega(t)\sin(\theta(t)) \\ \omega(t)\cos(\theta(t)) \end{pmatrix}$$

The acceleration of the patient's head is obtained by taking the derivative with respect to time of  $v(t)$ :

$$a(t) = r * \begin{pmatrix} -\alpha(t)\sin(\theta(t)) - \omega(t)^2\cos(\theta(t)) \\ \alpha(t)\cos(\theta(t)) - \omega(t)^2\sin(\theta(t)) \end{pmatrix}$$

The jerk of the patient's head is obtained by taking the derivative with respect to time of  $a(t)$ :

$$\begin{aligned} J(t) &= r * \begin{pmatrix} -\alpha'(t)\sin(\theta(t)) - \alpha(t)\omega(t)\cos(\theta(t)) + \omega(t)^3\sin(\theta(t)) - 2\alpha(t)\omega(t)\cos(\theta(t)) \\ \alpha'(t)\cos(\theta(t)) - \alpha(t)\omega(t)\sin(\theta(t)) - \omega(t)^3\cos(\theta(t)) - 2\alpha(t)\omega(t)\sin(\theta(t)) \end{pmatrix} \\ &= r * \begin{pmatrix} (\omega(t)^3 - \alpha'(t))\sin(\theta(t)) + (-3\alpha(t)\omega(t))\cos(\theta(t)) \\ -(\omega(t)^3 - \alpha'(t))\cos(\theta(t)) + (-3\alpha(t)\omega(t))\sin(\theta(t)) \end{pmatrix} \end{aligned}$$

Define the unit radial vector to be in the direction the stretcher is currently facing and the unit tangential vector to be in the direction tangent to the current direction of the stretcher:

$$u_R(t) = \begin{pmatrix} \cos(\theta(t)) \\ \sin(\theta(t)) \end{pmatrix}, u_T(t) = \begin{pmatrix} -\sin(\theta(t)) \\ \cos(\theta(t)) \end{pmatrix}$$

Taking the dot product of the velocity and acceleration vectors with respect to the unit radial vector and the unit tangential vector will yield values of tangential velocity, tangential acceleration, and radial acceleration. Instead of finding tangential and radial jerk, the magnitude of the jerk vector was calculated instead. This yields the following results:

$$v_T(t) = \langle u_T(t), v(t) \rangle = r * \omega(t)$$

$$|a_T(t)| = |\langle u_T(t), a(t) \rangle| = r * |\alpha(t)|$$

$$|a_R(t)| = |\langle u_R(t), a(t) \rangle| = r * \omega(t)^2$$

$$|J(t)| = \sqrt{\left( \omega(t)^3 - \frac{d\alpha(t)}{dt} \right)^2 + (3\alpha(t)\omega(t))^2}$$

Humans can typically survive large accelerations perpendicular to the spine, even up to 10g for 1 minute<sup>30</sup>. However, acceleration along the spine forces blood away or towards the

---

<sup>30</sup> [https://ntrs.nasa.gov/archive/nasa/casi.ntrs.nasa.gov/19980223621\\_1998381731.pdf](https://ntrs.nasa.gov/archive/nasa/casi.ntrs.nasa.gov/19980223621_1998381731.pdf)

head, causing severe damage in extreme cases. Most people can handle up to 5g along the spine, but our system will most likely be transporting injured patients. Thus, we will attempt to limit the radial acceleration to 0.5g at the patient's head. We chose 0.5g because it is less than the patient would experience while standing upright (1g), and choosing 0.5g would yield a large safety factor of 10. Furthermore, we will attempt to limit the tangential acceleration to 1g at the patient's head. We chose 1g because it is 10 times lower than the upper bound for tangential acceleration at 10g. Choosing the limit of tangential acceleration to be 1g is appropriate since we will likely be dealing with injured patients in the stretcher so a large safety factor is desirable. We can use these assumptions to obtain upper bounds on the angular velocity and angular acceleration. Using the fact that  $1g = 9.81(m/s^2)$ , and taking the value of r to be 1.1 meters

$$\begin{aligned} |a_R(t)| &\leq 0.5g & |a_T(t)| &\leq 1g \\ 1.1 * \omega(t)^2 &\leq 0.5 * (9.81) & 1.1 * |\alpha(t)| &\leq 1 * (9.81) \\ |\omega(t)| &\leq (2.11) \left( \frac{rad}{s} \right) & |\alpha(t)| &\leq 8.91 \left( \frac{rad}{s^2} \right) \end{aligned}$$

This yields an upper bound on angular velocity to be 2.11 (rad/sec) and an upper bound on angular acceleration to be 8.91 (rad/(sec<sup>2</sup>)). Note that these upper bounds are for the worst case scenario, where we assume that the patient's head is at the tip of the stretcher yielding the maximum r value of 1.1 meters. If the patient is shorter, they will experience less radial and tangential acceleration.

Unlike previous parameters, jerk helps determine patient comfort, not safety. Due to the rotational nature of the problem, magnitude of jerk is not a very good indicator of patient comfort. Looking at the magnitude of the jerk, it is evident that even when experiencing constant angular velocity, the jerk vector is non-zero. This makes the behavior of jerk not similar to the linear motion case, where constant linear velocity would result in jerk of magnitude 0. Furthermore, since the magnitude of the jerk formula uses the derivative of angular acceleration, the magnitude of the jerk is very sensitive to slight perturbations, yielding large values. To counteract this, we run the magnitude of jerk through a moving average filter to smooth out the values and to simulate dampening forces present in the stretcher and cables. Even so, these filtered magnitudes of jerk values are higher than the prescribed jerk values while riding in public transportation, being 0.6 to 0.9 m/(s<sup>3</sup>)<sup>31 32</sup>. While these jerk values seem large, it is not as bad as it seems. Children in merry go rounds regularly experience large magnitude of jerk values and are perfectly safe. To use magnitude of jerk to determine patient comfort, we compare the filtered magnitude of jerk with the compensated and uncompensated case to show that the operation of our device greatly reduces jerk.

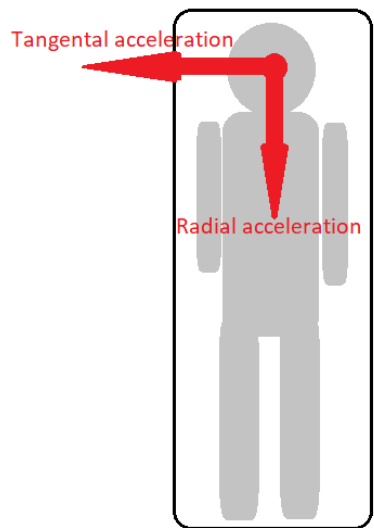
Below is a summary of the results derived in this section:

---

<sup>31</sup>

<https://peer.asee.org/an-investigation-of-acceleration-and-jerk-profiles-of-public-transportation-vehicles.pdf>

<sup>32</sup> <https://www.diva-portal.org/smash/get/diva2:839140/FULLTEXT01.pdf>



$$|a_R(t)| \leq 0.5g \quad |a_T(t)| \leq 1g$$

$$|\omega(t)| \leq (2.11) \left( \frac{rad}{s} \right) \quad |\alpha(t)| \leq 8.91 \left( \frac{rad}{s^2} \right)$$

$$|J(t)| = \sqrt{\left( \omega(t)^3 - \frac{d\alpha(t)}{dt} \right)^2 + (3\alpha(t)\omega(t))^2}$$

Figure: Acceleration experienced by patient on rotating stretcher

# System Design (All)

## System Dynamics

We will limit the stretcher motion to one degree of freedom; rotation about the cable axis.

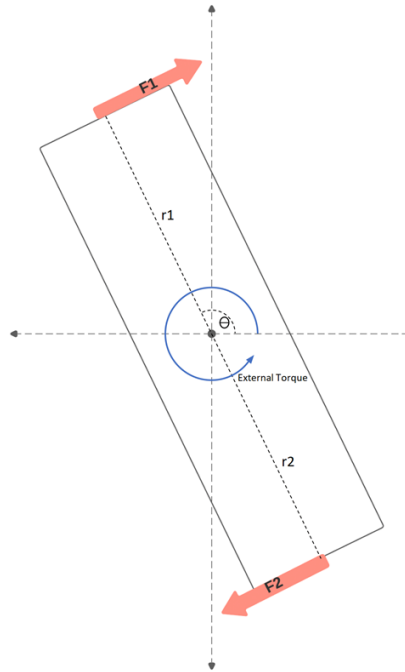


Figure: Stretcher free body diagram

To derive the system dynamics, we will make the following assumptions:

1. Our four actuators can be reduced down to two forces, since actuators pointing in opposite directions in a given module will never be activated at the same time
2. The torque from the cable,  $k\theta$ , and torque from wind resistance,  $c_w$  are negligible
3. All effects due to wind disturbances due to downwash and gusts can be simplified into some time dependent torque on the stretcher, labeled as  $\tau_{ext}(t)$ . As labeled in the diagram above, torque provided by external forces is opposed to the torque provided by the actuators on the stretcher

Angular acceleration of stretcher about center:

$$\sum \tau = I\alpha$$

$$\tau_{ext} - (r_1F_1 + r_2F_2) = I\alpha$$

$$\alpha = \frac{\tau_{ext} - (r_1F_1 + r_2F_2)}{I}$$

The forces and torque on the system are time varying, so

Angular acceleration:  $\alpha(t) = \frac{\tau_{ext}(t) - (r_1 F_1(t) + r_2 F_2(t))}{I}$

Angular Velocity:  $\omega(t) = \omega_{initial} + \int_0^t \alpha(\tau) d\tau$

Absolute angle:  $\theta(t) = \theta_{initial} + \int_0^t \omega(\tau) d\tau$

Using the above equations as a guideline, we derived the discrete time representation of the system as shown below:

State:  $x = \begin{bmatrix} \omega \\ \alpha \end{bmatrix}$

Inputs:  $u = \begin{bmatrix} F_1 \\ F_2 \end{bmatrix}$

Disturbance:  $w = [\tau_{ext}]$

Outputs:  $o = [\omega_{measured}]$

State Equation:

$$x_t = Ax_{t-1} + Bu_{t-1} + Cw_{t-1}$$

$$\begin{bmatrix} \omega_t \\ \alpha_t \end{bmatrix} = \begin{bmatrix} 1 & 0 \\ 0 & 0 \end{bmatrix} \begin{bmatrix} \omega_{t-1} \\ \alpha_{t-1} \end{bmatrix} - \frac{1}{I} \begin{bmatrix} r_1 \Delta t & r_2 \Delta t \\ r_1 & r_2 \end{bmatrix} \begin{bmatrix} F_1 \\ F_2 \end{bmatrix} + \begin{bmatrix} \Delta t \\ 1 \end{bmatrix} \frac{1}{I} \tau_{ext}$$

Output Equation:

$$o_t = Dx_{t-1} + N$$

$$\begin{bmatrix} \omega_{measured} \end{bmatrix} = [1 \ 0] \begin{bmatrix} \omega_t \\ \alpha_t \end{bmatrix} + Noise$$

In our mathematical formulation, our state only consists of angular velocity and angular acceleration. This is because our objective is to stop the stretcher from spinning, which involves driving the angular velocity to zero. We need information on angular acceleration as well because it will be used to determine the safety of the person within the stretcher. The output equation models the angular velocity measured by the IMU. Using information from the IMU system specification chart, noise is modeled as a normal distribution with mean 0 and variance being 2% of actual angular velocity at time t.

### Actuator Thrust Model

Typically, a motors RPM is not directly proportional to the input PWM signal. Additionally, RPM to thrust curve for the propellers is also not linear. For example, we can look at other examples of measured motors and propellers.

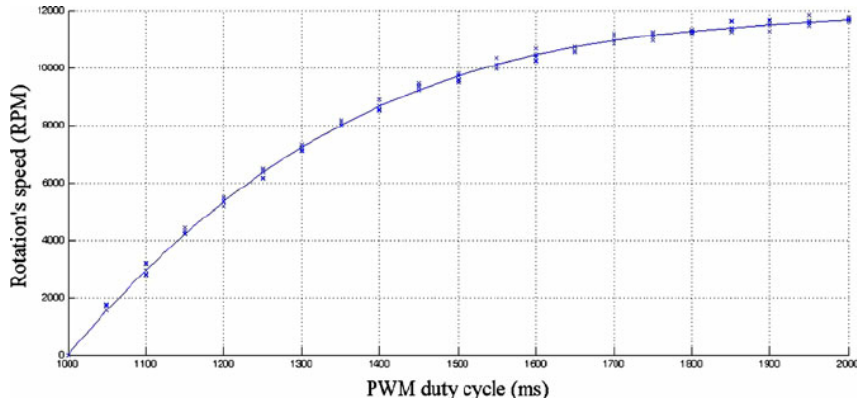


Figure : Measured rotational speed of the motor in various PWMS<sup>33</sup>

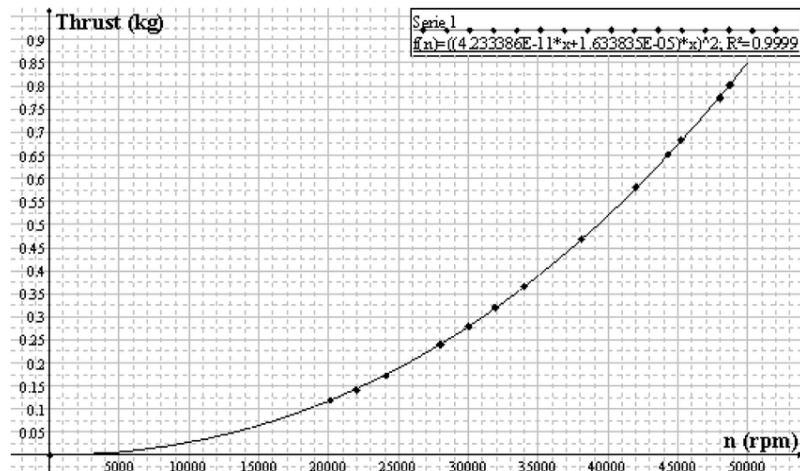


Figure 3: Propeller Thrust (kg) vs. rotational speed (rpm)<sup>34</sup>

These examples are for different motors and propellers than the ones we are using. We cannot find data on our specific actuators, so we will go forward assuming the ESCs and/or actuators have been programmed to output thrust that is directly proportional to the inputs.

### Rotational Inertia

In determining the rotational inertia of the stretcher system, we used the 3D model provided by Lifesavings Systems Corp. After applying materials to all the necessary components, we were able to get information on the center of mass and the axial moments of inertia. Below is an image showing the center of mass of the stretcher and inertial data.

<sup>33</sup> Mohammadi, Mostafa & Mohammad Shahri, Alireza. (2013). Adaptive Nonlinear Stabilization Control for a Quadrotor UAV: Theory, Simulation and Experimentation. Journal of Intelligent and Robotic Systems. 72. 10.1007/s10846-013-9813-y.

<sup>34</sup> Trancossi, Michele & Dumas, Antonio. (2011). A.C.H.E.O.N.: Aerial coanda high efficiency orienting-jet nozzle. SAE Technical Papers.

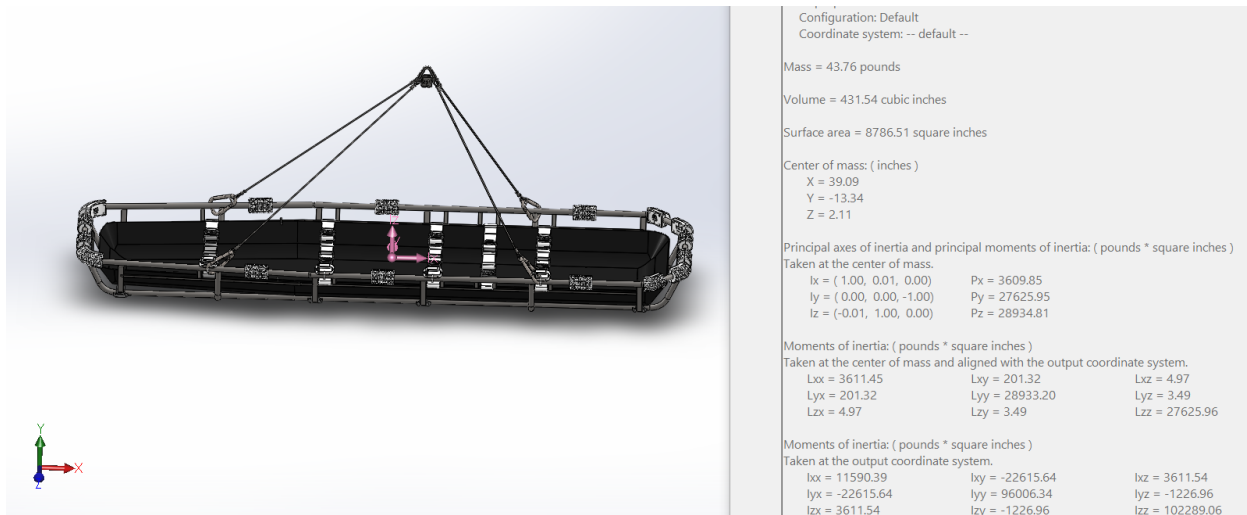
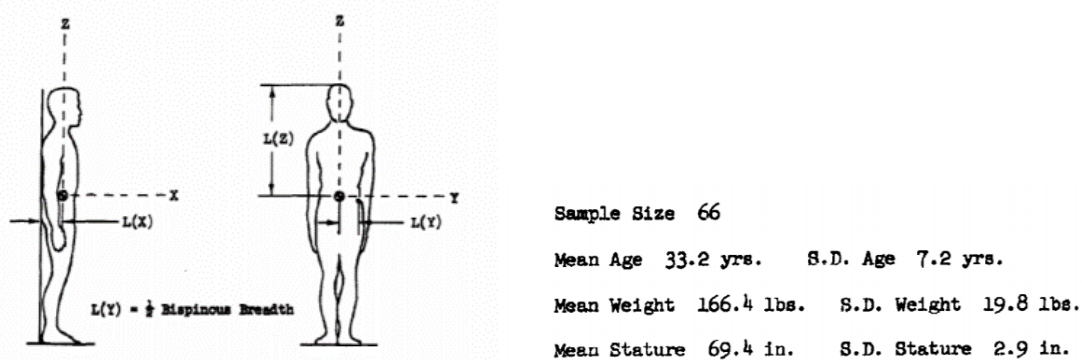


Figure: Center of mass of the stretcher.

The coordinate system in pink (created by mass properties feature) is the local coordinate system of the stretcher, which is used to define the directions for the moments of inertia. X is towards the head of the stretcher, Y is toward the side, and Z is towards the sling and the sky. This data is for the stretcher-sling system that connects to the rope. If necessary, we can also obtain inertial data without the sling system.

We used a paper on anthropometric data and inertia from the Department of Defense to begin modeling a body inside of a stretcher.<sup>35</sup> By taking data concerning the “standing” position and modifying the axes to fit a body laying down, we can approximate the added inertia of a patient in a stretcher. Below is a summary of inertial data for an upright individual, with standard deviations given for a sample size of 66 participants.

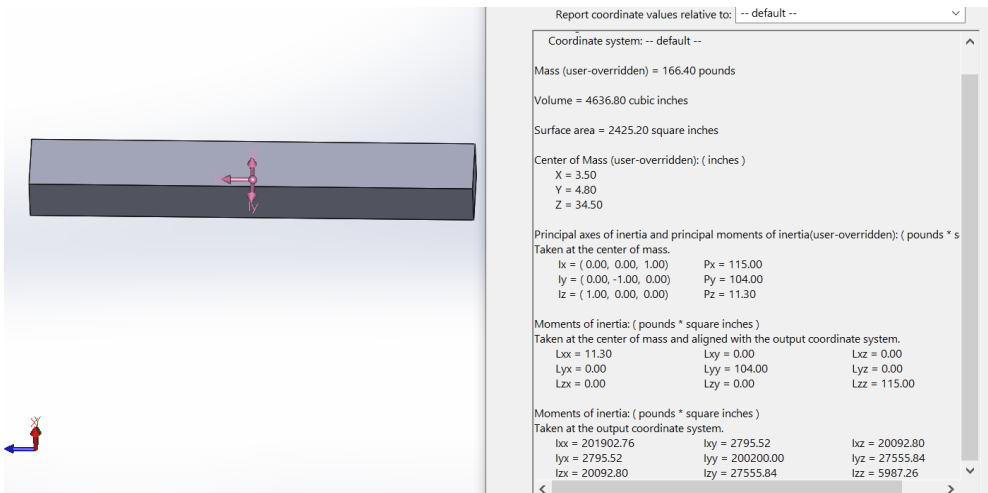


<sup>35</sup> Department of Defense Anthropometric Data : <https://apps.dtic.mil/dtic/tr/fulltext/u2/410451.pdf>

Axis	Center of Gravity (in.)		Moment of Inertia (lb.in.sec. <sup>2</sup> )	
	Mean	S.D.	Mean	S.D.
1. Standing	x	3.5	0.20	115.0
	y	4.8	0.39	103.0
	z	31.0	1.45	11.3
				2.2

Figure:

In Solidworks, we modeled the body as a prism with overridden mass and inertia properties. Since the body will rotate about its center of gravity and is strapped into the stretcher, this is adequate to model in our simulations. Below is a model based on the mean mass and inertia values.



Figure

We also modeled several more bodies that represent 3 standard deviations above and below mean DoD data to represent 99.7% of a possible patient population. We also planned for the cases of a maximum payload of 150kg and an empty stretcher, which serve as edge cases for our system to control. For the maximum payload case, the inertial values correspond to that 7 standard deviations from the mean. In planning our test cases, we will also vary the locations of the body inside the stretcher rather than strictly lining up the center of mass.

#### External Torque (Disturbance) Model

While the stretcher is being hoisted, it is subject to downwash from the helicopter, as well as wind from any direction, however, we are not coding a fluid dynamics simulation in python. Our goal is to model wind/downwash as an external torque, with reasonable magnitude and direction over time. We can approximate the bounds of this torque by estimating the maximum force exerted by wind on the stretcher's side.

To calculate the force exerted by wind, we will use the following equation,

$$F_{wind} = m_{air} \times V_{air}^2 \times \sin(\theta);$$

$$m_{air} = A_{surface} \times D_{air}$$

which describes the force exerted on a small object for a given wind speed and angle relative to the surface. The maximum wind speed a helicopter can safely operate in is about 90km/hr<sup>36</sup>. Additionally, wind from downwash can travel very quickly as seen from the plot below.

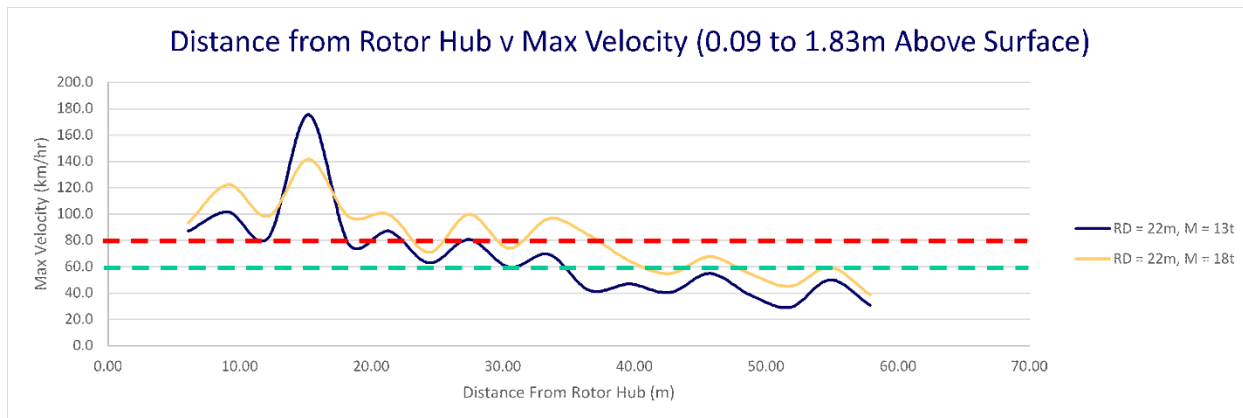


Figure : Distance from rotor hub versus maximum downwash velocity<sup>37</sup>

The wind speed of downwash can range from 40km/hr to 180km/hr depending on distance to rotors. However, it is directed down at the stretcher, and thus the angle at which the air hits the sides of the stretcher is likely low.

Using this information, we can calculate the total force wind or downwash could exert on the stretcher:

$$F_{wind} = 1.229 \times 0.38 \times 25^2 = 291N$$

$$F_{downwash} = 1.229 \times 0.38 \times 50^2 \times \sin(10^\circ) = 203N$$

Force of wind at 90 km/hr and Force of downwash at 180km/hr and 10°

These numbers look very large, but since this wind is exerted equally across the surface area, there is no torque exerted on the stretcher. Torque is only exerted when there is a difference in pressure along the surface area.

Let us assume the worst-case scenario, in which wind only acts on one side of the stretcher. Then the force exerted by the wind would be 145N spread out across one side. For

<sup>36</sup> STARS air ambulance:

<http://starshorizons.ca/when-is-it-too-windy-to-fly/#:~:text=The%20BK117%2C%20the%20helicopter%20we,rotating%20at%20a%20low%20speed.>

<sup>37</sup> JJ Ryan Consulting:

<https://jjryan.com.au/index.php/helicopter-rotor-downwash-excessive-wind-fod-and-brownouts-what-are-the-risks/>

simplicity, let us assume that equates to a single force acting at the halfway point between the center of the stretcher and the end. This produces a torque of 78 Nm. Likewise, the maximum torque we would see from downwash would be around 54 Nm. While 78Nm is larger than the maximum torque output of our actuators (61.6 Nm), our solution is not designed to handle extreme scenarios like this. However, we will test all scenarios within this range even if our actuators saturate.

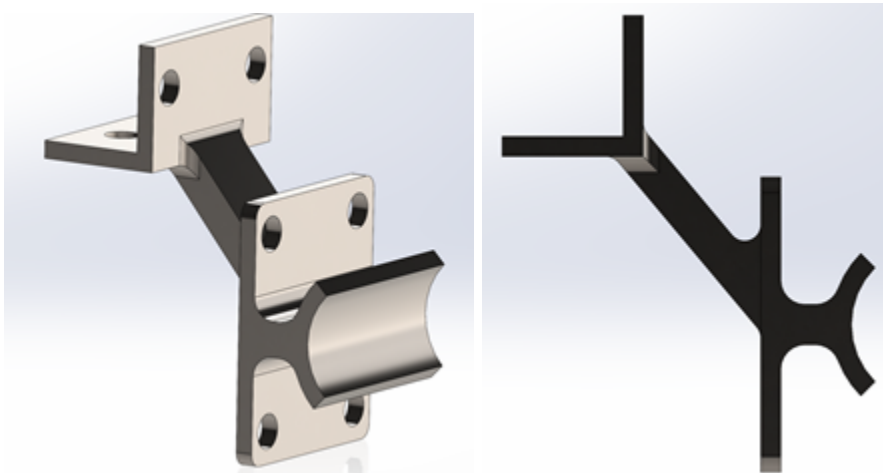
Our goal is to model the external torque over time (disturbance), and design a controller that can reject this disturbance. Since it is very hard to predict what the actual disturbances look like in the real world, we will conduct many tests with many disturbance models between these bounds.

## Mechanical Subsystem

### Mounting Hardware

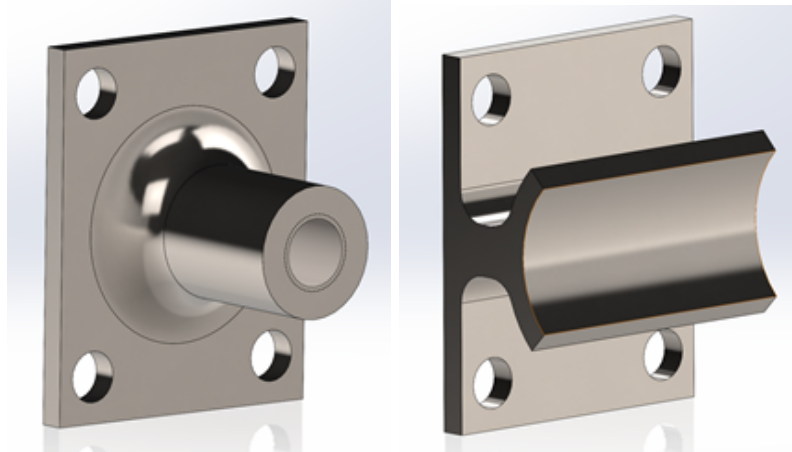
Off the shelf components were chosen when possible to decrease the effort and cost required. They also carry the added benefit of being designed by reputable engineers that have passed scrutiny tests. The horizontal mount uses U-bolts and  $\frac{1}{4}$ " – 20 threaded nuts, and washers. The U-bolts were chosen so that a user could tighten the mount around a pipe even if the pipe is smaller than one inch. The same U-bolts, nuts, and washers were also used in the vertical mounts. Other pieces used were a rod end ball joint, an inline ball joint linkage, a  $\frac{3}{8}$ " – 24 threaded rod, and  $\frac{3}{8}$ " – 24 nuts.

The horizontal mount has a custom-made piece named “Pipe Fitting Corner Mount”. It has through holes for  $\frac{1}{4}$ " diameter bolts and has a curved section to secure onto the horizontal pipes. The other half, seen on the left in both pictures shown below, is the piece that attaches to the chassis, again using  $\frac{1}{4}$ " diameter bolts. The reason for the angled piece is to allow a user to unscrew the nuts for the U-bolts while not having to take apart the chassis. Lowering the plate that attaches to the pipe lets the operator use a wrench without interfering with the chassis.

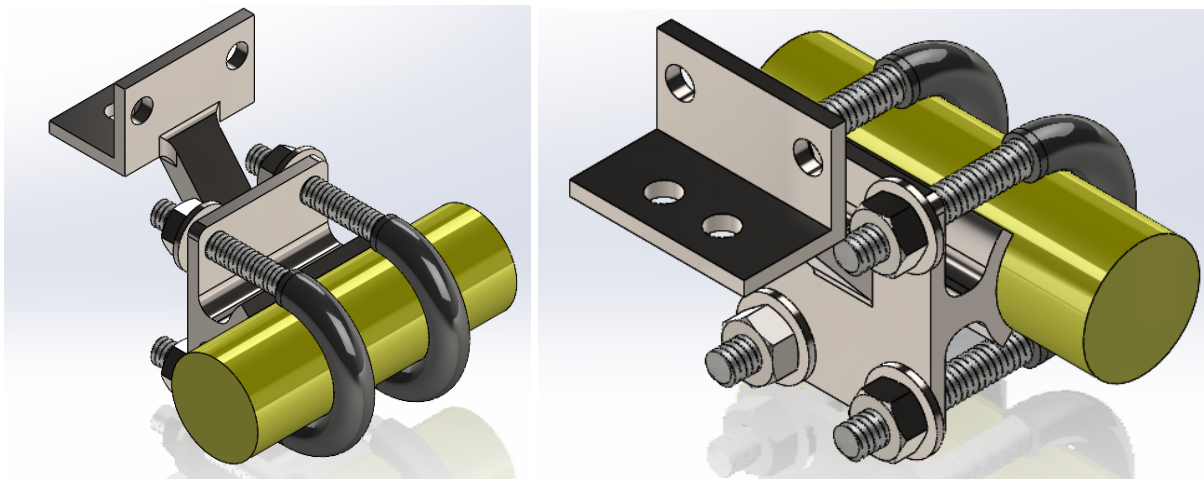


The vertical mounts required two unique pieces, called “Pipe Fitting” and “Pipe Fitting Hole”. Pipe Fitting is used to attach to the vertical pipes, and Pipe Fitting Hole is used to attach the mount to the underside of the chassis and the end of the inline ball joint linkage. The Pipe Fitting is similar to the Pipe Fitting Corner Mount, it was simplified because it did not share the

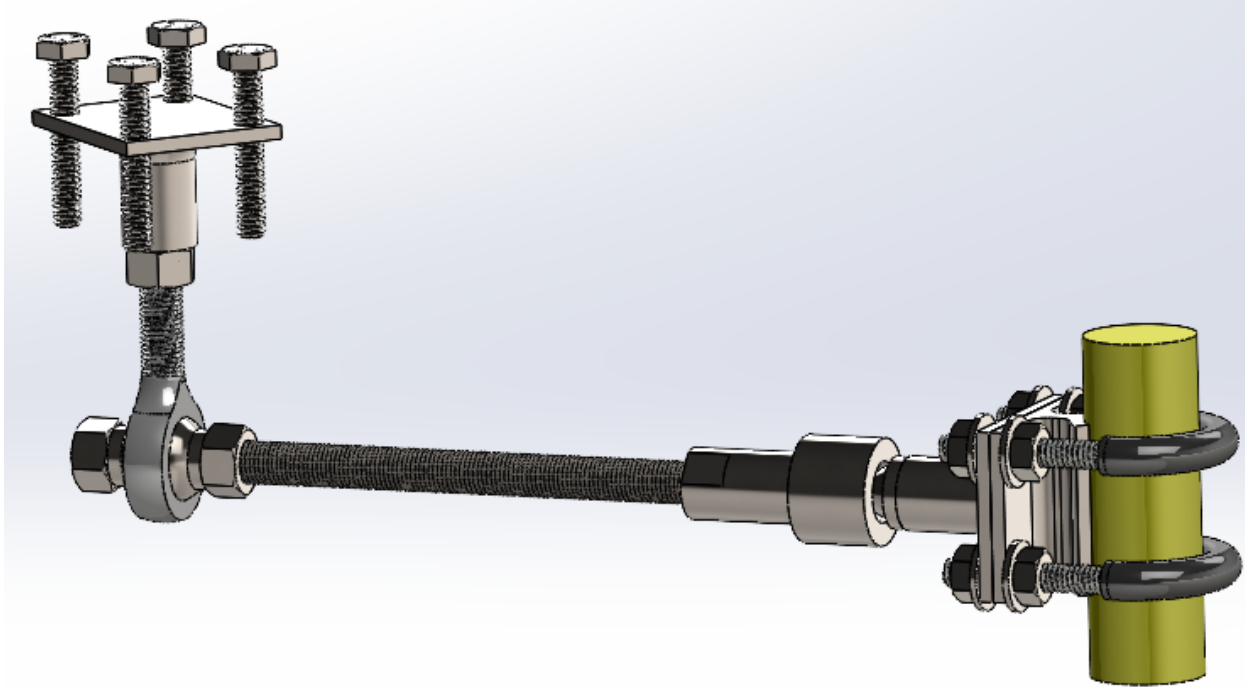
same constraint about removing the U-bolts while in close proximity to the chassis. The Pipe Fitting Hole is simply a plate with a threaded extrusion to accommodate 3/8" – 24 threaded rod.



The horizontal bracket is shown below with an example yellow pipe. The operator tightens the nuts to secure the mount in place. The U-Bolts are off the shelf components chosen from McMaster-Carr. The threaded ends were cut shorter in length so that a socket wrench can be used to tighten the U-bolts to the corner mount.

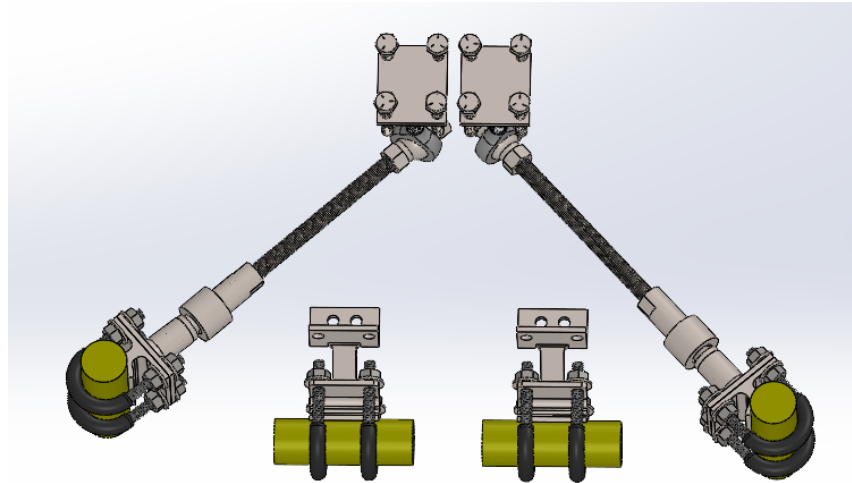


The vertical mount is more complex. First, the Pipe Fitting Hole part is secured to the chassis via four bolts. The rod end ball joint is then threaded into the Pipe Fitting Hole part and a nut is used to stop the rod end ball joint from spinning inside the Pipe Fitting Hole. A threaded rod is slipped through the ball joint and held in place by two nuts on either side of the ball. This allows an installer to specify the length of the threaded rod between the rod end ball joint and the inline ball joint linkage. The other end of the threaded rod is threaded into the inline ball joint linkage which is secured to a Pipe Fitting Hole part that is then fastened to the Pipe Fitting part and attached to the vertical pipe of the stretcher.

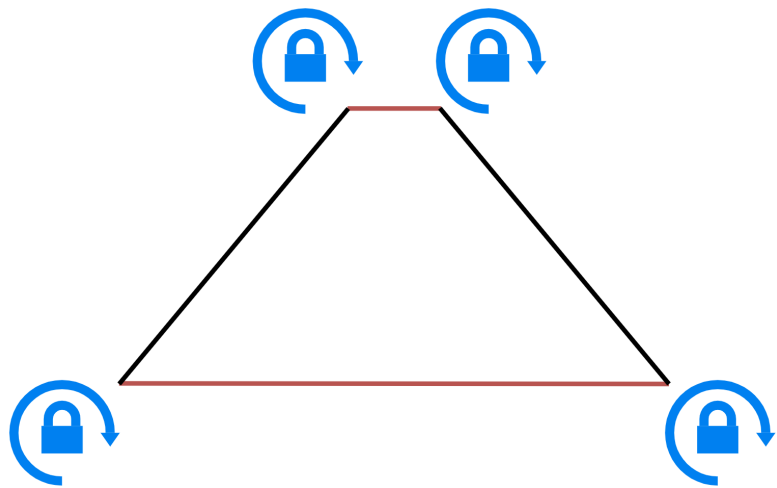


The rod end ball can be positioned a maximum of 23 degrees from being in plane with the rest of the joint, and the inline ball joint linkage can be positioned a maximum of 7 degrees from it's housing axis.

Ball joints were chosen to account for different orientations of bars on different models of stretchers. The downside of using ball joints is that they have three degrees of freedom a piece. The underside mounts are a mere 1.8 inches apart on the underside of the chassis.



A simplified model is shown below, where red lines represent distances between connectors that are constant because they are the physical distance between pipes on the stretcher or between bolt holes on the underside of the chassis. All four corners have rotational degrees of freedom because of the ball joints, but because the lengths of the threaded rods are held constant, the model is constrained. The U-Bolts have no degrees of freedom because friction will keep them in place. This friction is caused by tightening the nuts on the Corner Mount.



### Electrical Components

The following electrical component will be stored in the polycarbonate electrical housing, separated from the LiPo Batteries and the ESC via an electrical housing; the Arduino CPU, the IMU sensor, the voltage regulator, the CPU DC power socket to 2-pin terminal adapter, and the various wirings and connectors.

The aforementioned components use minimal amounts of power from the battery, and are not a major heat producer of our product. The large majority of our heat is produced from the 22.2V LiPo Batteries and the ESCs. To protect our critical components, a polycarbonate attachment was created to fasten the CPU and IMU and protect them from possible contact with the batteries and ESC. As for the small amounts of heat produced in the components within the housing, the holes that wires are allowed to exit will have slight gaps from being slightly larger than the wires, which will serve as ventilation. As the chassis itself is a competent water and debris-proof casing, the electrical housing will be safe from external threats.

The electrical housing also serves as a convenient way to change and replace batteries and ESC's without intruding on the electrical system. For a modular system, an extra layer of protection from debris, water, external forces, and convenience can allow a system to extend its life and use.

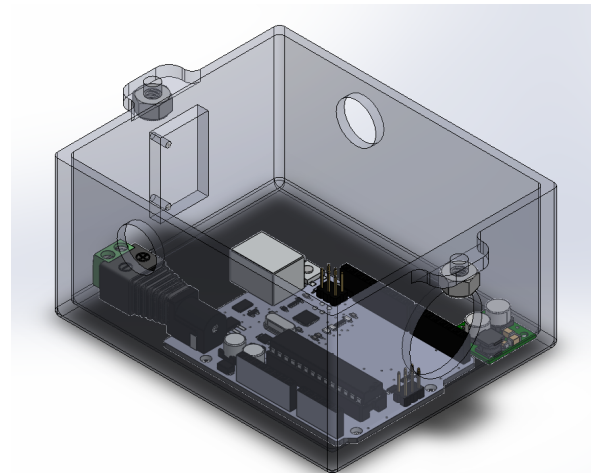


Figure: Electrical housing with electrical components

### Battery Integration

After further research, the product we concluded would meet our design specifications for the battery foam was the Tflex™ B200, a reliable compliant thermal material offering good thermal performance. It has high dielectric insulation which works to prevent dielectric breakdown and is made of ceramic filled silicone, a waterproof material. Placing this material in between the vent and the battery allows us to properly vent the heat from the batteries while keeping unwanted water, dirt, and oils outside. The foam also has a tacky side, used to attach to the battery, ESC, and the chassis to hold them together structurally.

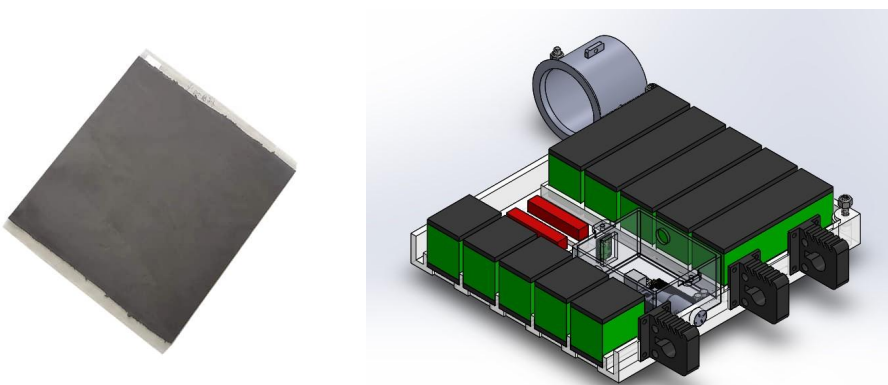


Figure: Tflex™ B200 from Digikey (left) on the batteries in chassis (right)

### Chassis

The figure below shows the final chassis design after numerous iterations. The two top and bottom components are very similar, allowing for easy revisions and updates.

The base was first extruded long enough to include the components within the chassis, including the batteries, ESC's, and other electronics. The holes were then created in the walled components, with room for  $\frac{1}{4}$ " socket head screws. The fan holders were then extruded out with their own screw holes to hold them in place. Cuts and wiring holes were created to ensure that the fan would be able to fit.

Once the fans were created, the ribs inside the chassis were created to hold the batteries, ESC's, and foam together without falling apart. The vents for these components were then created. Mounts were also attached to the corner of the chassis and the bottom of the chassis, with  $\frac{1}{4}$ " hex screws to keep the mounts in place. Finally, the electronic components were placed with the power button, ensuring that the CPU would remain separate from the batteries and ESC's and allow for easier exchange of parts.

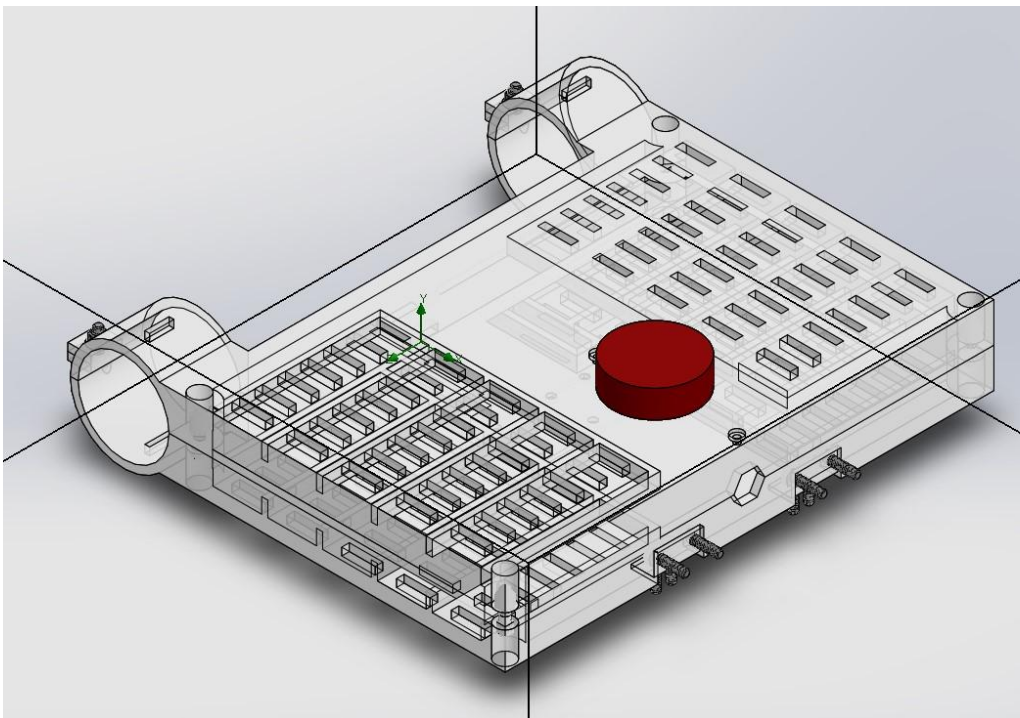


Figure: Chassis for module.

### Assembly

The assembly of all components was fairly simple to integrate given the comprehensive design of the chassis. The figure of the main assembly shows the final assembly's configuration which will be attached to the stretcher as shown in the figure following:

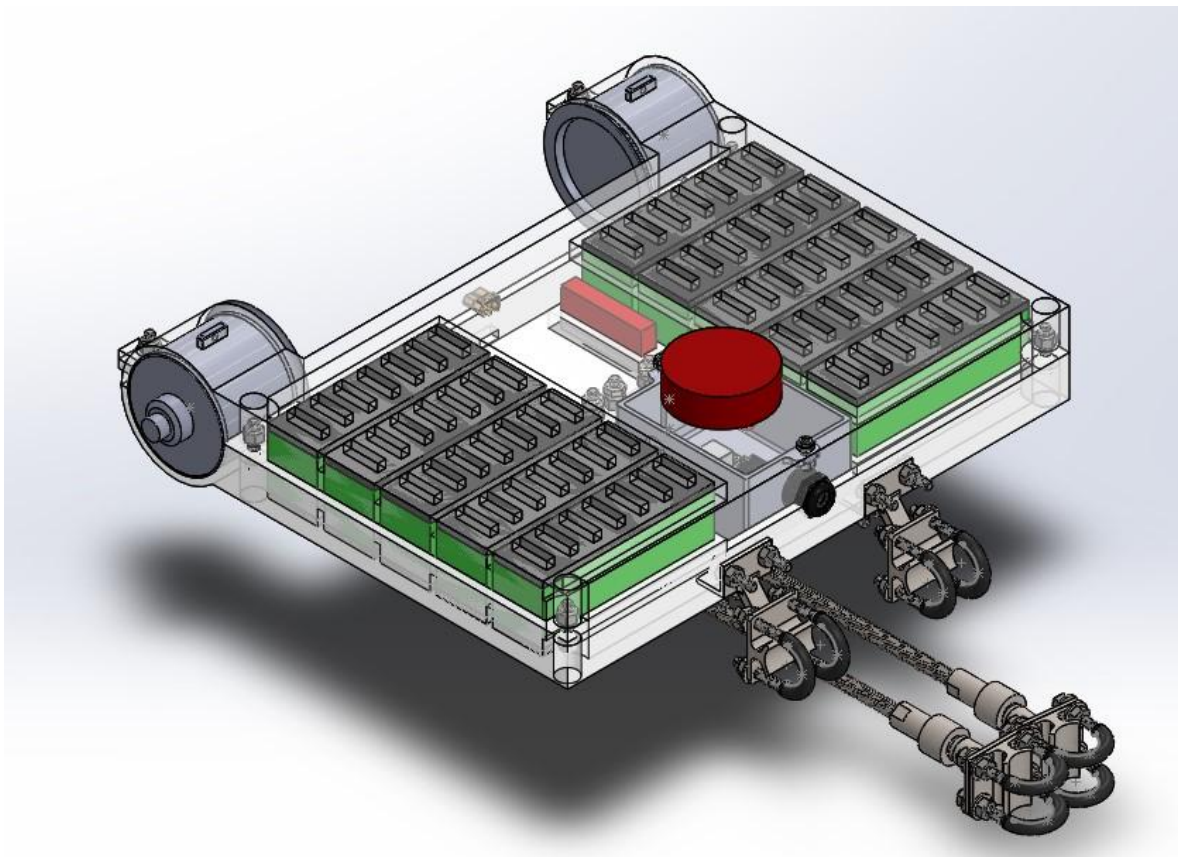


Figure: Main assembly including chassis, fans, mounts, electronics, and batteries.

The final chosen configuration was a device horizontal to the ground in parallel with the stretcher, offset from the stretcher itself. This configuration was chosen to avoid receiving the weight of the stretcher at the bottom, which may crush the modules when the patient is placed on the stretcher. We believe that the mounting system is strong enough with enough points of contact such that the device will not slip, rotate, or translate around the stretcher bars. This is yet to be confirmed through testing.

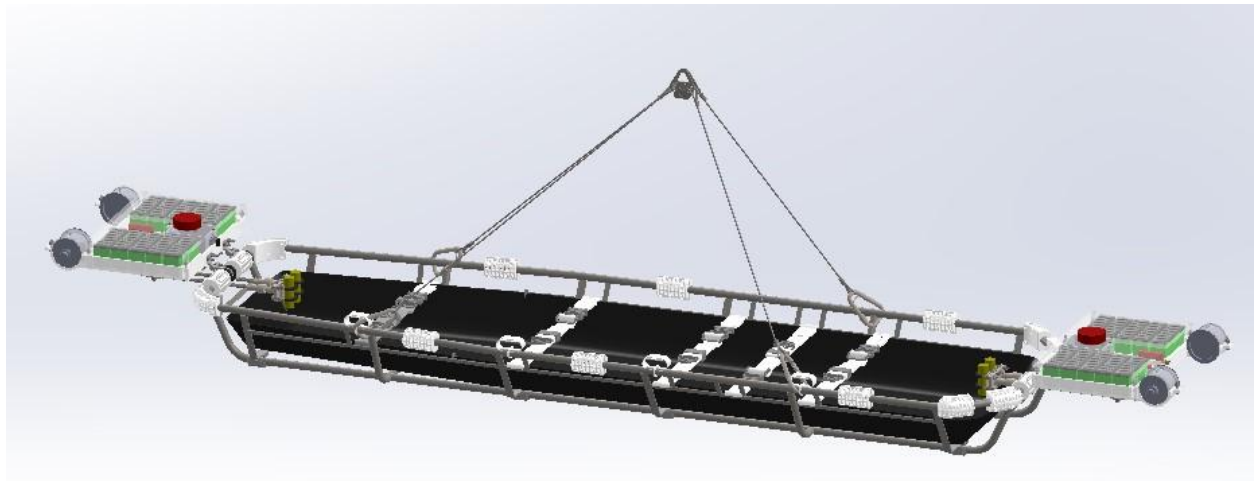


Figure: Assembly of the stretcher with the modules.

The assembly is designed to be able to fit in this formation on any stretcher. Though we have only been given one CAD model stretcher, we have been given drawings of other stretchers to be able to confirm this assumption.

## Electrical Subsystem

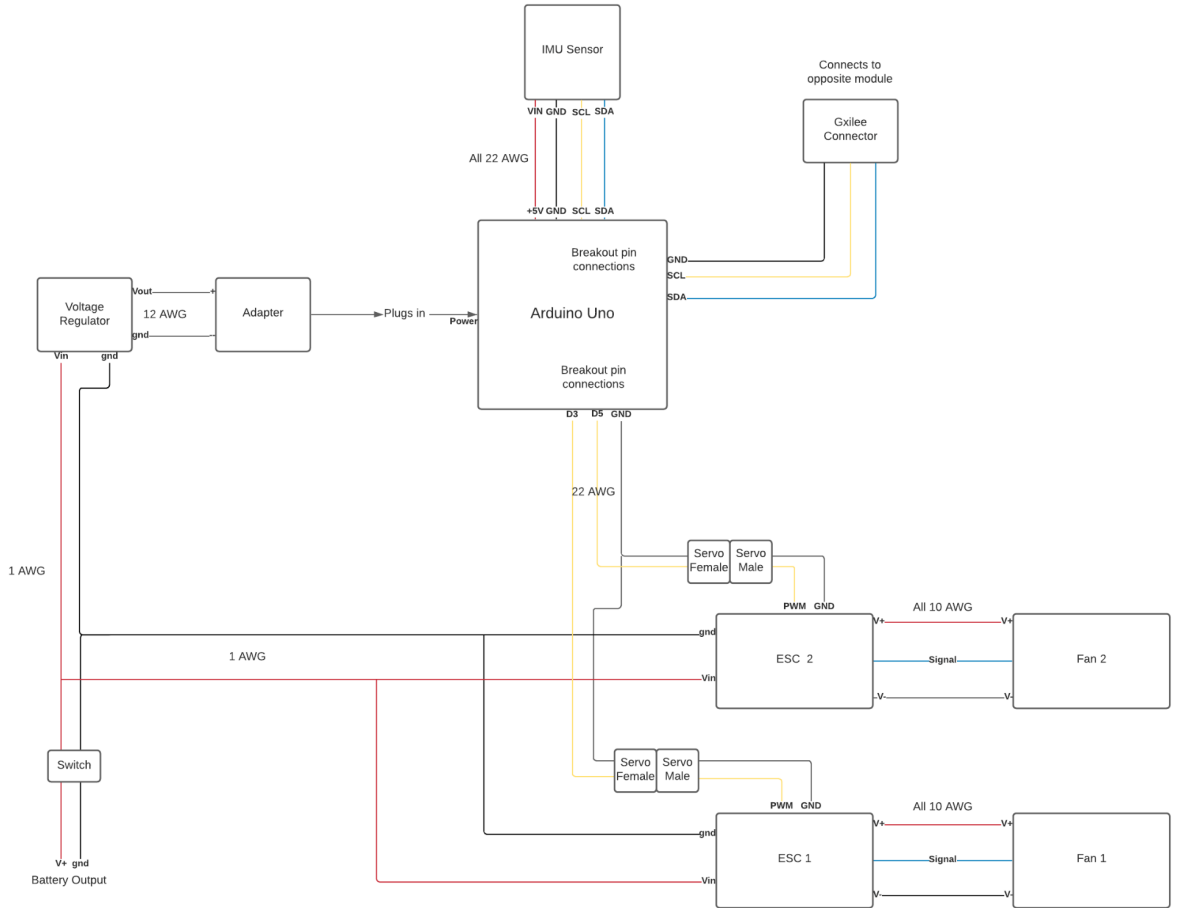


Figure: Module Electrical Schematic

Each Module is identical, and communicates with the opposite module via I2C. The communication will only be used to send the PID torque command from the master cpu to the slave cpu. This leaves one of the IMUs unused. However, future work could involve using the backup IMU as a failsafe in case the main one fails. The communication between CPU and IMU sensor is crucial for our autonomous system since the controlled actuators react on the angular velocity of the stretcher around its center of mass. We would connect them via I2C interface by using 22 AWG electric wire cables, which provide good connectivity and excellent uniformity for easy processing, stripping, and terminating. We would do the following instructions to connect the Arduino Board with the IMU sensor<sup>38</sup>.

- Connect IMU board VIN (red wire) to Arduino 5V
- Connect IMU board GND (black wire) to Arduino GND
- Connect IMU board SCL (yellow wire) to Arduino SCL
- Connect IMU board SDA (blue wire) to Arduino SDA

<sup>38</sup> <https://learn.adafruit.com/lsm6dsox-and-lsm330dhc-6-dof-imu/arduino>

By following the wiring instruction, the wires would be connected like the figure below.

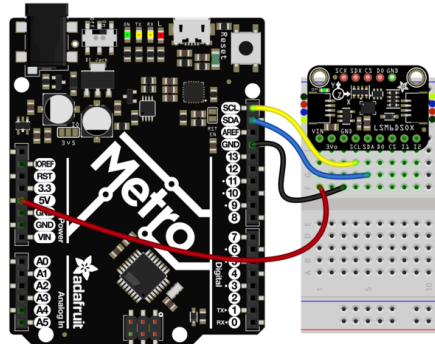


Figure: I2C Wiring with Arduino<sup>39</sup>

To connect the two modules, We would use 20 AWG-3 conductors-BELDEN B8772MN, which is covered by PVC Jacket. We picked this wire cable because PVC is known as resilient and durable to abrasion<sup>40</sup>. For the connector, we picked a Gxilee IP68 3 PIN DIN Female/Male Screw-on Solder connector<sup>41</sup>. The females will be installed into the chassis on each side facing the stretcher. The male parts of the connector will be soldered to each side of the BELDEN 20 AWG wire. This connection from the CPU in one chassis, to the 3 pin female, to the 3 pin male, through the BELDEN WIRE, and to the 3 pin female on the other chassis, will directly send the information from the CPU to the other chassis ESC.

This connector was chosen for several reasons. The nylon PA66 body and the silicon sealing element allows this connector to survive the harsh conditions of this product; it is waterproof grade, fireproof, debris-proof, and is resistant to corrosion. The screw-on connection also secures the fastening of the wire, preventing slight tugs from a person or object to sever the connection. The screw system also allows ease of deliberate detachment, making it a great choice for a modular, versatile device that still requires a strong wired connection between its parts.

A concern with the wired connection between the two chassis is its vulnerability to external forces, such as tugging, severing, cuts, and being caught. The wire will run inside the stretcher, which eliminates many of these problems, as we assume that the operating conditions make sure that all payloads in the system are relatively safe. The screw connections provide resistance to unintentionally tugging or tripping of the wires. A second protection is added by using a Safcord Cord protector; a 6 foot nylon sleeve that encapsulates the wire. Velcro is lined on both sides of the sleeve, and users may secure velcro on the stretcher and the sleeve to guarantee security. All in all, with these two measures, the wire and connection is as safe from the outside as the payload within the stretcher, which we will assume is not in significant danger. The external parts of the electrical system are fit for operations at emergency environments

<sup>39</sup> <https://learn.adafruit.com/lsm6dsox-and-lsm330dhc-6-dof-imu/arduino>

<sup>40</sup>

<https://www.elandcables.com/the-cable-lab/faqs/faq-what-are-the-benefits-of-pvc-insulated-cables#:~:text=Cable%20with%20a%20PVC%20insulation,durable%20and%20resistant%20to%20abrasion.>

<sup>41</sup> [https://www.digilaptopx.com/index.php?main\\_page=product\\_info&products\\_id=810484](https://www.digilaptopx.com/index.php?main_page=product_info&products_id=810484)

The charging port for the device will be located on the side of the chassis that holds the actuators. An XT60 will be used that will deliver power to all 10 batteries. During operation, a cap can be placed on the exposed charging port's xt60 to ensure that water and debris will not enter and result in failure of the charging system..

Since we are using LiPo batteries, we have designed our battery connections to allow for balanced charging. Each module contains two sub batteries, composed of five 3500mAh batteries. Below is the sub battery schematic.

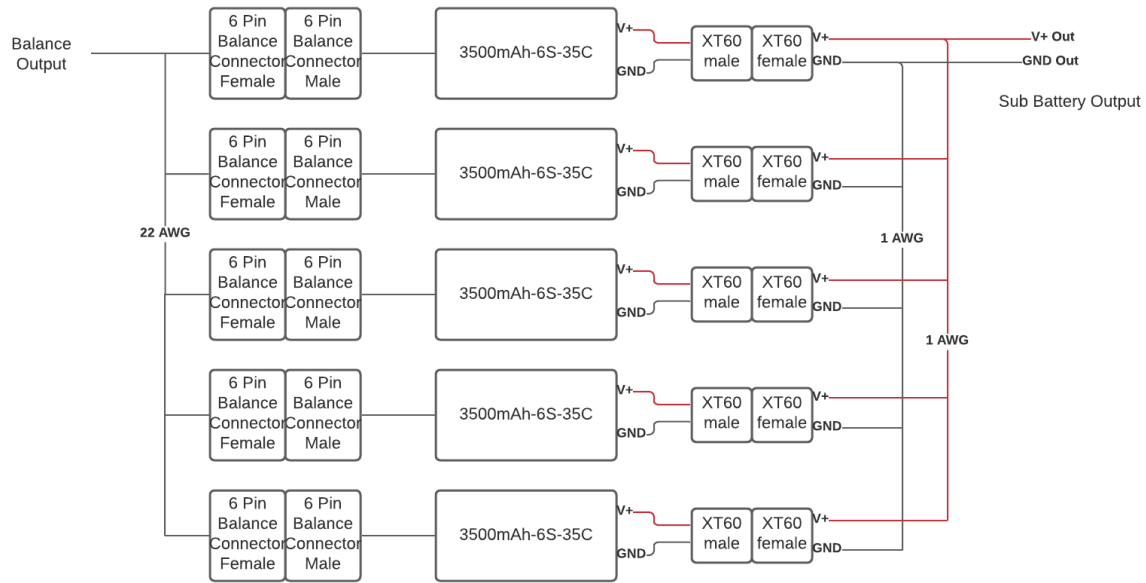


Figure: Sub battery schematic

Since the motors could draw 65A each, the total battery output could be 130A at times. Thus, we must use 1 AWG or equivalent for the battery output. The sub batteries will be connected according to the diagram below.

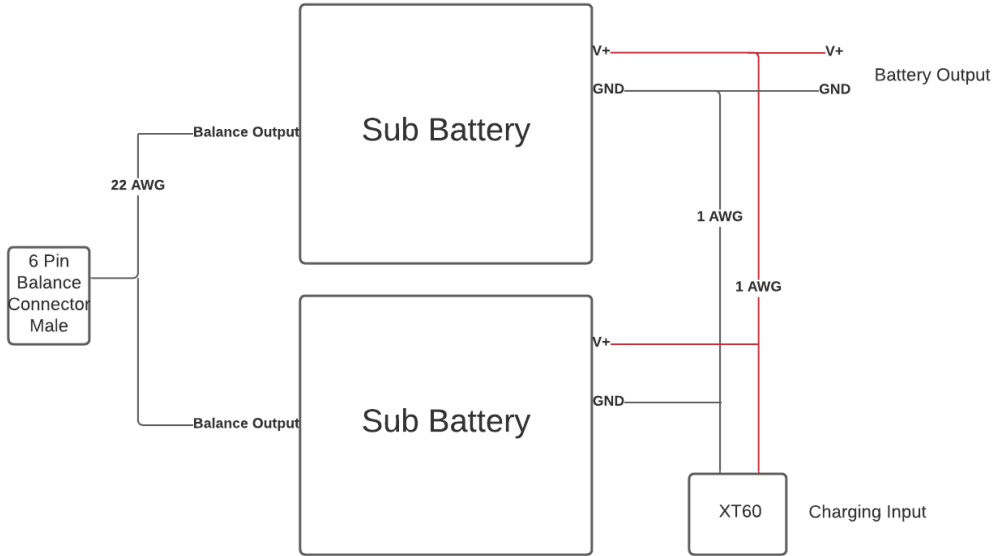


Figure: Full battery diagram

Currently, our solution to connect the batteries is a custom harness made from 1 AWG wire. This is not an easy harness to build, because there will be many solder connections to smaller gauge wires. We are looking into easier solutions, like a high amperage battery bus, but have not yet found a suitable product. For now, we will move forward with a custom harness.

## Software Architecture

To rapidly test our control algorithm, we created an analytical simulator which simulates the system dynamics given an external torque, moment arm, and actuator thrust. The advantage of the analytical simulator is that it runs simulations very quickly, and does not require a 3D model of the system. However, the analytical simulator assumes ideal actuator dynamics, and does not provide any visual representation of the system. Thus, we also simulate the system in WeBots to provide a more realistic physics and sensor simulation, as well as a visual representation of the system in action.

Since we are using both python and WeBots to run simulations, we will use the following software architecture that includes a simulation layer, interface layer, and algorithm layer.

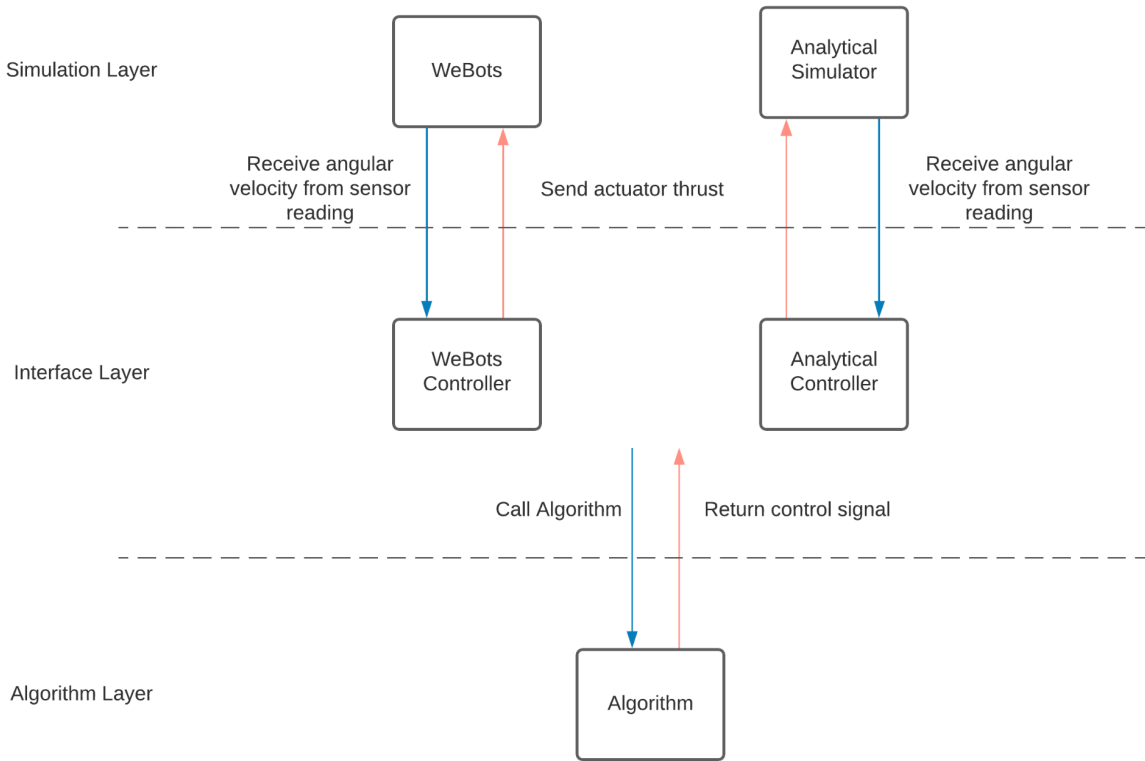


Figure: Software architecture block diagram

This architecture allows us to maintain a consistent control algorithm, and makes switching between simulations easy. Currently, our testing has mostly been done in the analytical simulation. However, as the mechanical model reaches completion, our focus will shift towards WeBots.

## Algorithm

Our goal is to drive the stretcher's angular velocity to zero, which requires us to reject any wind disturbance. The PID controller is the best candidate to solve the problem. Our job is to define appropriate proportional gain  $k_p$ , integral gain  $k_i$  and derivative gain  $k_d$ <sup>42</sup> such that our requirements are met.

Pseudo-code for one Arduino IDE:

*While IMU is available*

    Requesting data from IMU

    Call PID controller with IMU data as parameter

    Compute output from PID controller to get PWM values

    Send PWM values to slave arduino

*Command ducted fans with PWM values*

---

<sup>42</sup><https://web.archive.org/web/20150421081758/http://saba.kntu.ac.ir/eecd/pcl/download/PIDtutorial.pdf>

Pseudo-code for other Arduino IDE:

*While there is available info to receive*

    Command ducted fans with PWM values

Libraries that is needed for this algorithm are Servo<sup>43</sup> and Adafruit LSM6DS<sup>44</sup>. We would have to install Adafruit LSM6DS since it is not a default library.

Taking advantage of the Control System Toolbox in Matlab, we used the PID auto tuner to tune our controller with the average rotational inertia ( $26 \text{ kg.m}^2$ ). The table below contains controller gains, performance and robustness. The performance is superior to the baseline PI controller that Matlab automatically designs for the defined plant. Especially, with 6.92% overshoot, we might be able to avoid the case of angular velocity crossing over the safety threshold (2.1 rad/s).

Controller Parameters		
	Tuned	Baseline
Kp	82.2192	25.5118
Ki	26.5457	5.0149
Kd	2.6546	n/a
Tf	n/a	n/a
.....		

Performance and Robustness		
	Tuned	Baseline
Rise time	0.604 seconds	1.57 seconds
Settling time	5.84 seconds	12.6 seconds
Overshoot	6.92 %	11.6 %
Peak	1.07	1.12
Gain margin	-Inf dB @ 0 rad/s	-Inf dB @ 0 rad/s
Phase margin	90 deg @ 3.16 rad/s	78.9 deg @ 1 rad/s
Closed-loop stability	Stable	Stable

After figuring out the initial PID parameters, we tested this controller with different rotational inertia with step disturbance in the range of 12Nm-20Nm, which is the average range for external torque shown in the Guardian News video<sup>45</sup>. The figure below shows the simulink model that we used to test these cases.

<sup>43</sup> <https://www.arduino.cc/reference/en/libraries/servo/>

<sup>44</sup> <https://learn.adafruit.com/lsm6dsox-and-lsm330dhc-6-dof-imu/arduino>

<sup>45</sup> <https://www.youtube.com/watch?v=yhKZCy41g5w>

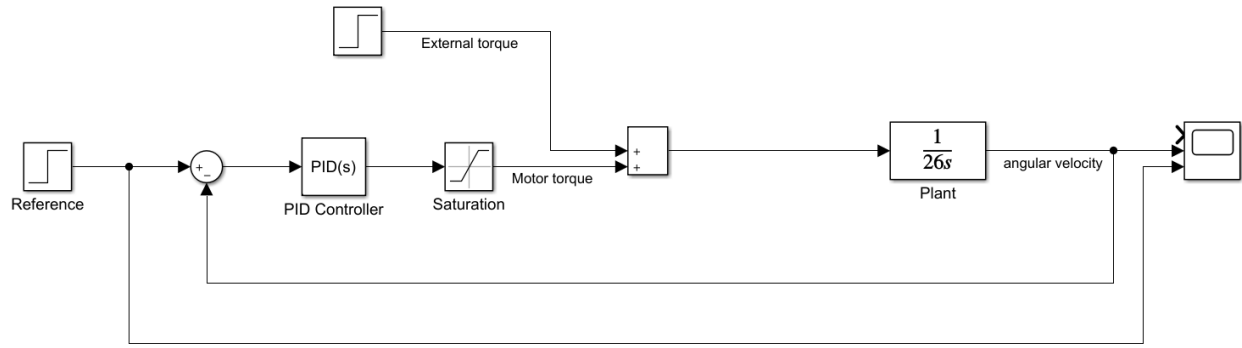


Figure: Simulink Model for Closed-Feedback Loop

Here is the detailed-level block diagram for the PID controller that we used for the helicopter payload self stabilizer system. The filter coefficient was set to be 100.

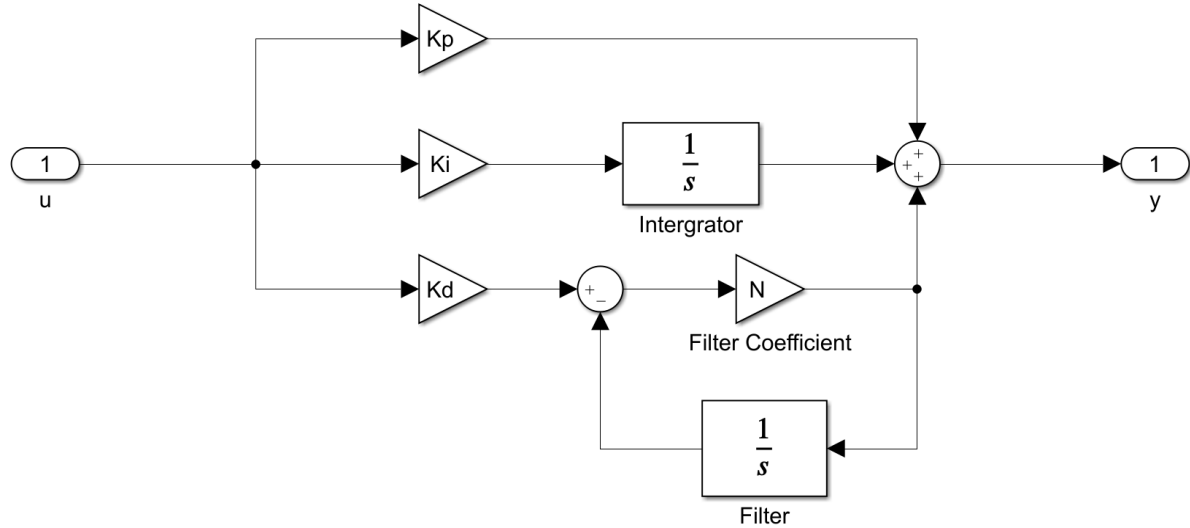


Figure: PID Controller Model

$$\frac{Y(s)}{U(s)} = K_p + K_i \frac{1}{s} + K_d \frac{N}{1+N\frac{1}{s}}$$

To evaluate the closed loop stability of our algorithm, we performed a frequency response analysis. Plotting the frequency response of our loop transfer function (below) yields the following results.

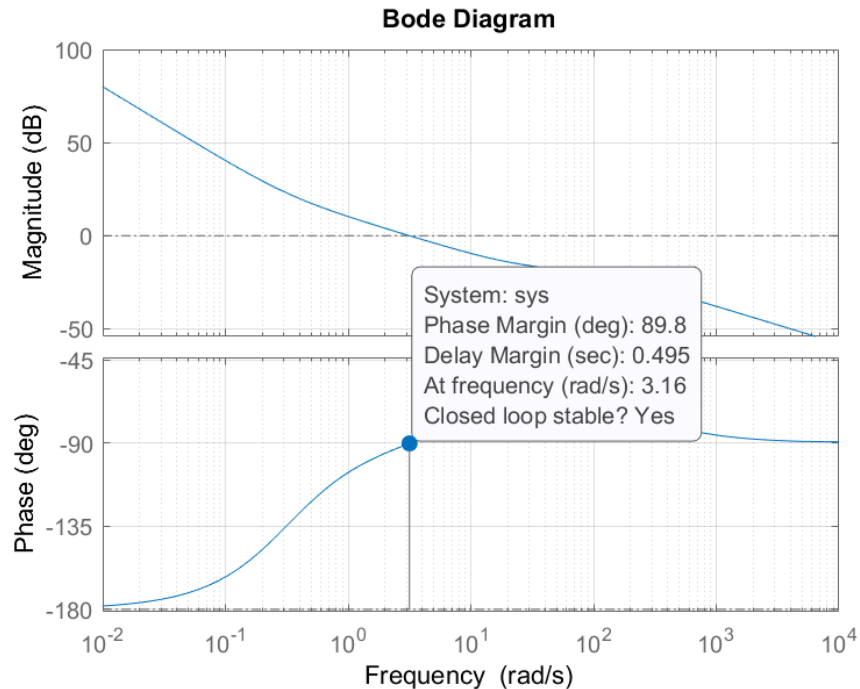


Figure: Bode plot of loop transfer function (above plot)

$$332 s^2 + 8226 s + 2600$$

Loop Transfer Function:  $C(s)P(s) = \frac{332 s^2 + 8226 s + 2600}{26 s^3 + 2600 s^2}$

We have designed our controller to have large gain at low frequencies where we expect to see most of the disturbances. At our crossover frequency of 3.16 (rad/sec), we have a comfortable phase margin of about 90°. This results in a delay margin of about 0.5 seconds.

During testing of our algorithm, we noticed that the system would react to sensor noise and jitter as it made its larger corrections. This jittering greatly increased the jerk experienced by the patient. To reduce jerk from tiny noise induced adjustments, we implemented a lowpass filter on the last 21 sensor readings. This adds a 10ms delay, but greatly reduces jerk. After some experimentation, we settled on a windowed sinc FIR filter with a 100 Hz cutoff frequency. As expected, the filter reduced the small controller adjustments, reducing jerk greatly. In the following example, we compare the results for the actuated stretcher without a low pass filter and with a low pass filter, subject to an arbitrary disturbance.

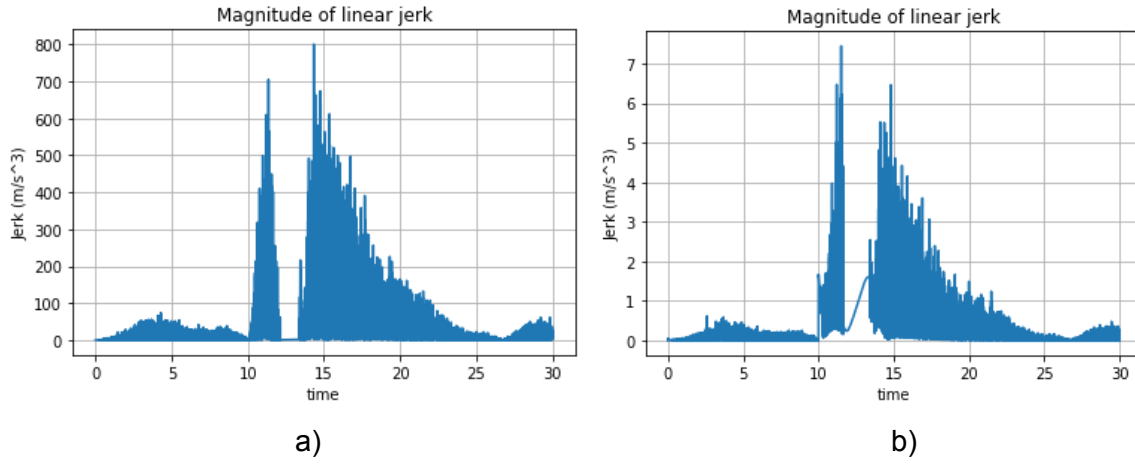


Figure: a) Jerk before lowpass b) Jerk after lowpass

Although the filter adds 10ms of delay, it reduces the jerk greatly. We expect that a real life stretcher is not completely rigid, and that the propellers cannot instantaneously produce tiny adjustments. Thus, the actual jerk experienced in real life is likely lower than in our simulations. Regardless, the lowpass filter is a worthwhile tradeoff.

# Analysis (All)

We will analyze the effectiveness of our system by evaluating the control algorithm performance in both simulation types, as well as the mechanical robustness. In order to test our control algorithm, we must test it on different wind disturbance scenarios and different payloads.

## **Formulation of Test Scenarios**

To make sure our control algorithm is robust, we are testing it thoroughly in many different conditions. The unknowns we can test it on include the wind disturbance, differences in stretchers (payload), and differences in body position within the stretcher.

## Wind disturbance modeling

In order to build a library of disturbance models, we created a wind disturbance toolbox. This toolbox includes a set of basis disturbances that can be added quickly into the overall disturbance model. So far, we have gusts, sinusoids, and step disturbances.

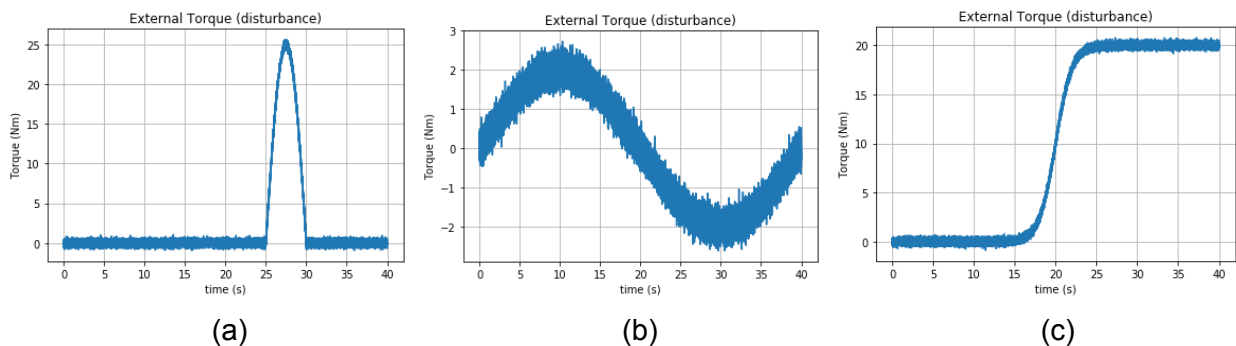


Figure: a) 25Nm gust, b) Low frequency sinusoid, c) 20Nm step

By combining these basic disturbances, we can come up with many unique test scenarios. As defined in our system dynamics, the maximum external torque we expect to see is 78Nm. Below are examples of disturbances that fall within these bounds.

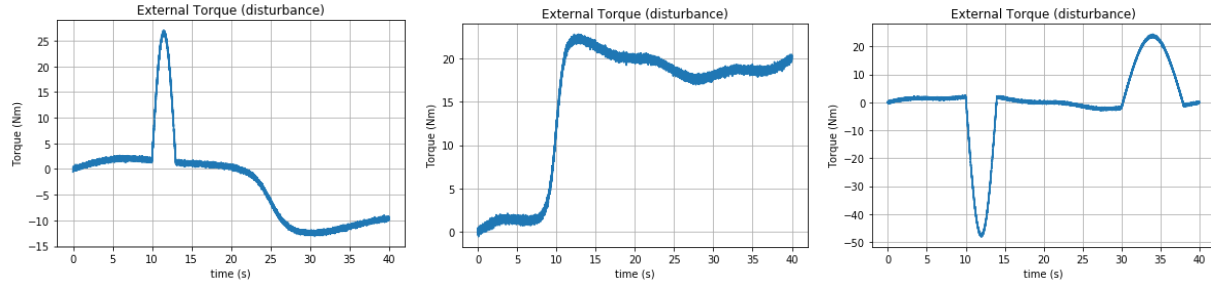


Figure: Various disturbance models created with toolbox

## Numerical Simulation

Since the rotational inertia of the payload (stretcher and human) is unknown to the controller, we have estimated a few different rotational inertia due to the information of rotational inertia that we have obtained in the System Dynamics session.

$$\text{Rotational Inertia of human: } 115 \text{ lb.in.sec}^2 = 13 \text{ kg.m}^2$$

$$\text{Standard deviation: } 19.3 \text{ lb in sec}^2$$

$$\text{Minimum: } 115 - 19.3*3 = 57.1 \text{ lb.in.sec}^2 = 6.5 \text{ kg.m}^2$$

$$\text{Maximum: } 115 + 19.3*3 = 172.9 \text{ lb.in.sec}^2 = 19.5 \text{ kg.m}^2$$

$$\text{Rotational inertia of stretcher: } 115 \text{ lb.in.sec}^2 = 13 \text{ kg.m}^2$$

### Total Rotational inertia:

- Average: 26 kg.m<sup>2</sup>
- Minimum: 19 kg.m<sup>2</sup>
- Maximum: 32 kg.m<sup>2</sup>
- Empty stretcher: 13 kg.m<sup>2</sup>

Using the initial controller to test with different rotational inertia, we obtained the below results.

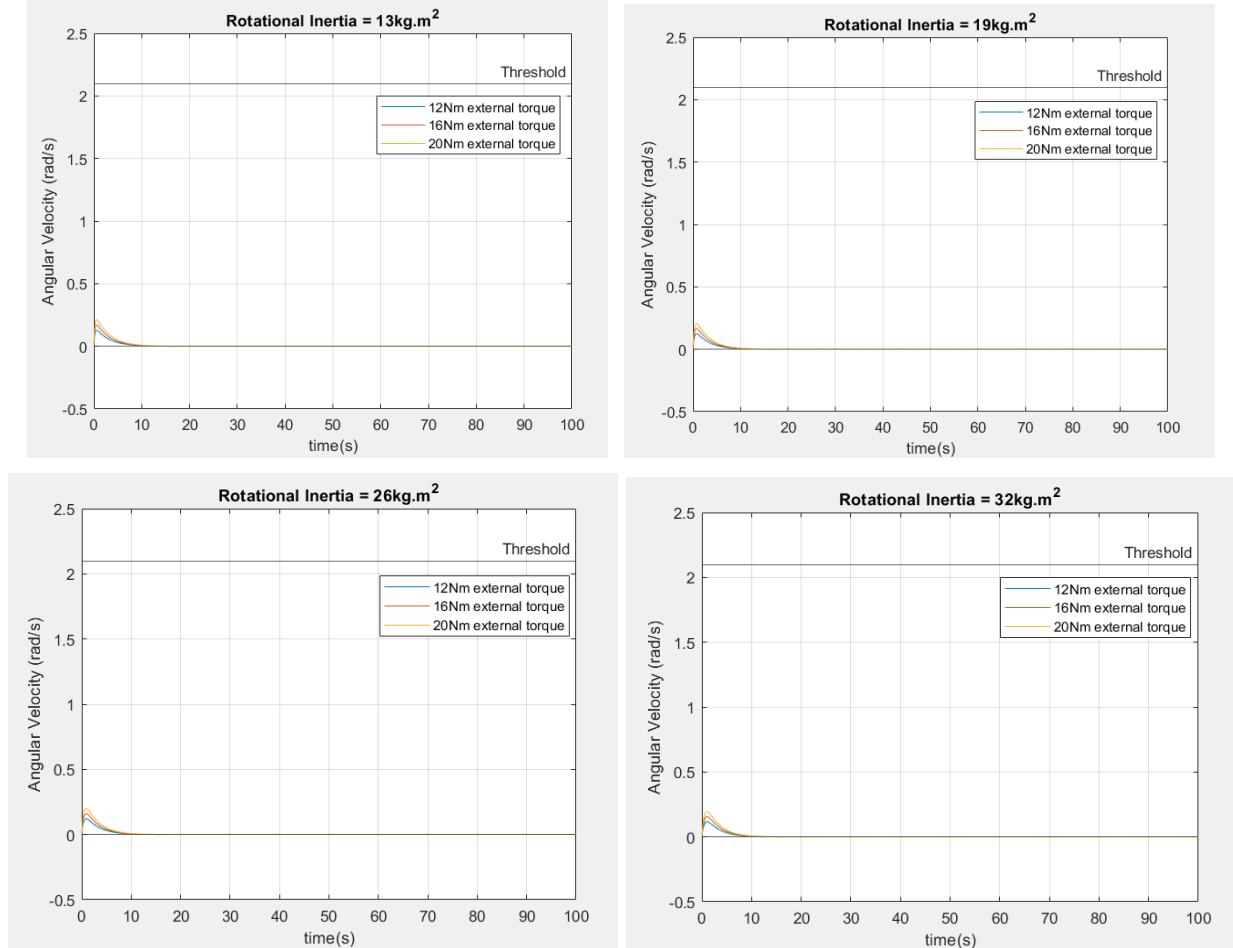


Figure: Test Runs with Rotational Inertia Variance and External Torque Variance

According to the results shown in the above figure, the angular velocity never crosses the threshold line ( $2.1 \text{ rad/s}$ ) which we define to be the upper limit that the person can handle during hoisting operation. Therefore, we decided to keep the parameters for the PID controller and we would test the controller with more complicated disturbance in the Physics base simulator to evaluate and optimize the controller by following the safety measure that we defined.

### Preliminary Results

To make sure the control algorithm is working as expected, we have run several simulations using the average rotational inertia of  $26 \text{ kg m}^2$ .

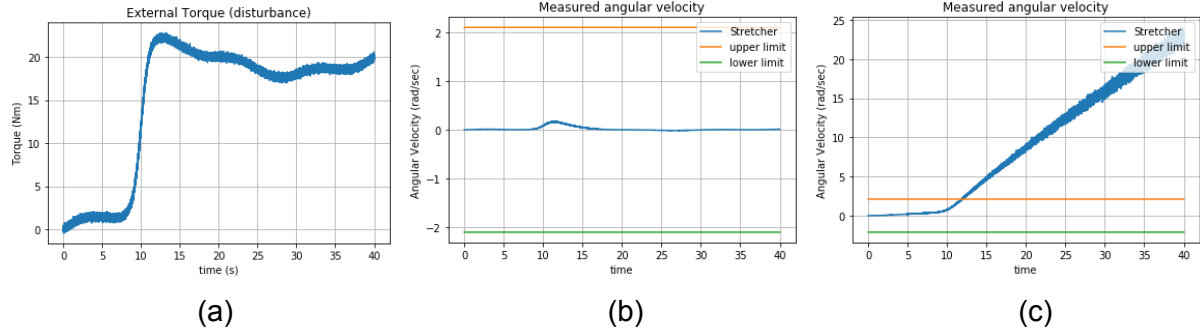


Figure: a) Disturbance, b) Compensated c) Uncompensated

In the above figure, the disturbance is less than our maximum actuator output, and the stretcher's angular velocity stays well within the limits. In this case, the uncompensated stretcher goes very far above the safety limits. In the next scenario, we tested our algorithm on a three second gust of 80Nm.

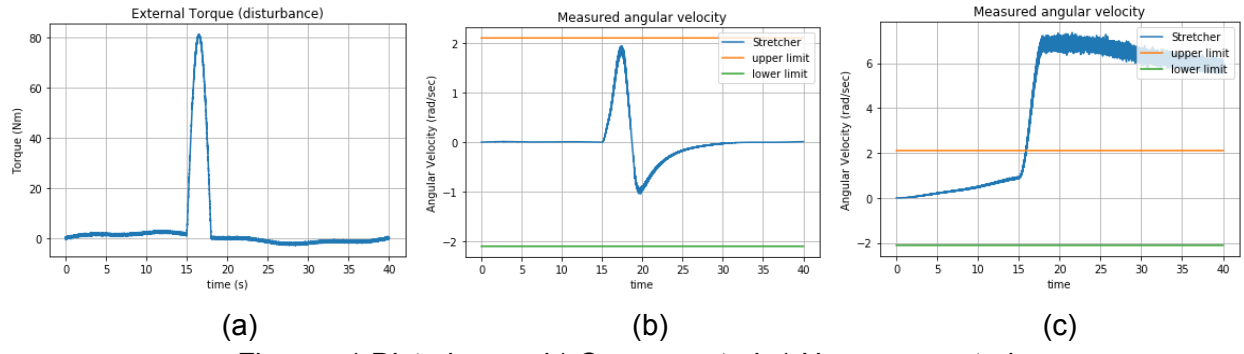


Figure: a) Disturbance, b) Compensated c) Uncompensated

Again, the compensated stretcher manages to stay within the bounds even when the external torque exceeds the maximum actuator output. However, a longer duration gust of this magnitude would force the stretcher into the unsafe zone. Next, we test the control algorithm on a sinusoidal disturbance.

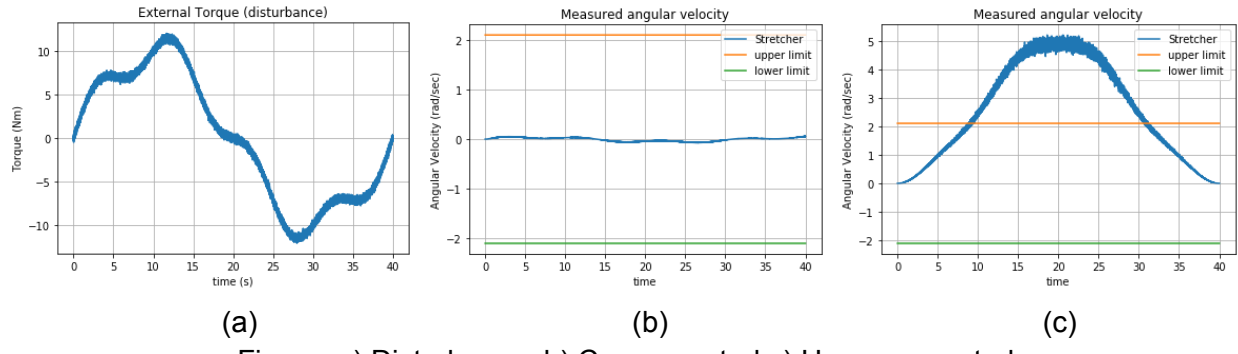


Figure: a) Disturbance, b) Compensated c) Uncompensated

The compensated stretcher has some difficulty rejecting the sinusoid, but does much better than the uncompensated stretcher. We will continue to test and improve our control algorithm as we shift our focus to the mechanical simulation

## Mechanical Simulation

### Webots

In order to validate our system design and numerical simulation, we also modeled our stretcher-body-device system in Webots. Webots is an open-source physics and robot simulator from Cyberbotics LTD that allows us to accurately model the kinematics of our system. Through this software, we can model the bodies, sensors, and controllers necessary to validate and expand on the results of the numerical simulation.

To model our components in the Webots environment, we imported the solidworks models of our stretcher in VRML format as 3D objects. Due to the complex nature of our stretcher and device models used in the design process, we created simplified models with approximate geometries to use in Webots. By specifying the components' mass and inertia values to be the same as determined by our final solidworks design, the models are accurate for our simulation purposes.

In order for our Webots simulation to match the kinematic numerical simulation, we made use of various webots structures and simulation parameters to apply our design and test restrictions to the environment. The Connector structure locks the location and orientation of two models, which we used to "strap in" our body model to the stretcher as well as attach our stabilization devices to either end in the correct location. Similarly, a HingeJoint modeled at the base of our stretcher restricts the movement to a one degree-of-freedom spin. The external inputs on the system are modeled through the Supervisor node of our robot as a torque on the body, similar to our numerical solution. Our rotors are modeled using the Propellor node, which allows our robot to input a specific fan speed that results in a corresponding thrust force. The IMU in our device is modeled as a Gyro and Accelerometer to track angular velocity, acceleration, and jerk, and placed in its corresponding location in the chassis. The controller mimics that of the numerical solution and our system PID algorithm, receiving angular velocity inputs from the chassis and actuating the fans accordingly to stabilize the system.

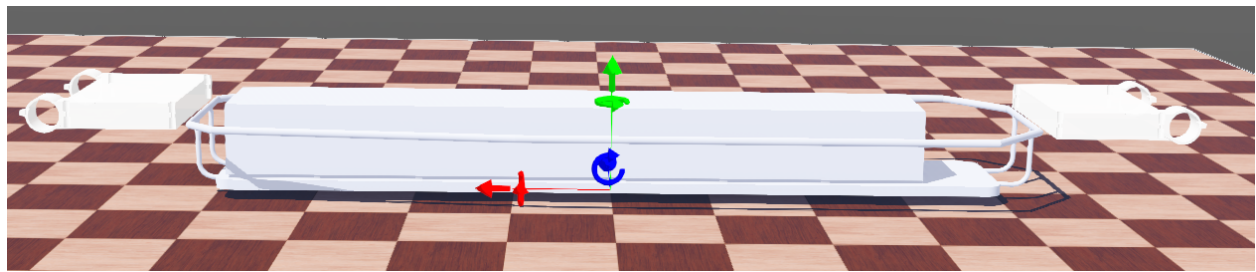


Figure: Stretcher, Body, and Stabilization Device Modeled in Webots

We recreated different wind disturbances such as gusts, step, and sinusoidal by setting torque data on the combined robot system from the Webots Supervisor node. Payload variance will be achieved by swapping the body model in the stretcher with that of our anthropometric

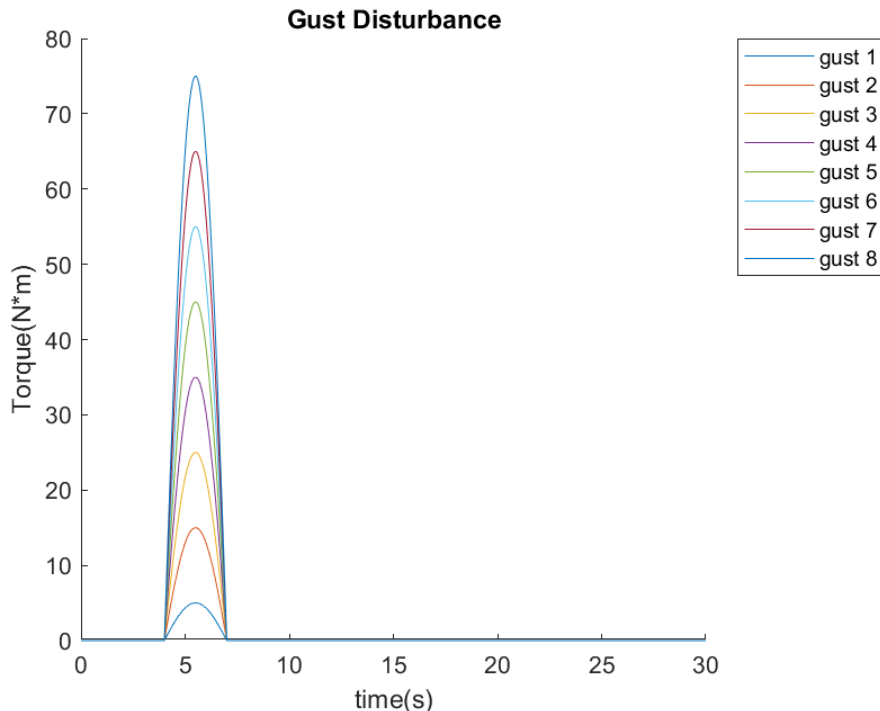
data. We can also vary the payload positioning in Webots by initializing the location of the body and its connector at different locations in the stretcher. Together, these give us a variety of test scenarios to validate our system design in Webots.

### Disturbances:

Using the external torque disturbance toolbox we developed, we formulated 8 gust disturbances, 16 sinusoid disturbances, 15 step disturbances, and 7 miscellaneous disturbances. Each of these disturbances last for 30 seconds, with exception to the last two miscellaneous disturbances which last for 60 seconds. We exported these disturbances into webots to test with various cases, such as payload variance, payload position variance, and device position variance. Below are charts and graphs describing the nature of the disturbances generated:

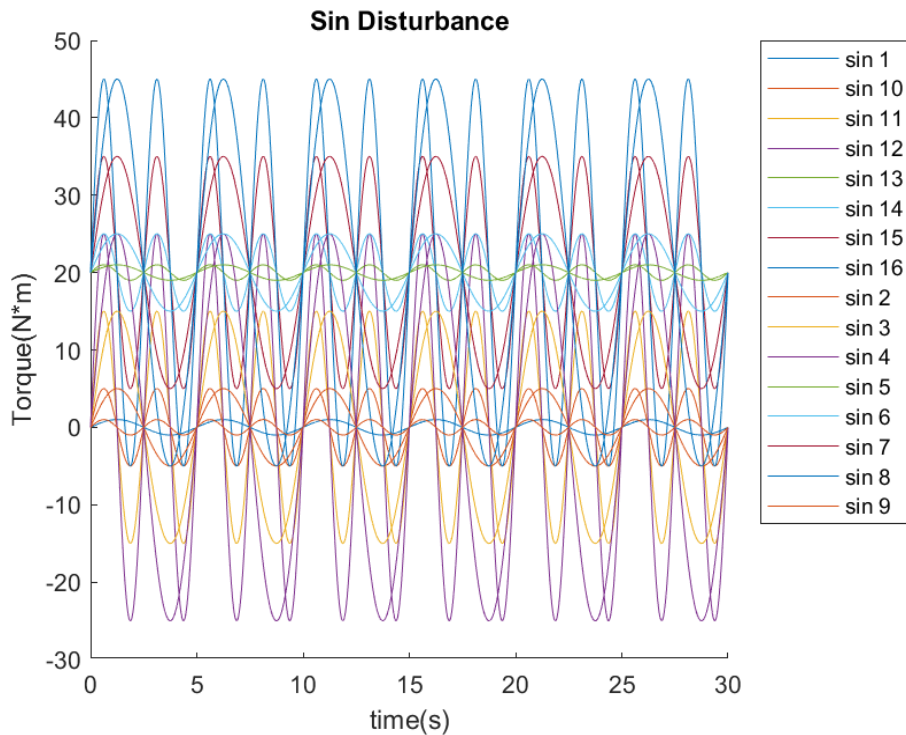
The gust disturbances are high external torque spikes that last for a short period of time. They are meant to simulate the effect of a sudden strong gust of wind. The gusts disturbances generated have an amplitude ranging from 5 to 75 newton meters and have a duration of around 3 seconds

Disturbance	Amplitude (N*m)	Duration (Seconds)
Gust 1	5	3
Gust 2	15	3
Gust 3	25	3
Gust 4	35	3
Gust 5	45	3
Gust 6	55	3
Gust 7	65	3
Gust 8	75	3



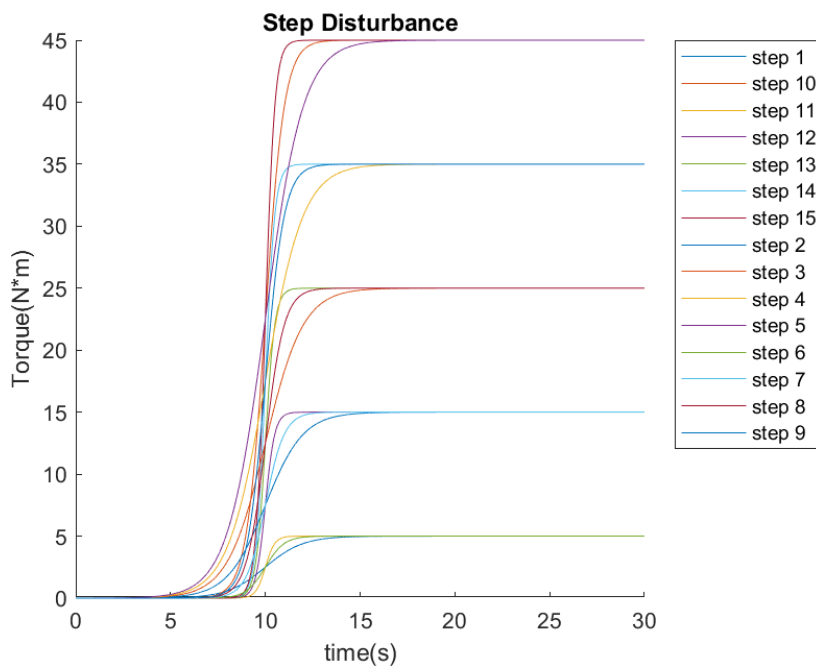
The sinusoid disturbances represent a wind of varying speed or direction. The sinusoids generated have amplitude ranging from 1 Newton Meter to 25 Newton Meter. The sinusoids either have a period of 5 seconds or 2.5 seconds. The sinusoids also have a bias that can be up to 20 Newton Meters. These features allow us to generate sinusoidal torque disturbances in the range of -50 Newton Meters to +50 Newton Meters

Disturbance	Amplitude (N*m)	Period(Seconds)	Bias(N*m)
Sine 1	1	5	0
Sine 2	5	5	0
Sine 3	15	5	0
Sine 4	25	5	0
Sine 5	1	5	20
Sine 6	5	5	20
Sine 7	15	5	20
Sine 8	25	5	20
Sine 9	1	2.5	0
Sine 10	5	2.5	0
Sine 11	15	2.5	0
Sine 12	25	2.5	0
Sine 13	1	2.5	20
Sine 14	5	2.5	20
Sine 15	15	2.5	20
Sine 16	25	2.5	20

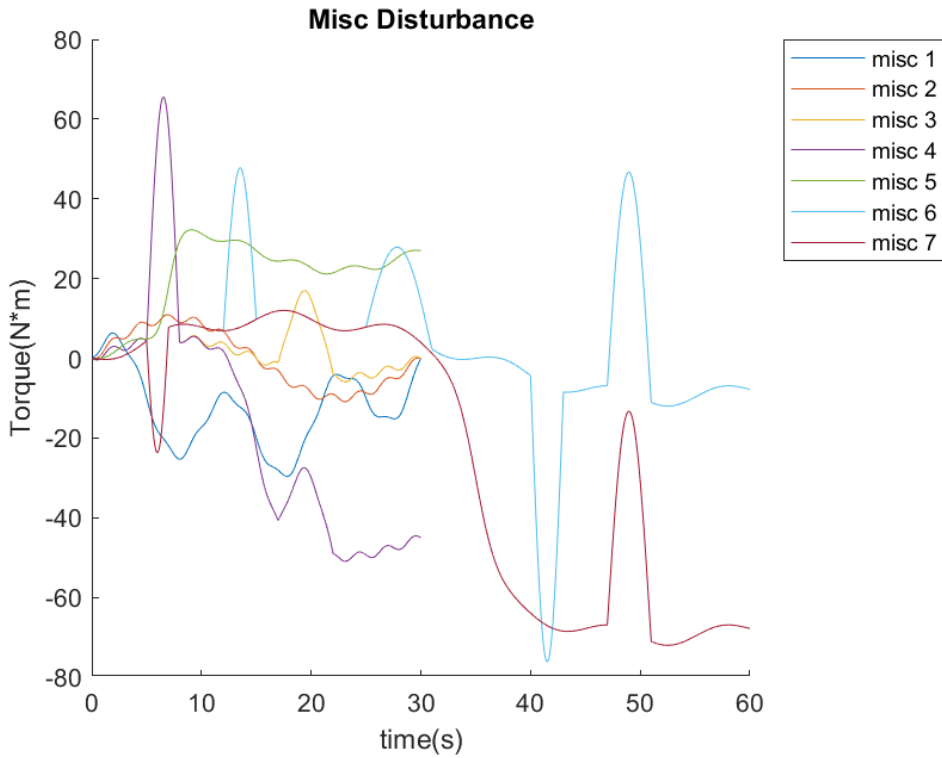


The step disturbance is meant to represent a worse case scenario, where all the wind generated by downwash blows on one side of the stretcher, yielding constant torque. The step torques range from amplitudes 5 Newton meters to 45 Newton meters, have a midpoint at 10 seconds, and have a varying slope parameter from 1 to 4

Disturbance	Max Value(N*m)	Midpoint(Seconds)	Slope
Step 1	5	10	1
Step 2	15	10	1
Step 3	25	10	1
Step 4	35	10	1
Step 5	45	10	1
Step 6	5	10	2
Step 7	15	10	2
Step 8	25	10	2
Step 9	35	10	2
Step 10	45	10	2
Step 11	5	10	4
Step 12	15	10	4
Step 13	25	10	4
Step 14	35	10	4
Step 15	45	10	4



The miscellaneous disturbances are a combination of step, gust, and sinusoid disturbances. The first 5 miscellaneous disturbances last 30 seconds. The last two miscellaneous disturbances last for 60 seconds.

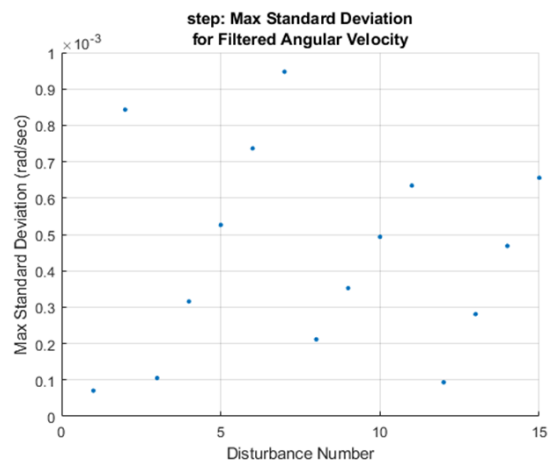
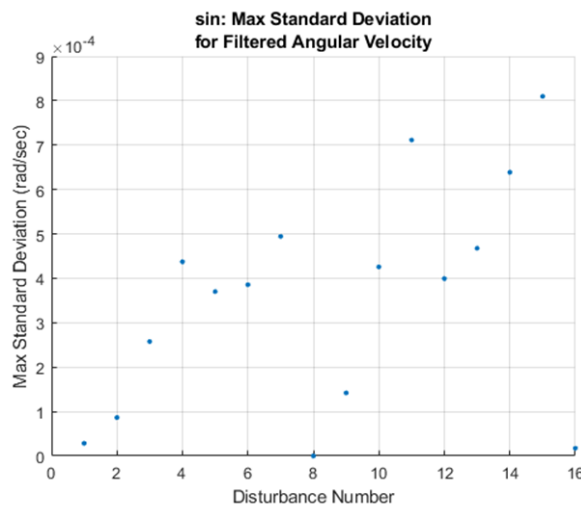
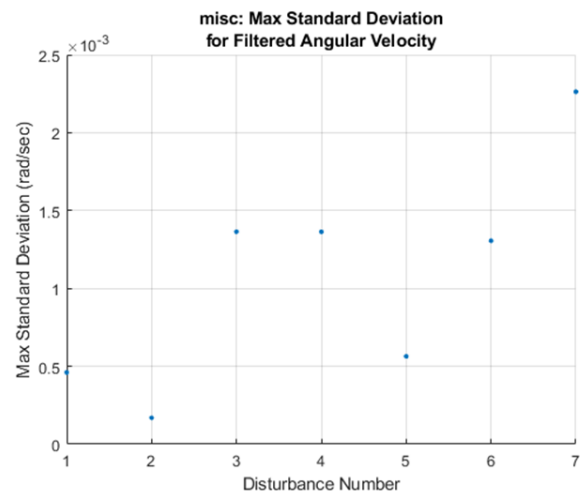
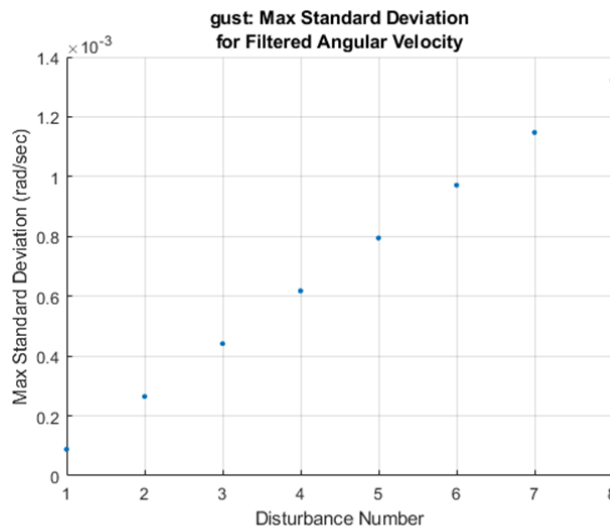


### Statistical Uncertainty Analysis

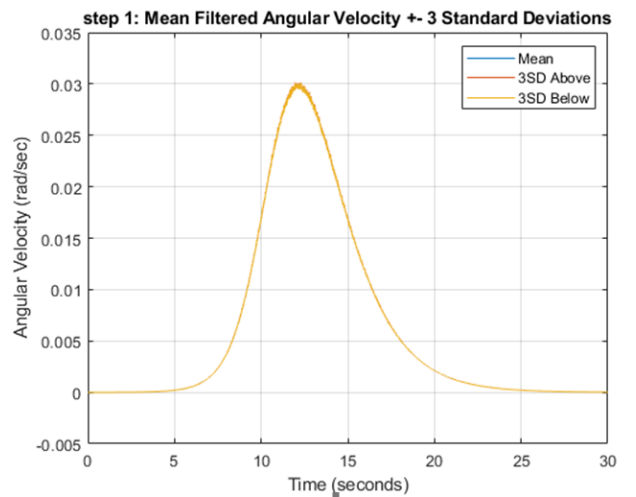
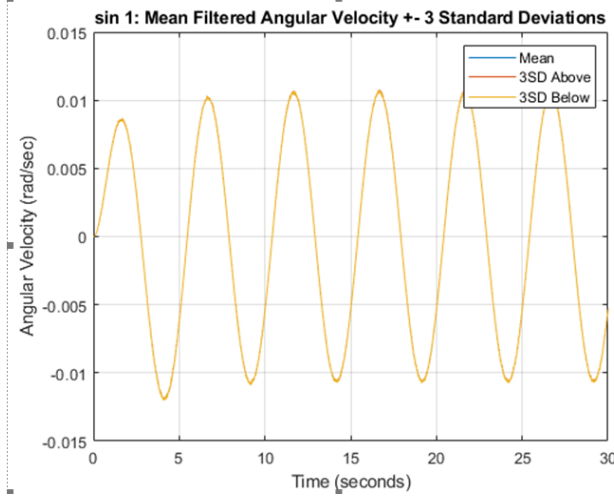
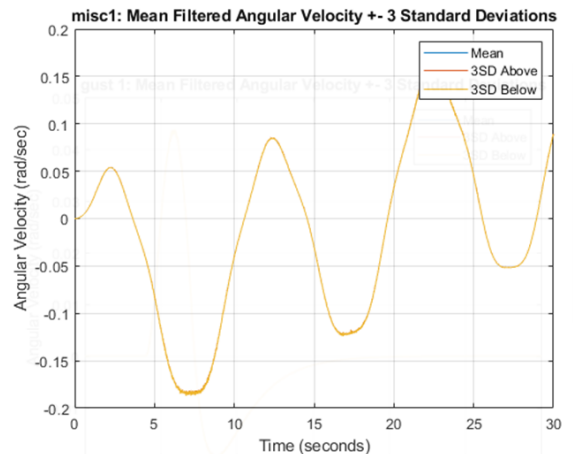
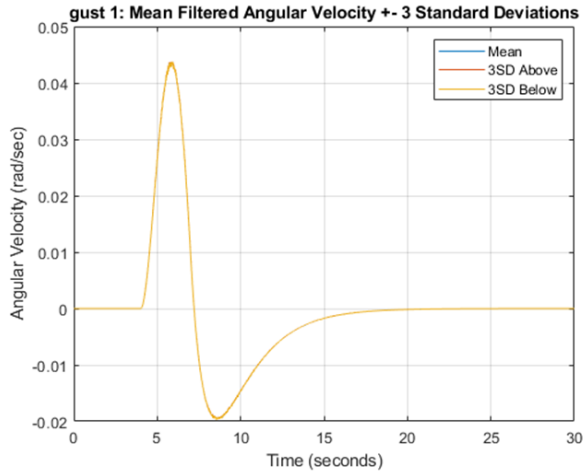
The system's sensors and actuators were modeled as realistically as possible in webots, with associated errors. Due to the robust nature of the PID controller as well as the low-pass filter on our gyro readings, We expected minimal variation in the stem and a stable result.

The only random process in our system is the IMU measurement of angular velocity, which has 2% noise on reading. This value is then filtered and passed into the PID controller. Therefore, the effect of randomness on the system can be examined by looking at the behavior of filtered angular velocity across the same input disturbance. To determine the behavior of filtered angular velocity, all sin, gust, step, and miscellaneous disturbances were run 3 times on the average body case with no payload position variance and no device position variance.

Below are graphs showing the maximum standard deviation of filtered angular velocity vs. disturbance for gust, sin, step, and misc disturbances:



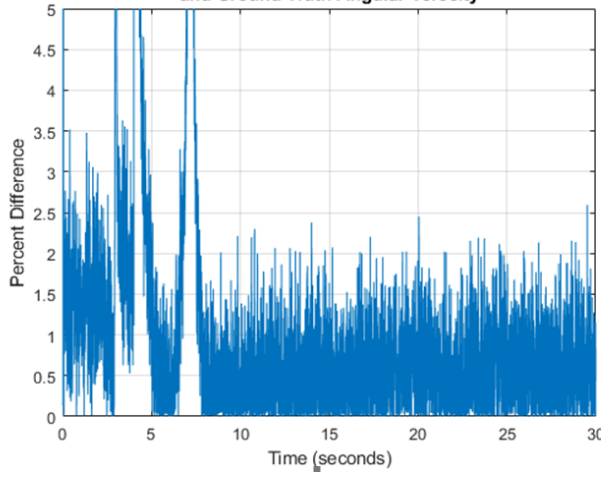
From these graphs, it is evident that the maximum standard deviation across each disturbance is extremely small, in the range of  $10^{-4}$  to  $10^{-3}$  rad/sec. These values are minuscule compared to the actual measured angular velocity. To demonstrate these points, below are graphs showing mean filtered angular velocity plus or minus 3 standard deviations vs. time for disturbances gust 1, misc 1, sine 1, and step 1.



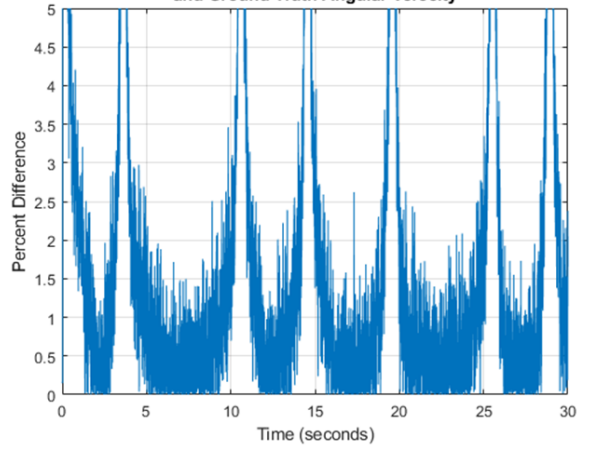
From these graphs, it appears that only the yellow line is showing because the mean, 3 standard deviation above, and 3 standard deviation below graphs are all extremely similar. This shows how little the noise from the IMU affects the filtered angular velocity readings. This justifies why the system is not affected greatly from random processes. We can run the same disturbance twice and obtain similarly identical results.

The graphs below show percent difference between mean of the filtered angular velocities and ground truth angular velocity for disturbances gust 1, misc 1, sin 1, and step 1

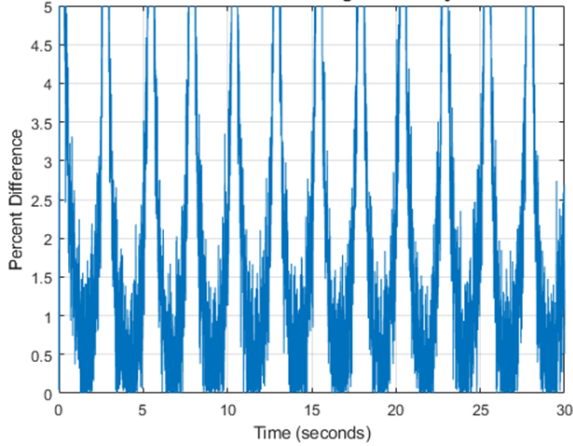
**gust 1: Percent Difference Between Mean of Filtered Angular Velocity and Ground Truth Angular Velocity**



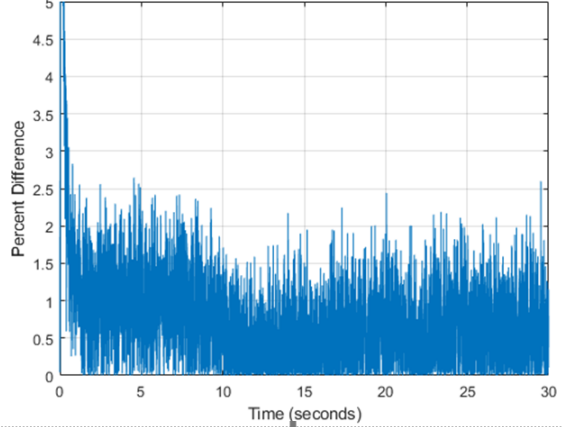
**misc1: Percent Difference Between Mean of Filtered Angular Velocity and Ground Truth Angular Velocity**



**sin 1: Percent Difference Between Mean of Filtered Angular Velocity and Ground Truth Angular Velocity**



**step 1: Percent Difference Between Mean of Filtered Angular Velocity and Ground Truth Angular Velocity**



In these graphs, there are some infinity spikes, however this only occurs when the ground truth angular velocity goes to zero. From the graphs, it is evident that the percent difference between the mean filtered angular velocity and ground truth angular velocity is between 0 to 2 percent. This makes sense as the IMU outputs 2% of noise on measured angular velocity. As seen in the later sections, this small deviation from ground truth angular velocity does not drastically affect the system in meeting safety requirements for all disturbances.

If more detail is necessary, please look at the Statistical\_Analysis file posted in the github repository linked in the appendix.

### Payload Variance

We varied the payload of our stretcher device by swapping out our modeled patient body with the 5 total body models as mentioned in the System Dynamics section. This represents a wide range for the possible payloads that our system can control. In Webots, we can simply replace the body model with a different one and change the mass and inertia properties accordingly.

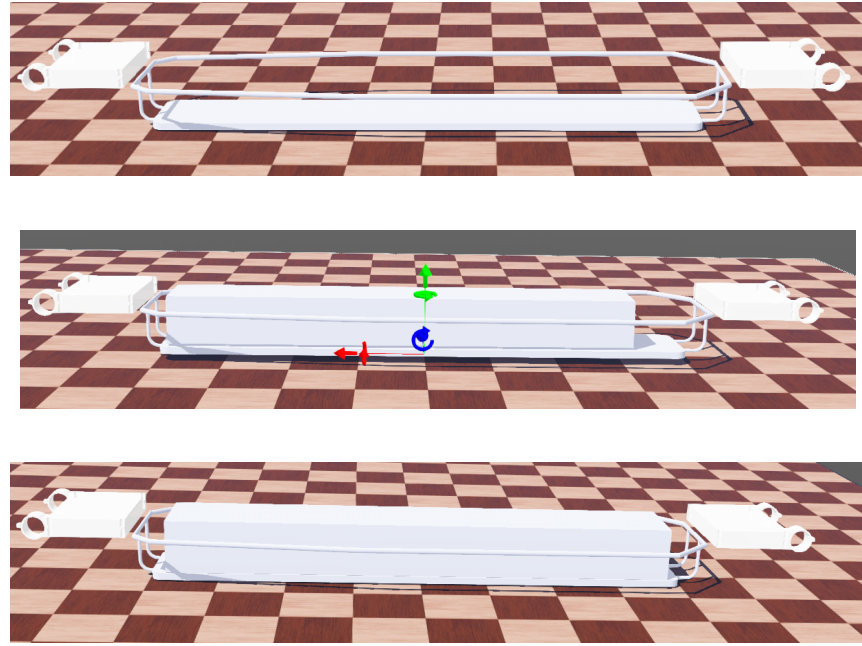
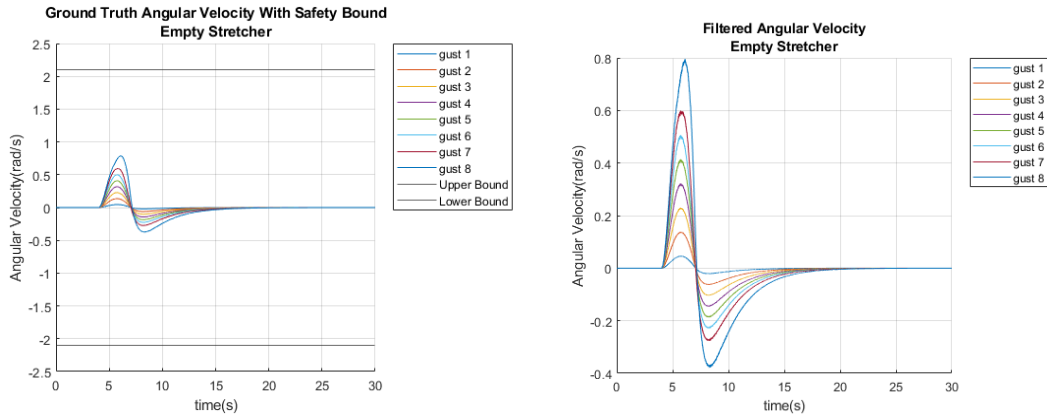
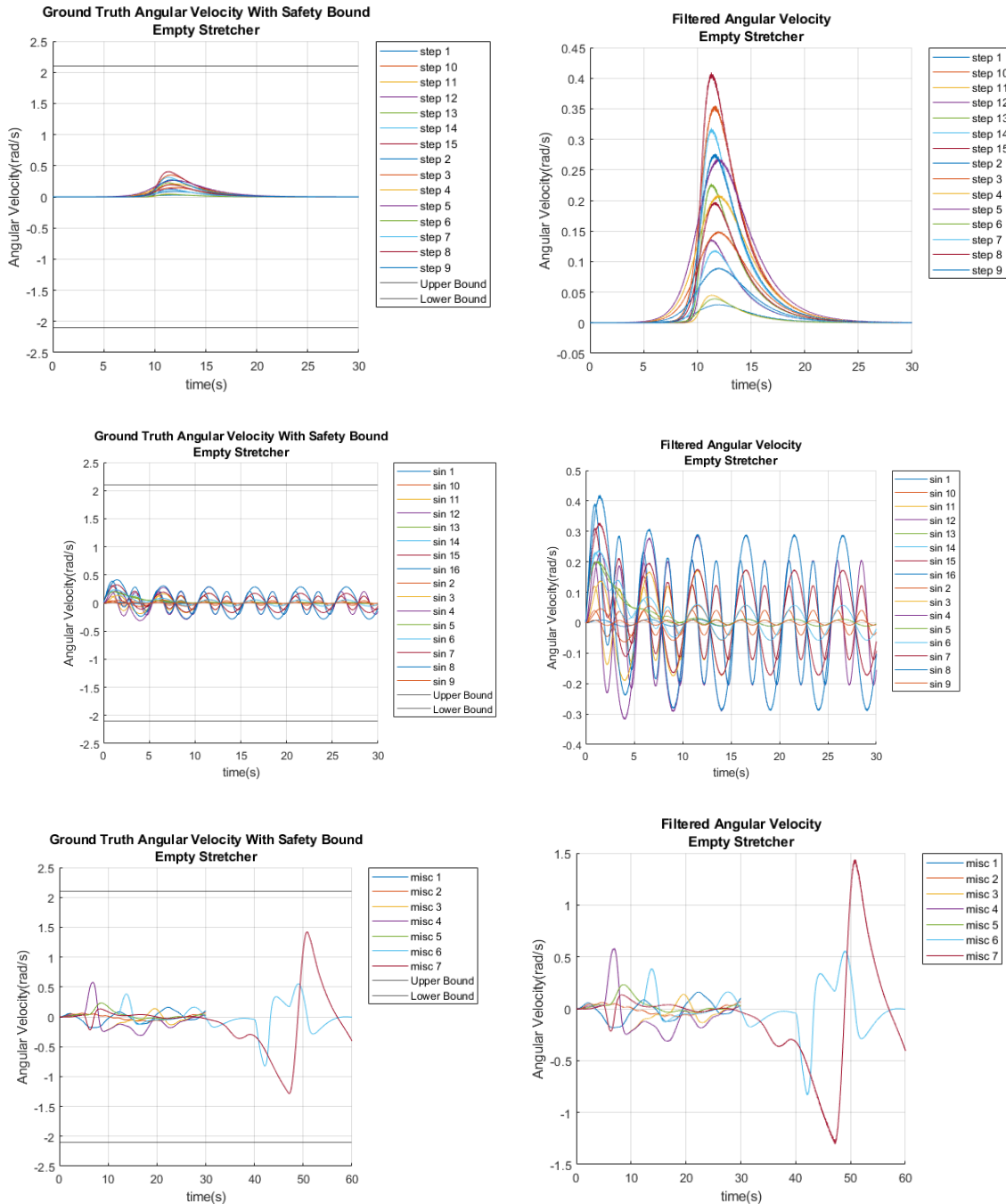


Figure: Stretcher systems with payloads of various sizes

We found that any added mass acted as an inertial damper for the system, as it would resist changes in momentum from the external wind disturbance. As a result, the case of maximal disturbance was that of an empty stretcher, which serves as our worst-case scenario. Below are our full data for the empty stretcher disturbance. This and all remaining data is available in our project Github folder linked in Appendix 3.

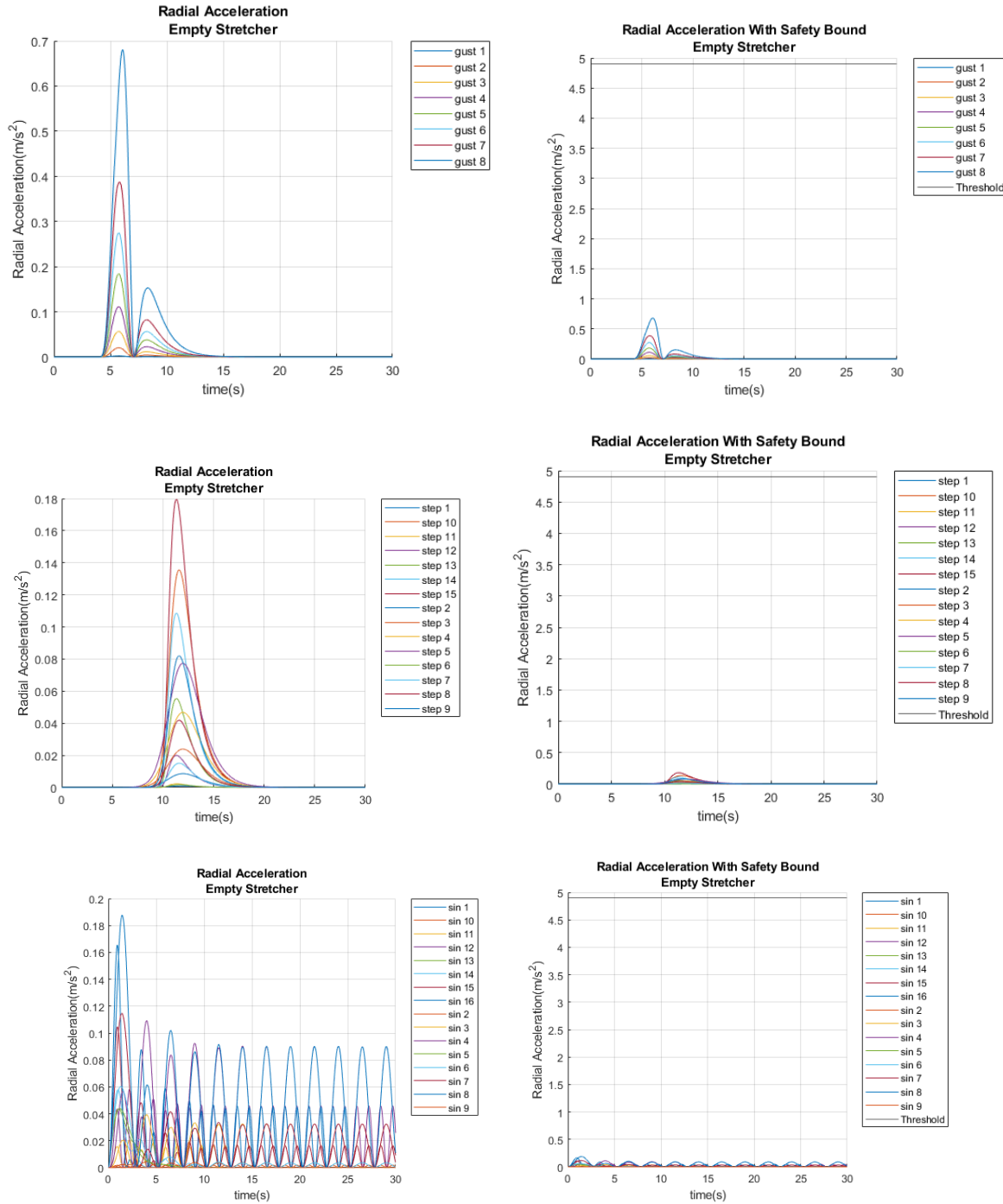
Below are the following graphs that show ground truth angular velocity and filtered angular velocity for gust, step, sin, and misc disturbances using empty stretcher:

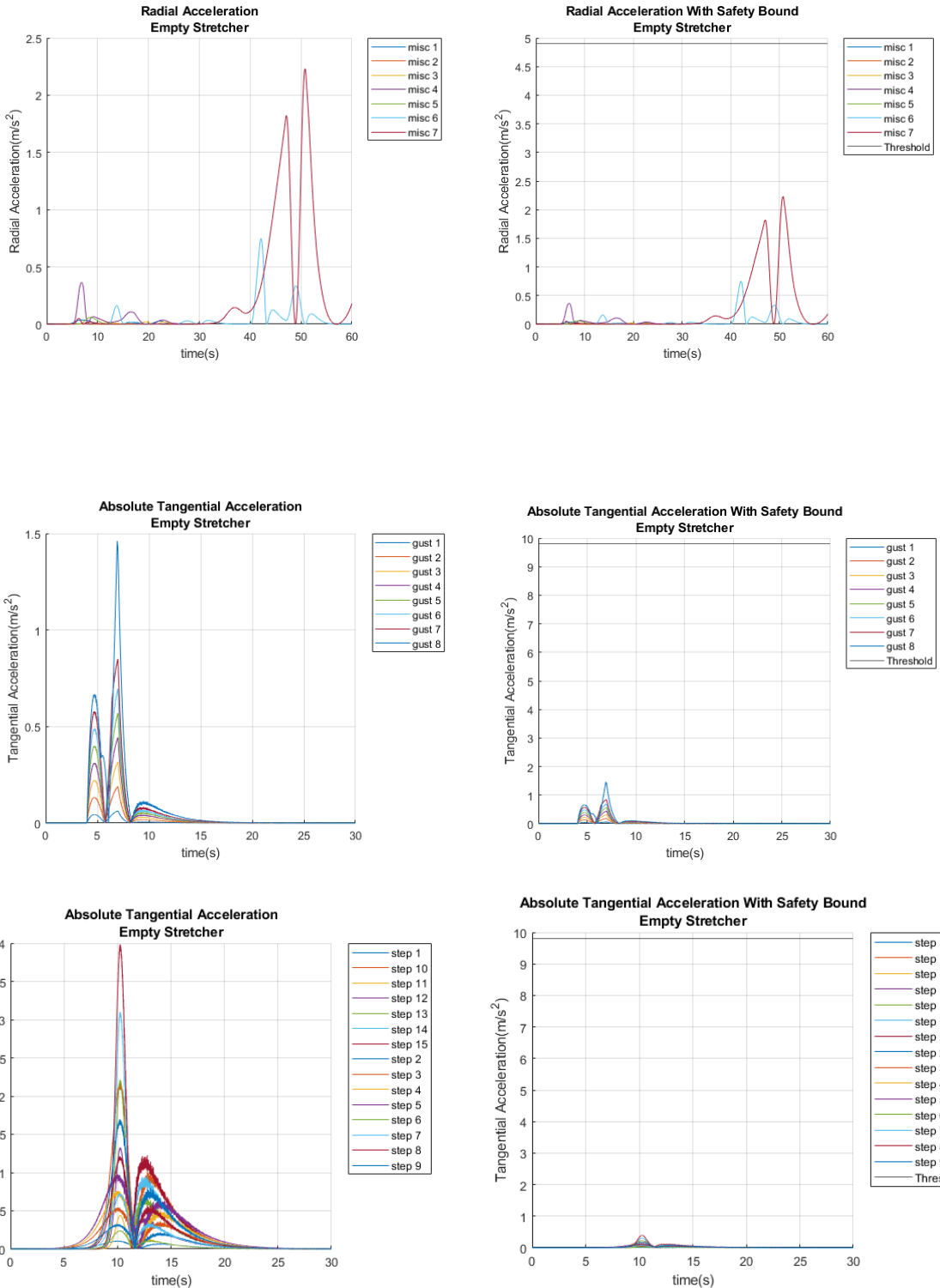


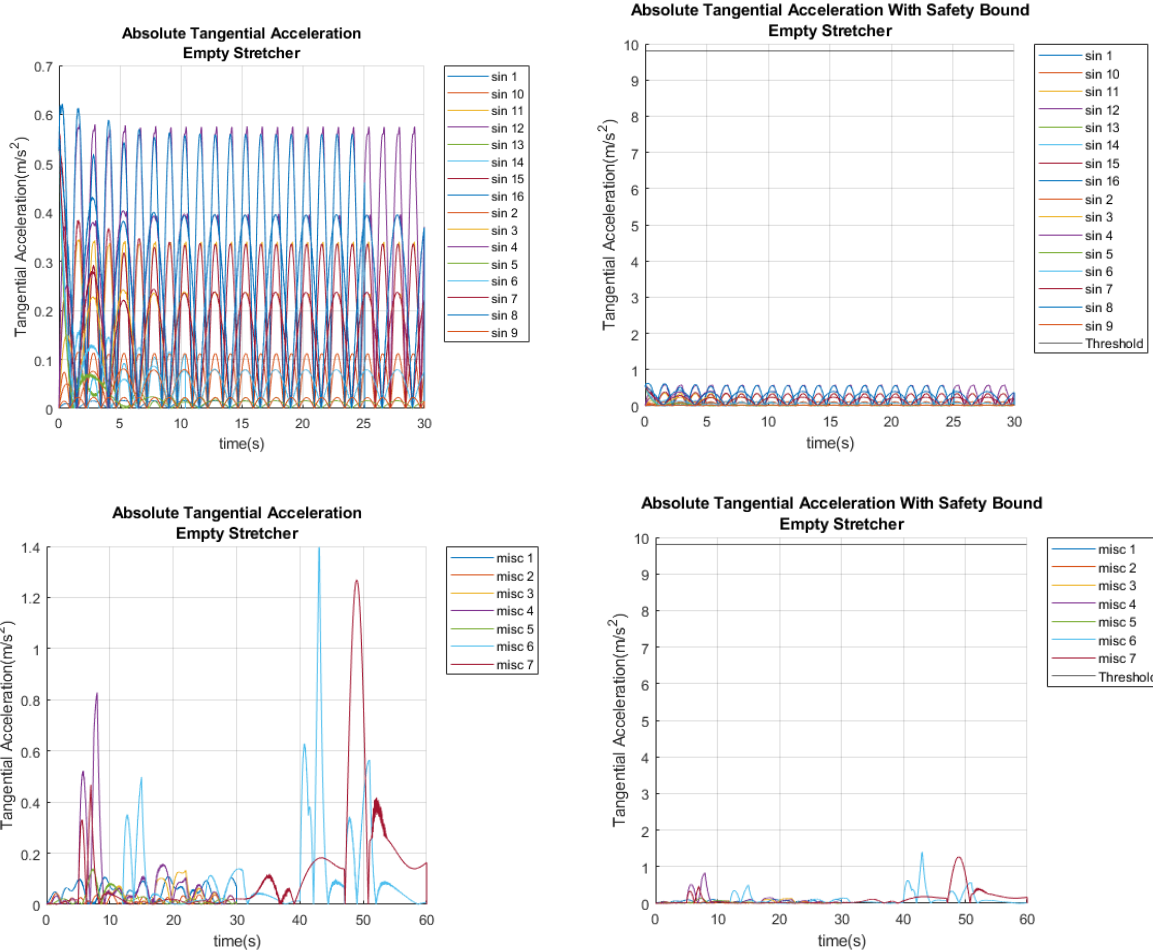


From these graphs, it is evident that the ground truth angular velocity does not cross the  $\pm 2.11$  radians/sec limit established in the safety measures. The filtered angular velocity is shown next to the ground truth angular velocity without safety bounds to show a clearer view and to demonstrate measured and filtered angular velocity value is close to the ground truth angular velocity values.

The graphs below show absolute radial acceleration and absolute tangential acceleration for gust, step, sin, and misc disturbances using the empty stretcher.

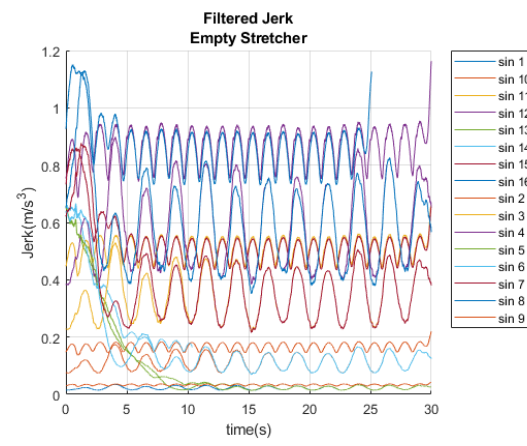
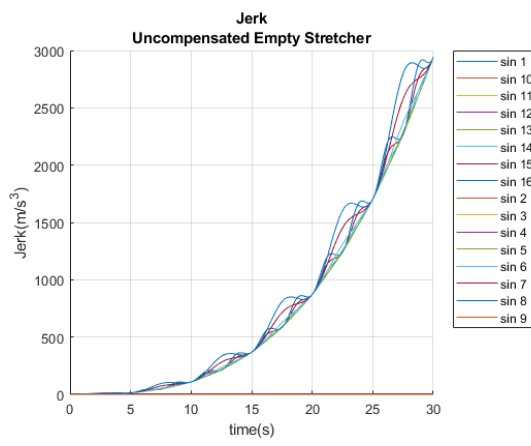
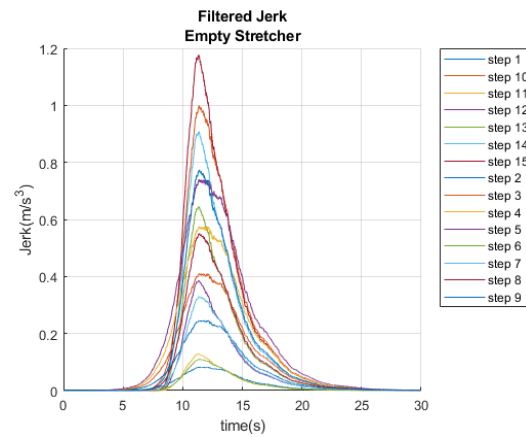
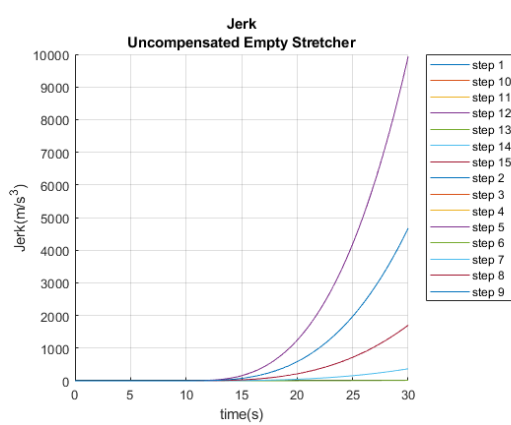
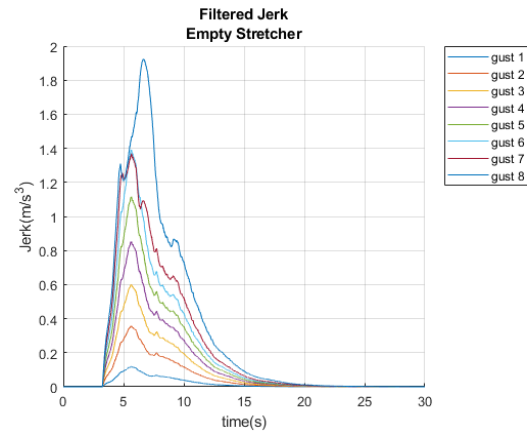
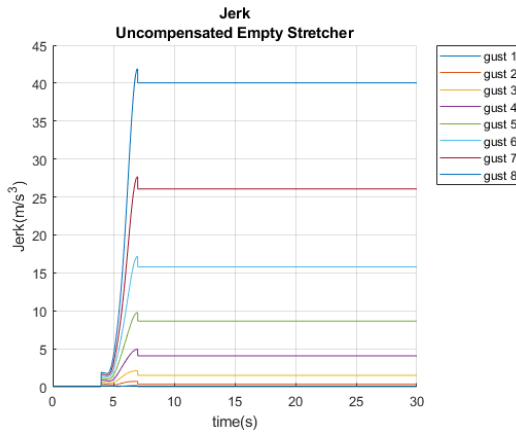


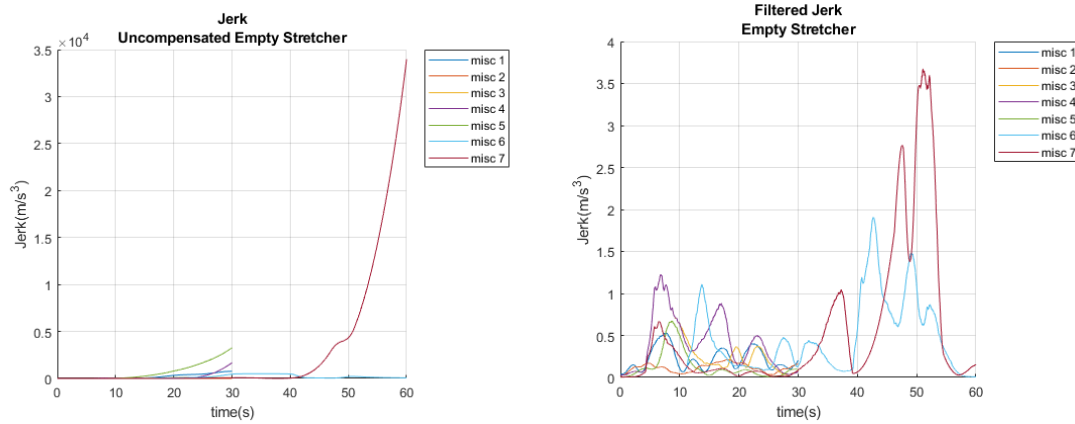




From the graphs above, it is evident that the empty stretcher stays within the safety bounds regarding absolute radial acceleration and absolute tangential acceleration for all disturbances. Radial acceleration graphs were shown without the safety bound of 0.5gs and Tangential acceleration graphs were shown without the safety bound of 1gs in order to give a better view of the acceleration response.

Below are graphs that display the filtered jerk for gust, step, sin, and misc disturbances using the empty stretcher in both the compensated and uncompensated case. Note that the filter used was a moving average filter over 1.2 seconds. This filter was used to make the jerk graphs readable and to simulate the damping found in the stretcher and the hoisting cable.





Despite jerk values reaching high values of around  $3.75 \text{ m/s}^3$  in the compensated case, the compensated jerk was magnitudes lower than the uncompensated jerk, which could go into the thousands or tens of thousands. Therefore, our system does a better job of ensuring comfort over the uncompensated case.

### Patient Position Variance

We also varied the position of the payload inside the stretcher to account for non-perfect alignments of the body and stretcher centers of mass. Through the Webots environment, we prepared two cases in varying the location of the body inside the stretcher: One such that the head reached the top of the stretcher (Head), and one such that the feet reached the bottom of the stretcher(Tail). In this situation, we tested our device and controller's ability to stabilize an asymmetric system. Below are images of these two cases.

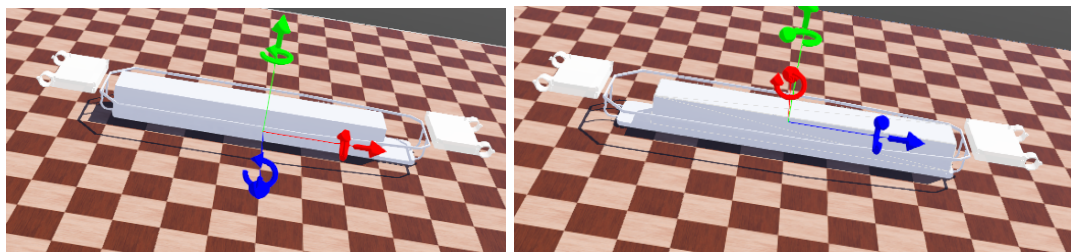
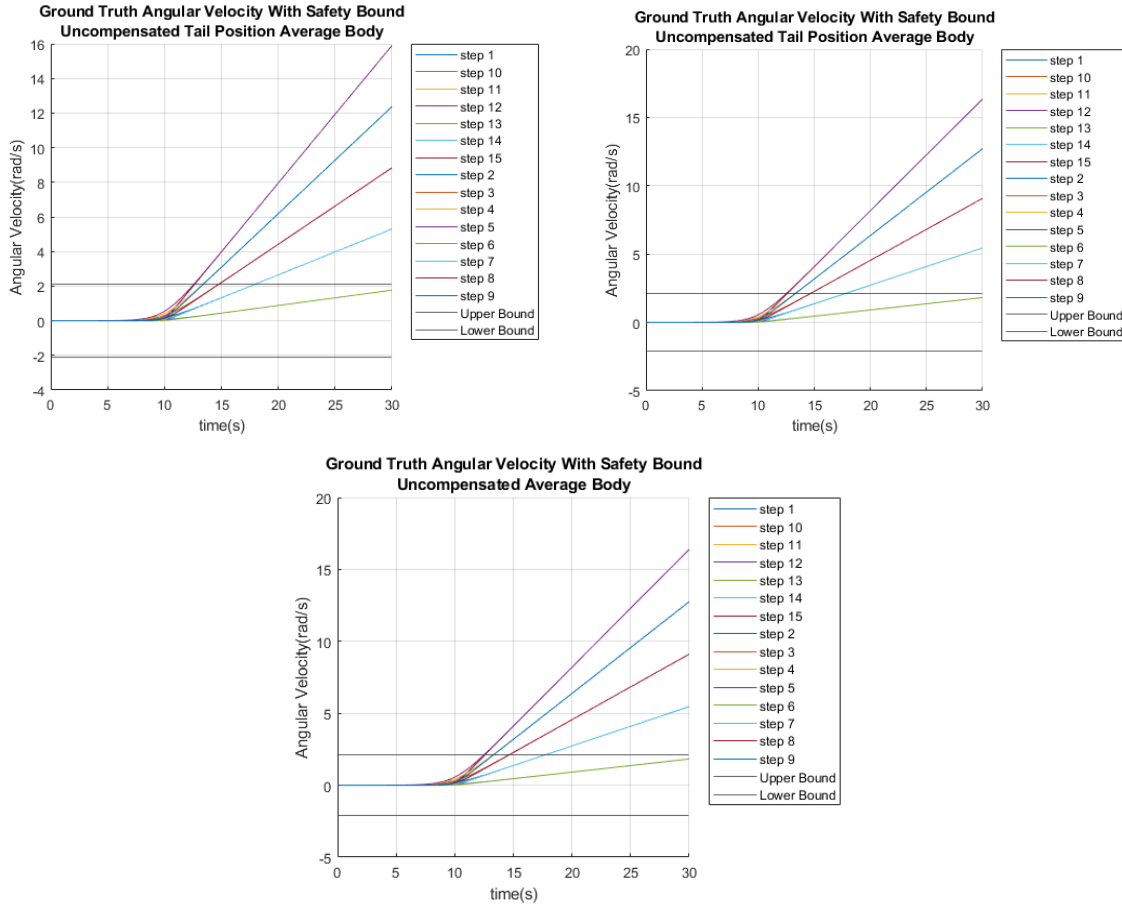
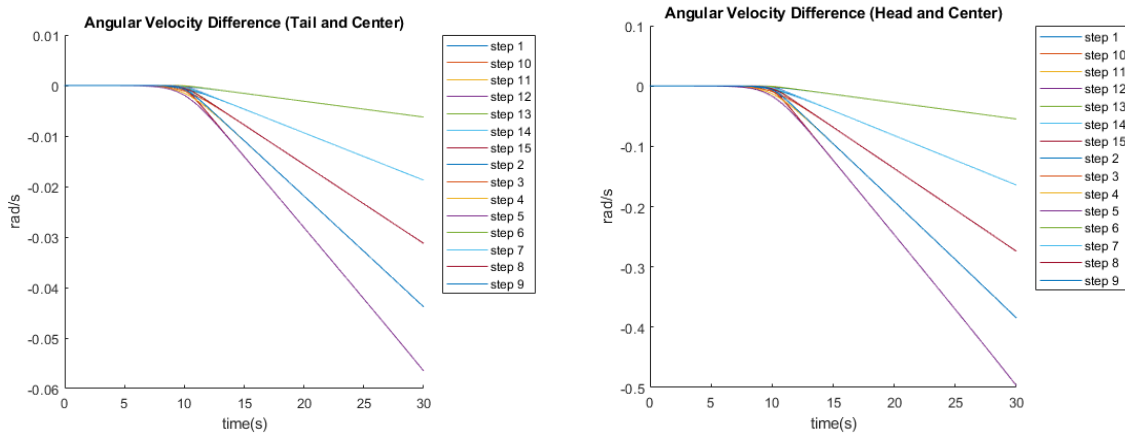


Figure: Body model placed in the head (right) and tail (left) configurations

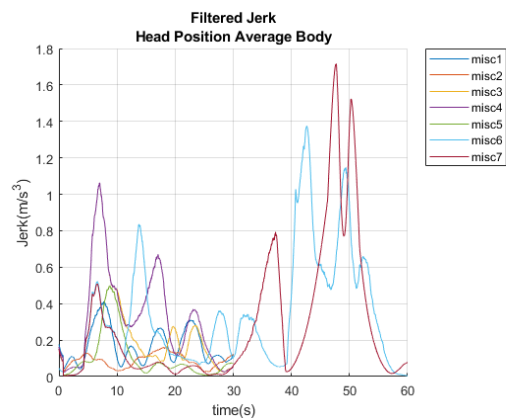
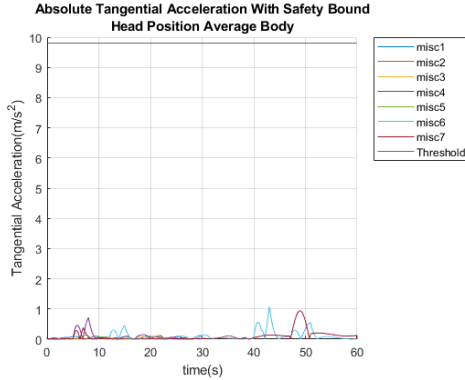
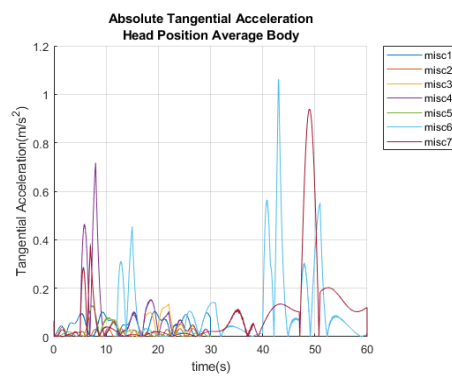
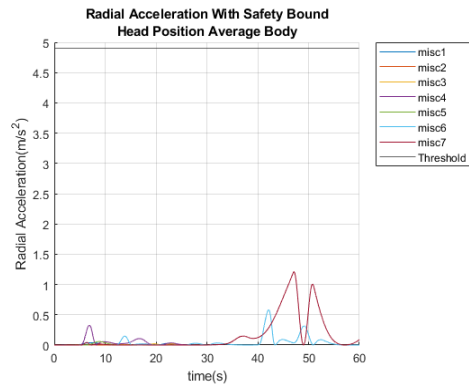
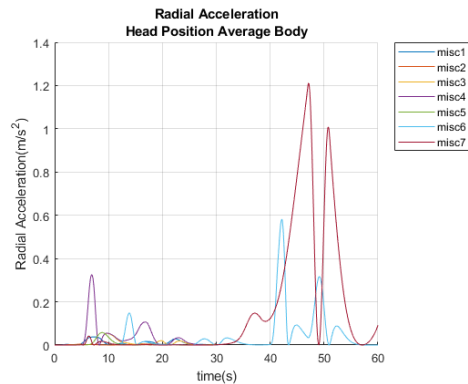
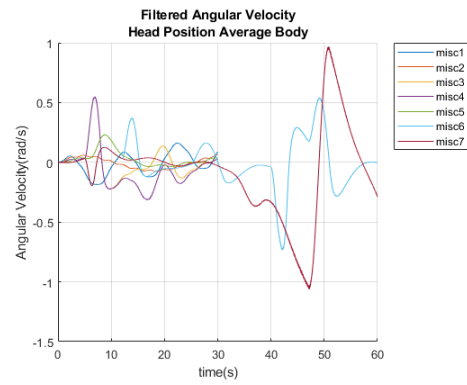
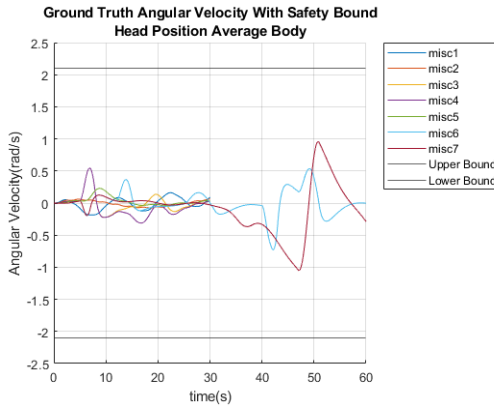
Due to differences in the heights and weights of our modeled bodies, The 3 Standard deviation below model moved farther from the center than the average body, and is expected to have a greater effect on the system rotational inertia. Similarly, the 3 SD above model and the maximum payload model did not deviate much from the stretcher center of mass, and was not tested as a result. Below are comparisons of angular velocity, acceleration, and jerk for this variance.



The graphs below display the difference between angular velocity from tail and center case as well as head and center case. Notice all the values are negative showing that the center case has the greater angular velocity.



The graphs below show the ground truth angular velocity, radial acceleration, tangential acceleration, and jerk for miscellaneous disturbance for head position case using average body. The graphs shown without safety bounds are there to give a clearer look at the graph behavior not seen when the safety bound is displayed.



From this data, we see that our velocity threshold is not crossed, and that the difference in angular velocities between scenarios is negligible. The uncompensated system where the device is non-functioning shows the system well exceeds the safety bounds, showing success of our system. As with the velocity, the acceleration and jerk of the compensated system is comparable to that of the centered body cases, showing that the variance of the body has little effect on the success of our system.

### Device Position Variance

In the field, the stabilization devices may not be centered directly along the center of mass of the stretcher system. Our device needs to function properly in the case of an imperfect setup. We varied the location of the devices along the top and bottom bars of the stretchers in three cases: one module off-centre, both modules off-center in the same direction, and both modules off-center in different directions. In all cases, the modules were placed as far as possible along the top and bottom bars to represent a worst-case scenario.

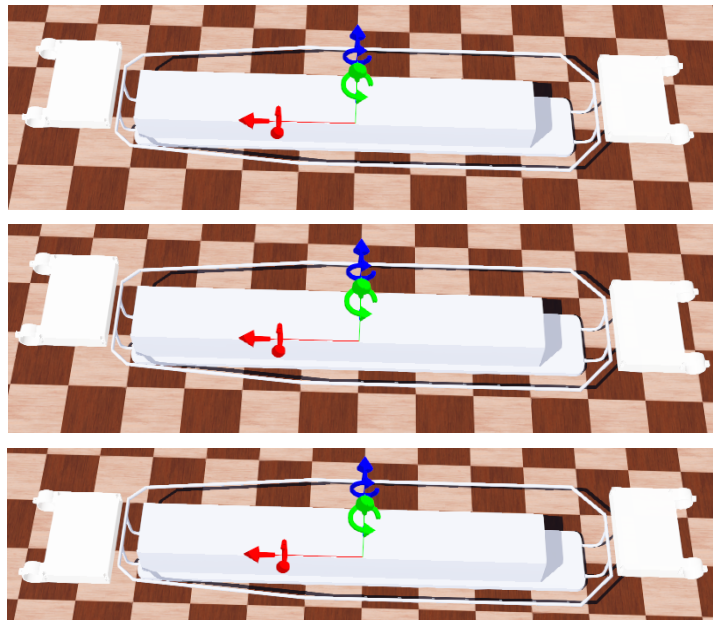
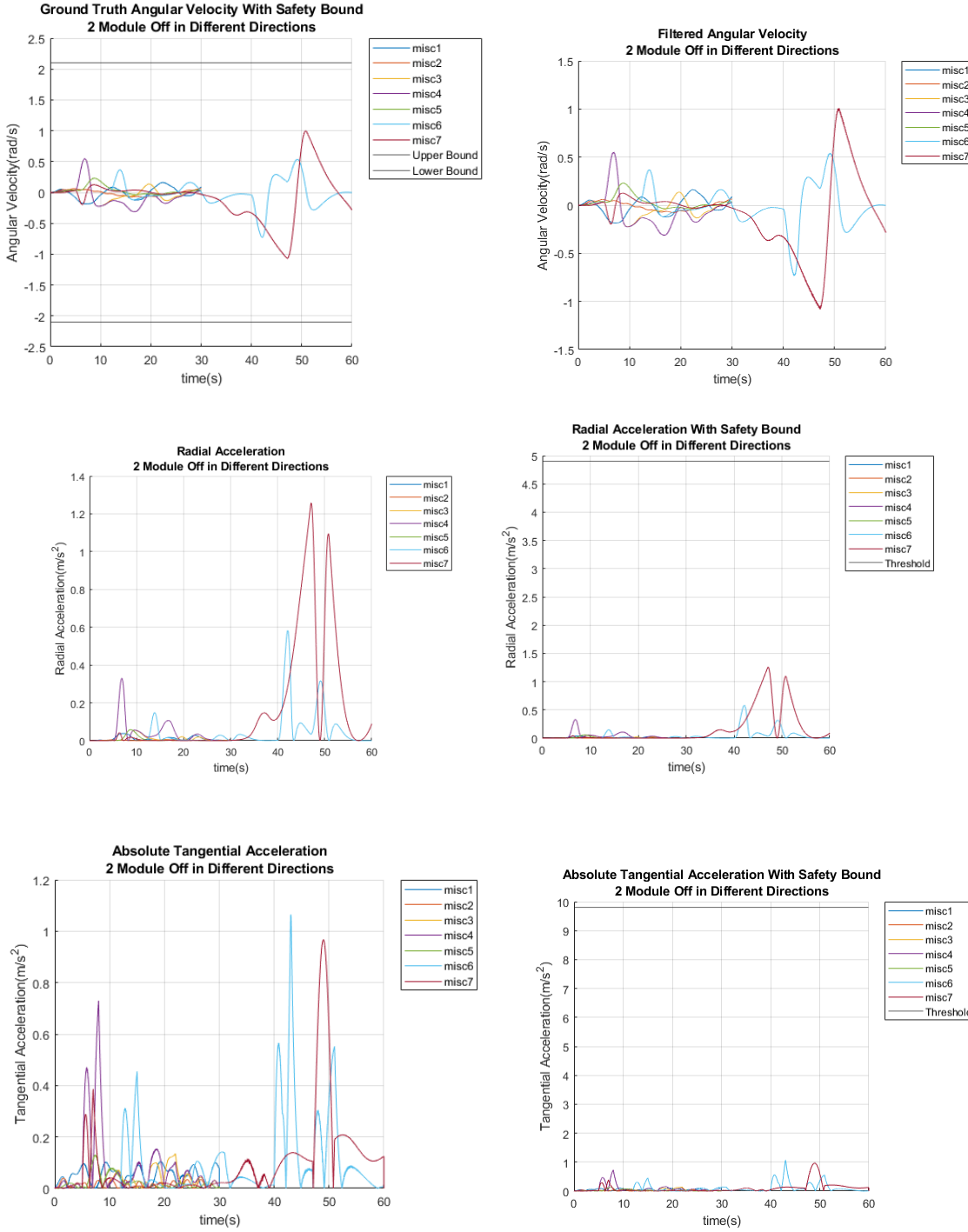


Figure: Devices Positioning configurations: One module offset (top), Both offset same direction (middle), Both offset different directions (bottom)

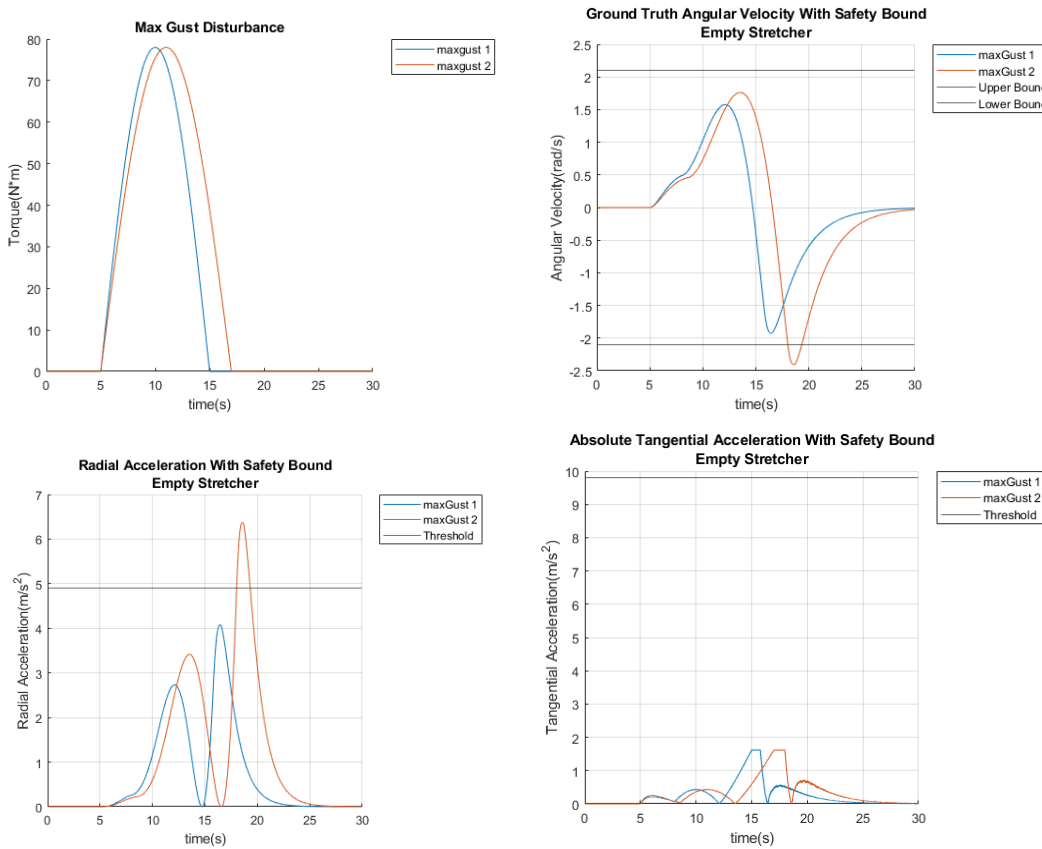


According to the results from above figures, which focus on the case that 2 modules off the center in different directions, we can say that the angular velocity never crosses the safety limit. The same thing happens to radial acceleration and absolute tangential acceleration, they never cross their own limit. As for the other 2 cases of device positioning variance, we counter the same behavior and the results can be found in the github link (Appendix 3). We can conclude that the system will be able to function as it can in fine setup even though the devices are positioned off center.

## Device Limitations

With the device attached, the actuators have a 1.4m moment arm each, resulting in a maximum torque output of 61.6Nm. Thus, any constant external torque above 61.6Nm will result in constant angular acceleration. We calculate that 61.6Nm corresponds to about 80km/hr winds constantly applying torque. We also looked at the maximum duration gust our system could handle in 90km/hr winds (maximum wind speed a helicopter will fly in).

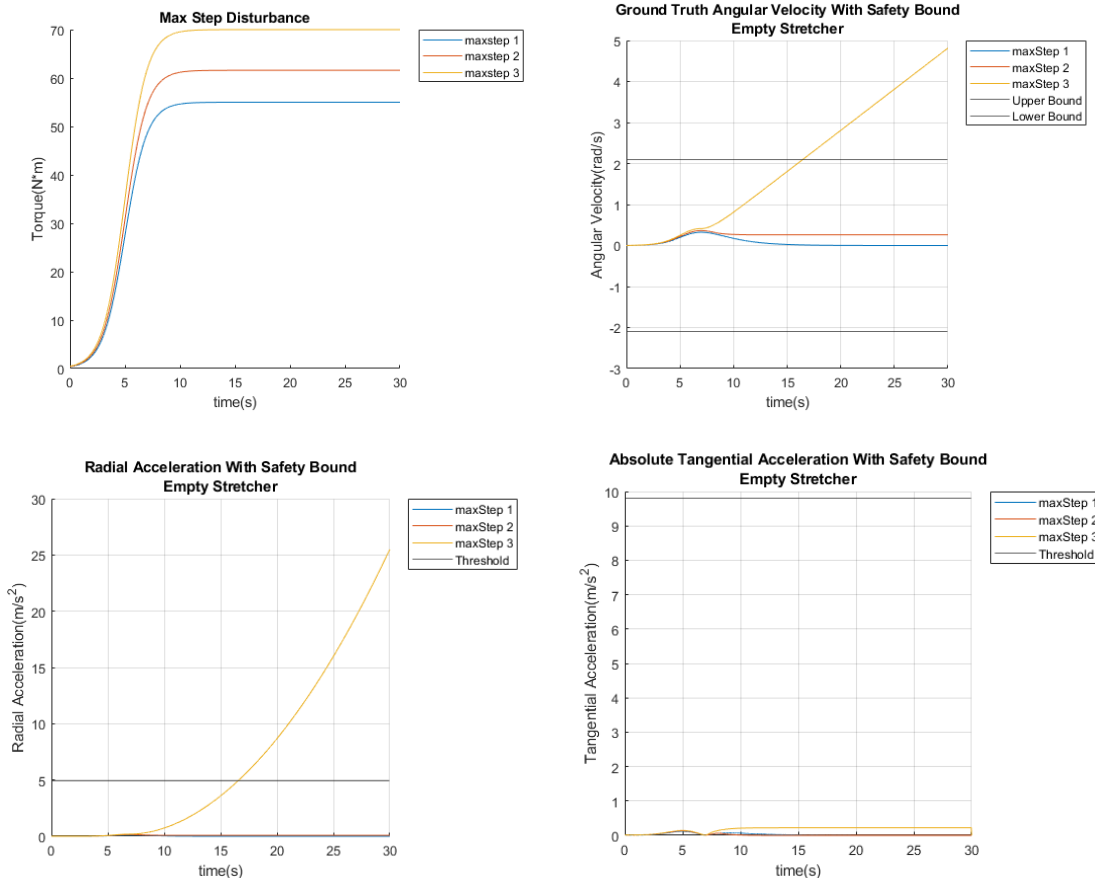
Disturbance	Amplitude (N.m)	Duration (seconds)
Maxgust 1	78	10
Maxgust 2	78	12



According to the results from above figures, our system can sustain 78Nm gusts within 10 seconds without breaking the safety limit.

Disturbance	Max Value(N.m)	Midpoint(Seconds)	Slope
Maxstep 1	55	5	1
Maxstep 2	61.6	5	1

Maxstep 3	70	5	1
-----------	----	---	---



According to the results from above figures, we can say that our system can meet the safety requirement as long as the step external torque is under 61.6 N.m. This makes sense since the saturated torque that actuators can produce is also 61.6N.m, which causes the net torque to be zero if the external torque is 61.6N.m. If the disturbance is a step external torque that is larger than 61.6N.m like “maxStep 3”, the system will break the safety limit at some point due to the constant angular acceleration.

### Frequency Analysis

FEA Frequency analysis was conducted in Solidworks, using the frequency studies in SolidWorks Simulations.

Our device operates in turbulent environments with several actuators. This means that the system receives several types of frequencies, such as from the helicopter, stretcher, winds, torque, and mainly, its own actuators. It is important to check if any of these frequencies arrive

at the device's natural resonant frequency and affect the device through deformation or threats to critical locations.

The chassis was used as a baseline for frequency analysis; the electrical housing of the same material as the chassis provides protection to critical parts of the electrical system, however frequency analysis will still be necessary to guarantee safety.

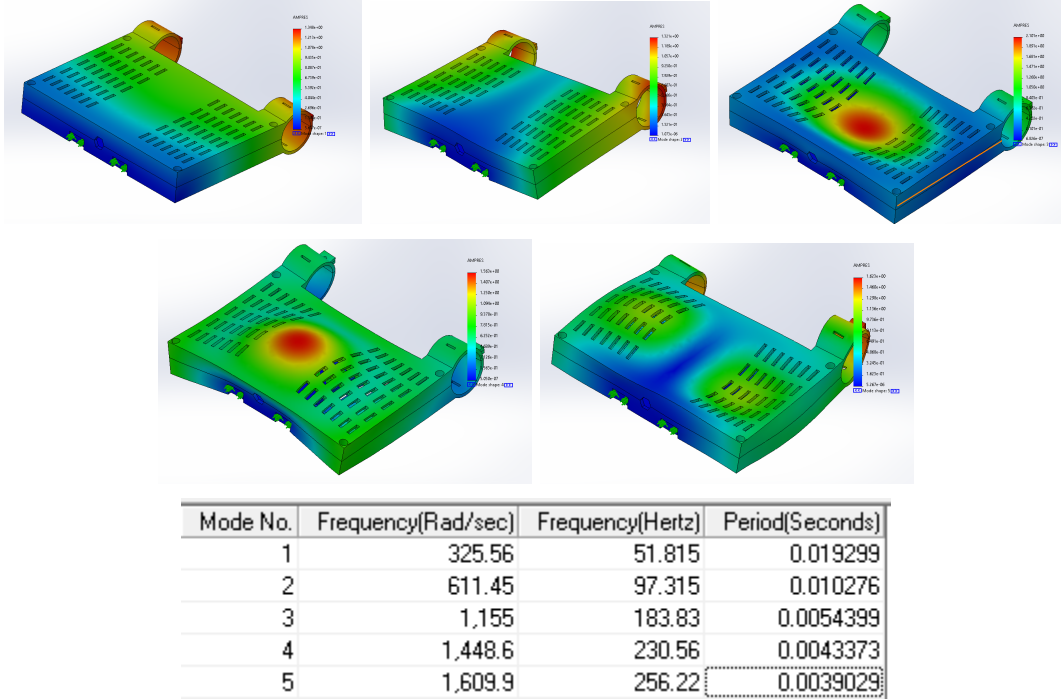


Figure: Natural Frequency Analysis results; Modes 1 ~ 5 with Resonant Frequencies

The Powerfun 70mm EDFs have a maximum RPM as standard max EDF RPMs, which is 52000 RPM. This converts to 866 Hz, which is our assumed max frequency applied onto the chassis.

Under this limit, 5 mode frequencies were found when the chassis was meshed and conducted through natural frequency analysis. The controller can be modified to intentionally avoid the following 5 frequencies; 51, 97, 183, 230, and 256 Hz. The mode shapes suggest that Mode 3 and 4 may directly affect the location where the electrical components are stationed; although there is an electrical housing that will provide protection, other preventative measures were made. The controller now actively avoids the 5 frequencies mentioned above.

Generally, the environment that the device will operate in does not receive a constant frequency, especially its resonant frequency; because the environment, forces, and actuators itself are dynamic, it can be confidently said that the chassis will not receive neither a constant or strong enough frequency to falter to resonance and experience plastic deformation that will threaten the critical components of our system.

## Thermal Analysis

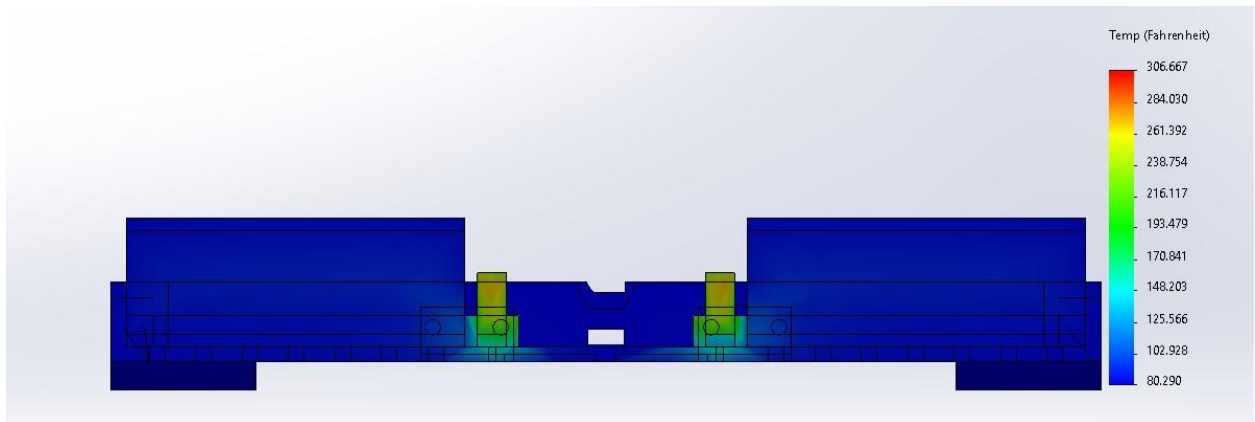


Figure: Front cross-sectional view of temperature distribution in the chassis. Notice that the ESC's are the highest temperature components.

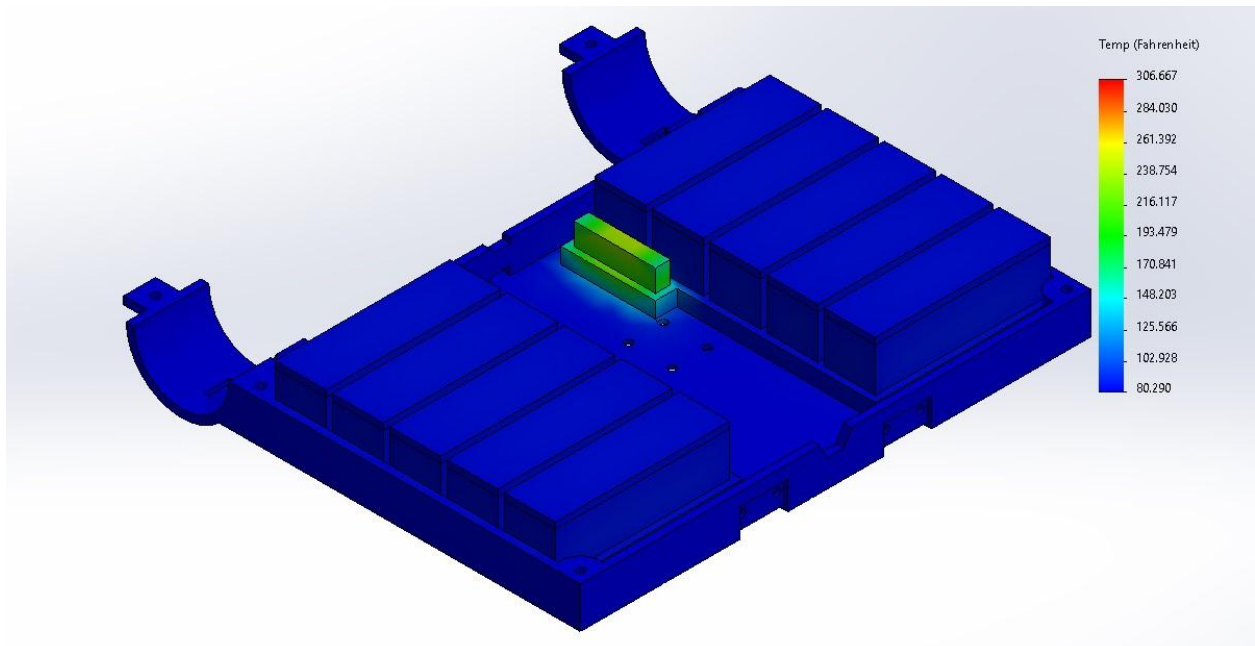


Figure: Isometric view of chassis components.

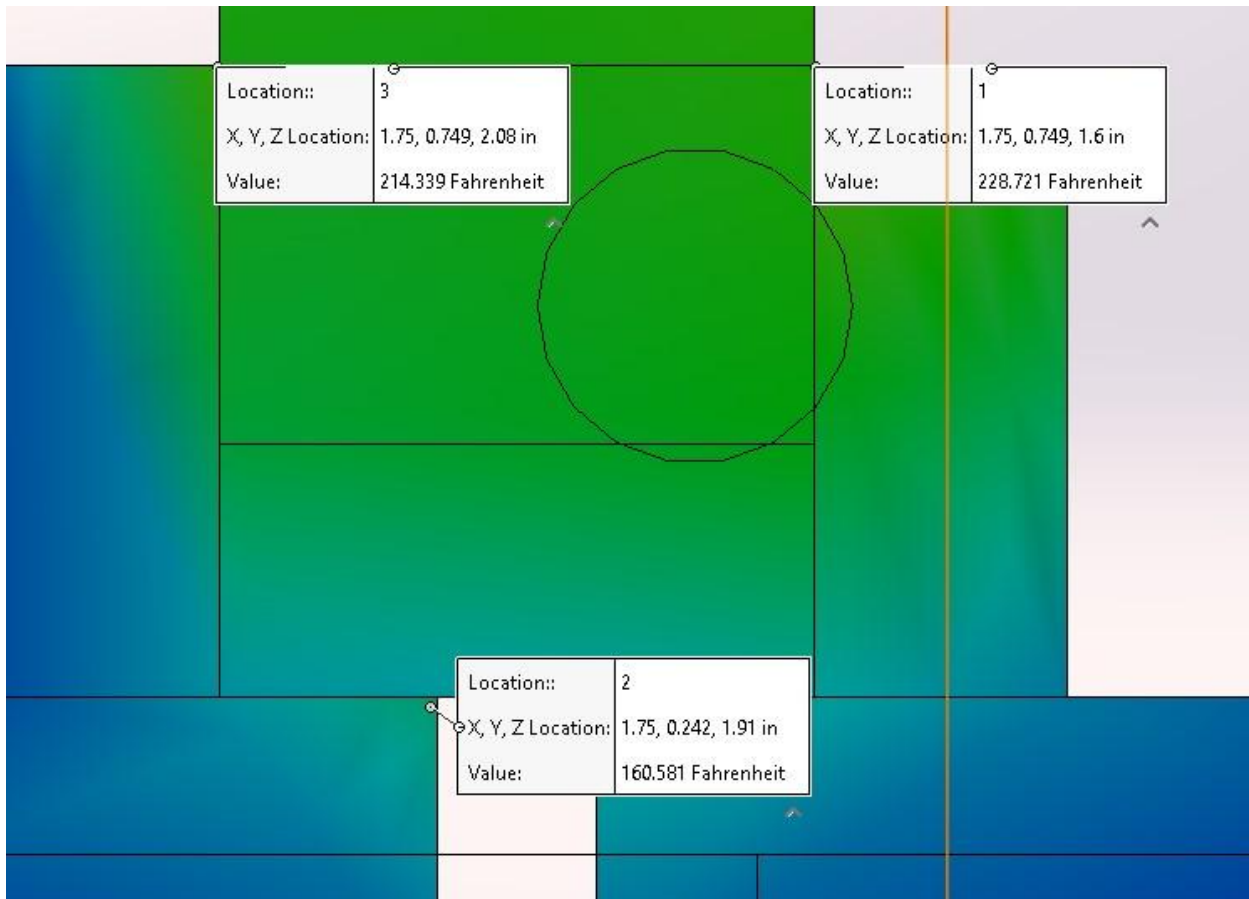


Figure: Temperature distribution near the ESC's. Notice that the temperature near the top approaches 230°F.

We could not find any specifications on the exact heat generated for our ESC's and batteries. However, we can create estimates to determine the power consumption on our battery using the following formula:

$$P = I^2 R$$

To determine the power, we must determine the current and internal resistance. We know that the actuator specified runs at 65A. An efficiency of 80% is a reasonable estimate for the ESC, meaning that the ESC will run at 81.25A<sup>46</sup>. By estimating an efficiency of 80% for the 5 batteries per speed controller, we can determine that the current running through each battery is 20.3125A.

The internal resistance of a good quality ESC is predicted to be around 0.001 to 0.002Ω. We assume a value of 0.002Ω for the ESC.<sup>47</sup> The internal resistance of a lipo battery is

<sup>46</sup> 1 Gong, Andrew & Verstraete, Dries. (2017). Experimental Testing of Electronic Speed Controllers for UAVs. 10.2514/6.2017-4955.

[https://www.researchgate.net/publication/318294444\\_Experimental\\_Testing\\_of\\_Electronic\\_Speed.Controllers\\_for\\_UAVs](https://www.researchgate.net/publication/318294444_Experimental_Testing_of_Electronic_Speed.Controllers_for_UAVs)

<sup>47</sup> "ESC Resistance: Does It Matter?" RC Groups RSS, [www.rcgroups.com/forums/showthread.php?197679-ESC-resistance-does-it-matter](http://www.rcgroups.com/forums/showthread.php?197679-ESC-resistance-does-it-matter).

assumed to be about 2 to 6mΩ. However, this is for optimal performance. The value is closer to 8mΩ as a more conservative estimate.<sup>48</sup> <sup>49</sup>

With these values, we determined that the estimated heat generation from the ESC is 13.2W. We also determined that the heat generated from the battery is 3.3W for each battery. Using these values, our simulation determined that the temperature on the chassis reaches about 230°F at parts non-critical to the design, while other critical parts maintain temperatures negligible to the heat generation created.

### Airflow Analysis

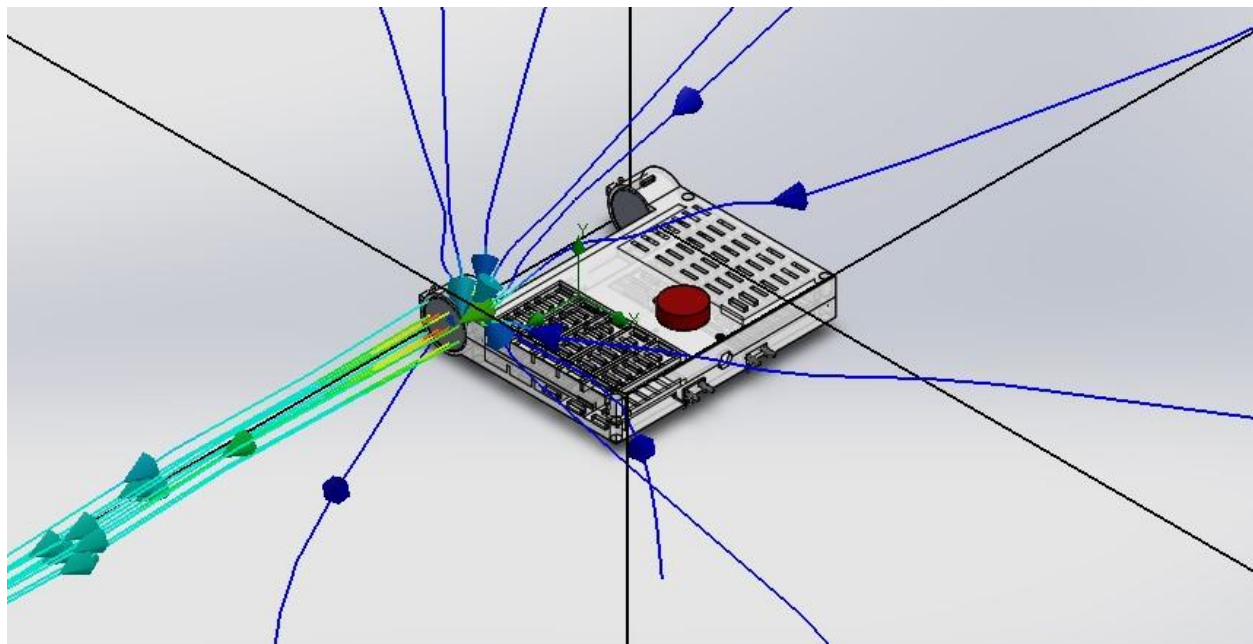


Figure: Airflow analysis of actuator fans on chassis.

An airflow analysis was conducted to determine if the flow of the air through the actuator fans was interrupted by the chassis or by the other actuator. Recall that each actuator is pointed in opposite directions, meaning that only one actuator on a module operates at a time. The analysis was modelled using inlet and outlet lids for one actuator while the other actuator received lids with a mass flow rate of zero (this is only an estimate, as the opposing fan will not be capable of completely blocking the airflow in the reverse direction). We determined that the lines of velocity approaching the inlet of the fan only increase to a substantial amount right up against the fan, meaning that the actuator placement and chassis size has negligible effect on the input velocity of the fan. Additionally, the figure shows a very high output velocity (as seen by the green and lighter blue colored lines) of the fan pointing away from the chassis, showing that the fan is capable of providing high thrust in this orientation.

### Load Tests

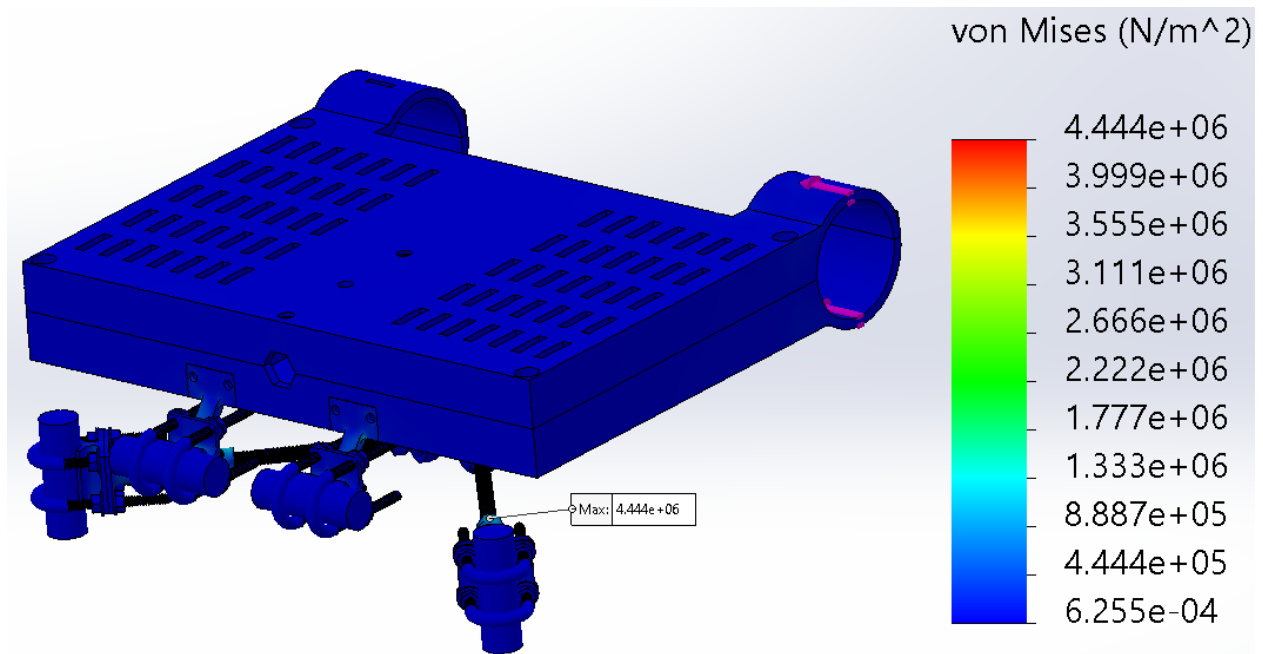
<sup>48</sup> “LiPo Internal Resistance - Why It's Important.” *RCHelicopterFun.com*, [www.rchelicopterfun.com/lipo-internal-resistance.html](http://www.rchelicopterfun.com/lipo-internal-resistance.html).

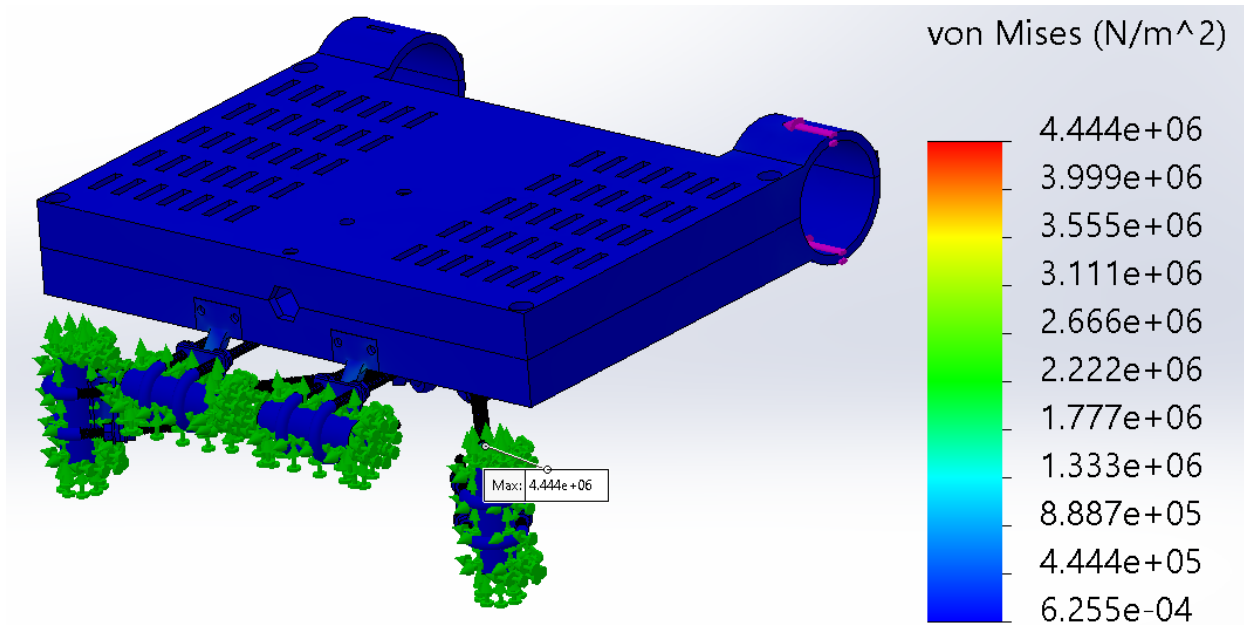
<sup>49</sup> “A LIPO BATTERY GUIDE TO UNDERSTAND LIPO BATTERY.” *GensTattu*, [www.genstattu.com/bw/](http://www.genstattu.com/bw/).

Load testing is done entirely in Solidworks, a professional grade CAD software. All CAD parts and assemblies were also made with Solidworks, making it the de facto choice for simulations. Running simulations is a tedious task that uses a good deal of computing power. For this reason we ran different simulations to determine factors of safety on various parts so that our hardware could handle our simulations.

The purpose of a load test is to determine where stresses are concentrated on a part, to what extent the parts/assemblies are deformed, and to inform on whether or not any pieces fail. It is also critical to know that components' stresses are within our factor of safety during the most rigorous testing scenarios. The components that face the most difficult challenges in a load test are the mounting hardware and the chassis. The other components simply need to be kept in their places to be operational.

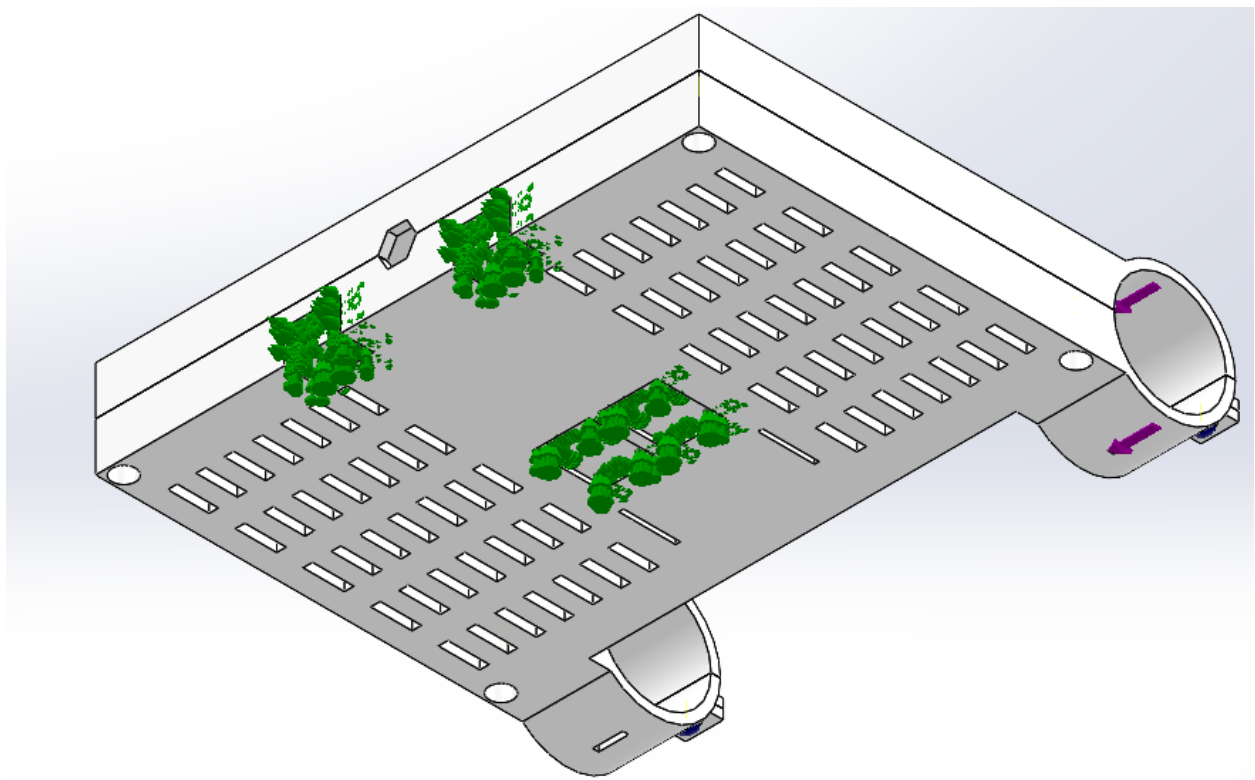
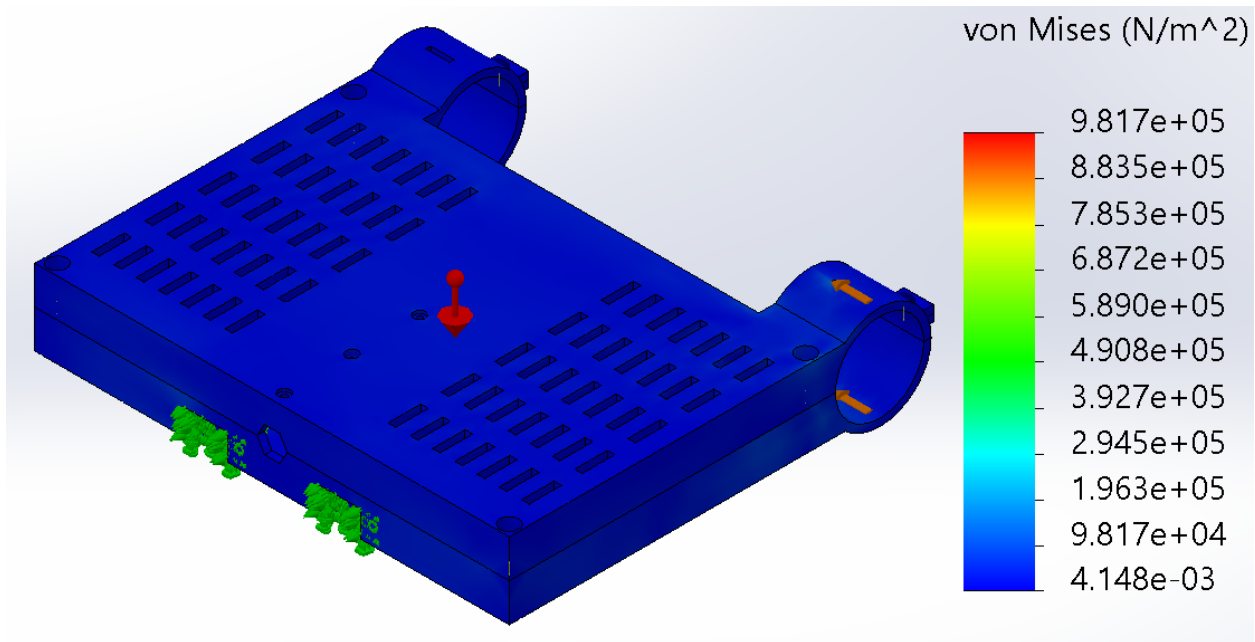
Our device was tested in two different simulations. The first was a static simulation in which the mounting hardware and the chassis were in a simulation and treated as "bonded". This is a simple assumption to make, and while it does not have all the complexity that a global "no penetration" contact set would have, it is a reasonable assumption and allowed us to actually run the simulation successfully. The four example pipes were fixed, and the maximum load of 16 Newtons was applied where the tabs from the actuator come into contact with the chassis. All visuals showing results of static simulations are shown with true deformed scale.





The maximum von Mises stress was reported to be  $4.444\text{e}+06 \text{ N/m}^2$  and was applied on one of the inline ball joint linkages which is made of alloy steel. In the Solidworks library, the yield strength is reported to be  $6.204\text{e}+08 \text{ N/m}^2$ . The factor of safety on the part with the highest stress is 139.6, well over our required factor of safety.

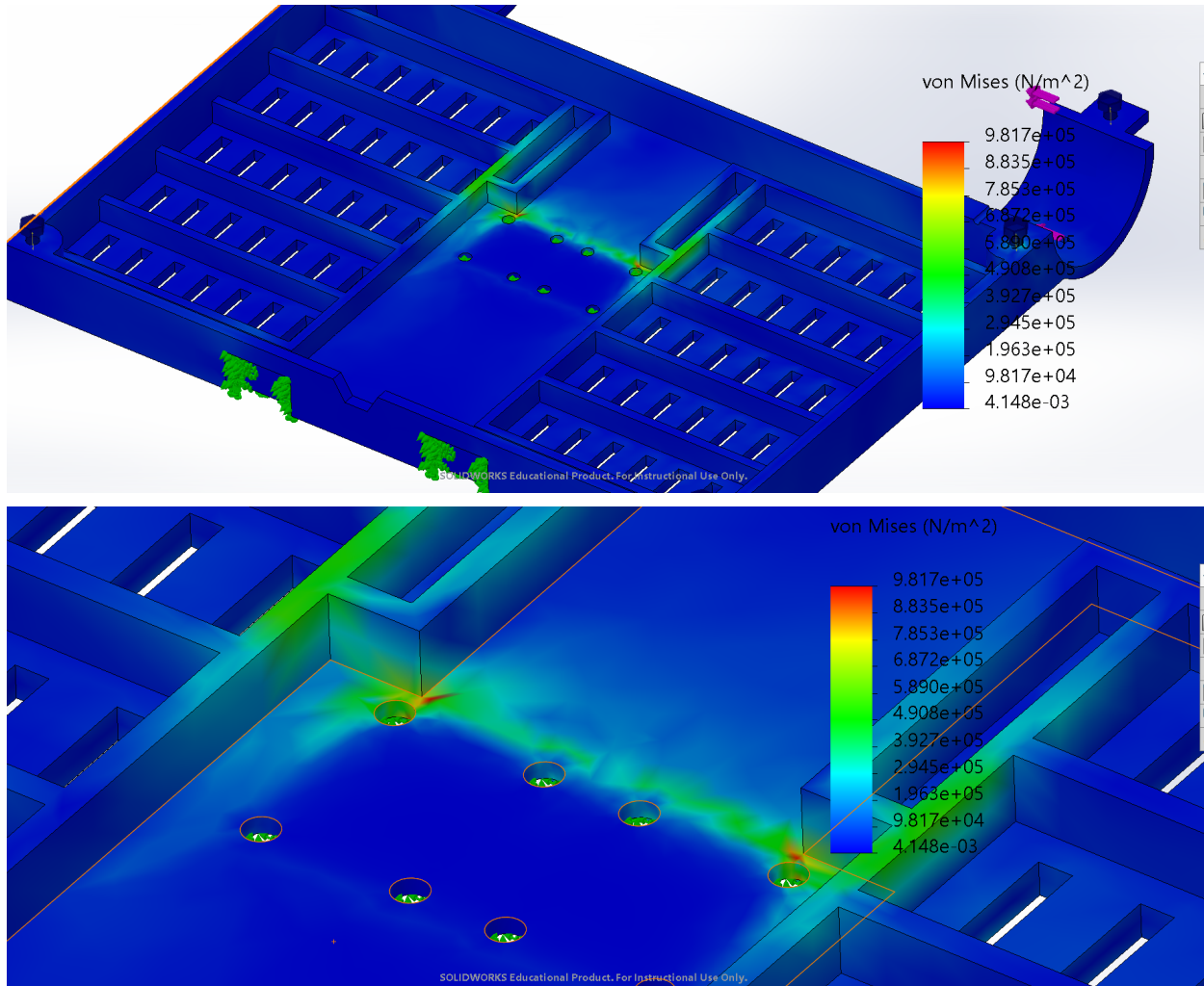
The second static simulation was done on the top and bottom halves of the chassis. They had a global “no penetration” contact and we used bolt connectors where appropriate. The faces where mounting hardware attaches to the bottom half of the chassis were chosen to be fixed geometry, and the same force was applied as in the first static simulation. The purpose of this simulation was to investigate how and where stresses accumulated with a more realistic set of assumptions for how the chassis interacts with itself and applied loads.



The stresses in this part do not exceed  $9.8e+5$  N/m<sup>2</sup>. The top and bottom halves of the assembly are made of PC High Viscosity plastic, which (according to Solidworks) has a tensile strength of  $6.27e+7$  N/m<sup>2</sup>. While factors of safety are normally calculated using the yield strength of materials, plastics behave differently than metals and so the yield strength is not a parameter that is used. Regardless, the maximum stresses experienced in the chassis due to

maximum output by an actuator is far below the threshold for material failure. If we use tensile strength to calculate the factor of safety, this chassis assembly has a factor of safety of 64.

The maximum stresses on the chassis parts accumulated on the corners inside the bottom chassis parts shown below in red:



If required, fillets could be applied to the edges inside the chassis cavity to reduce stress, but because of the high factor of safety, no further changes are necessary. The chassis survived rigorous loads and we are confident it will survive, not become plastically deformed, and function in our most extreme designed-for scenarios.

## Structural Analysis

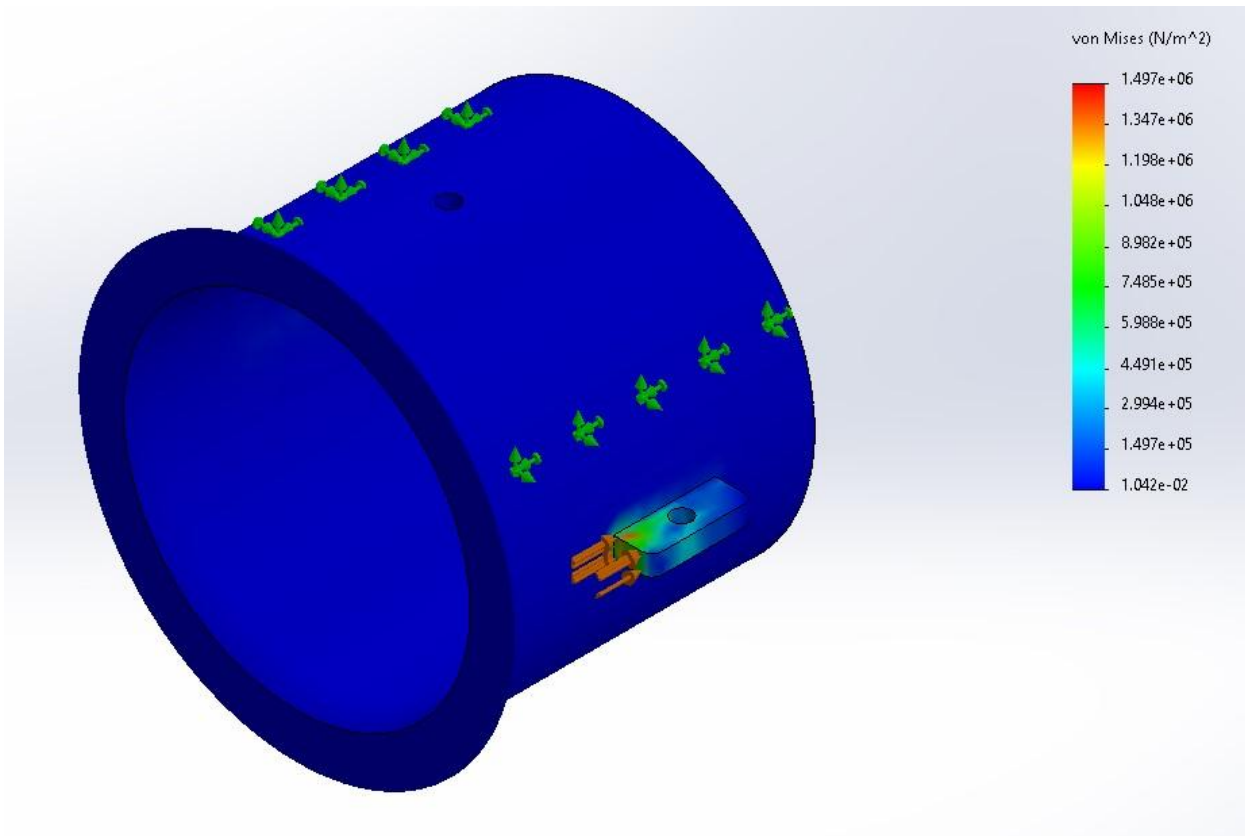


Figure: Von Mises stress of the actuator. For a yield stress of 30MPa, the actuator tabs are well below failure.

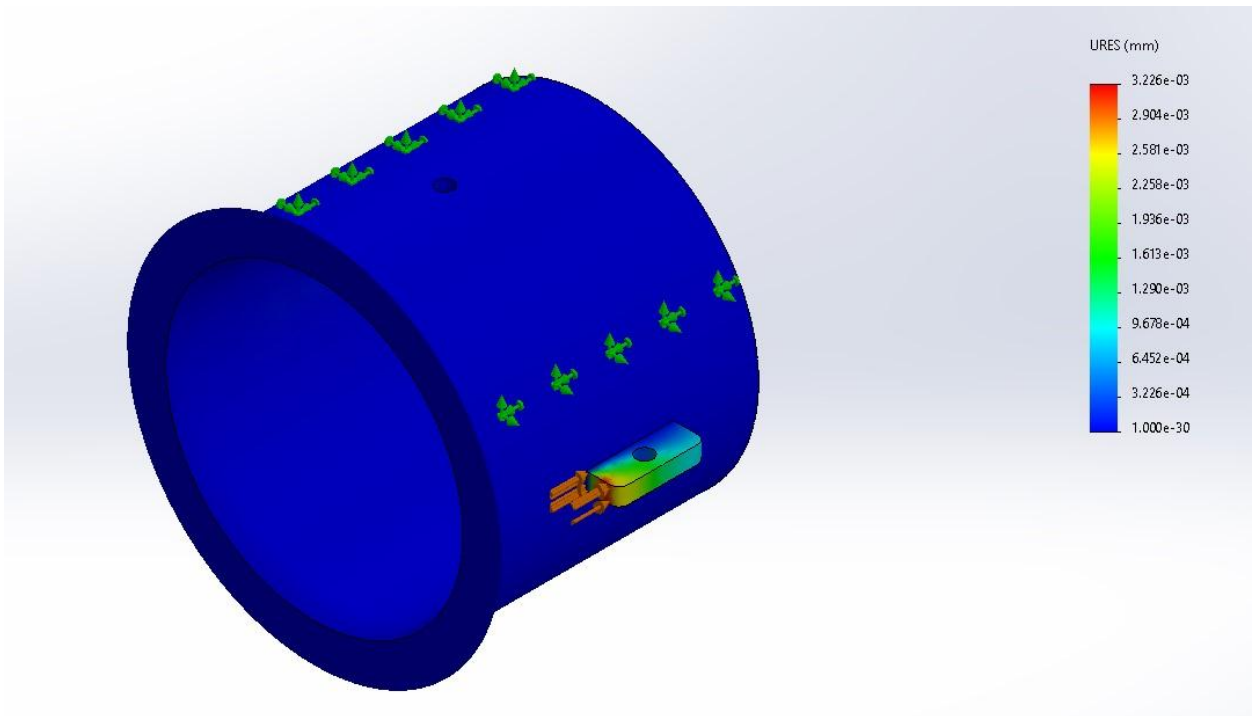


Figure: Displacement of the actuator in the range of micrometers.

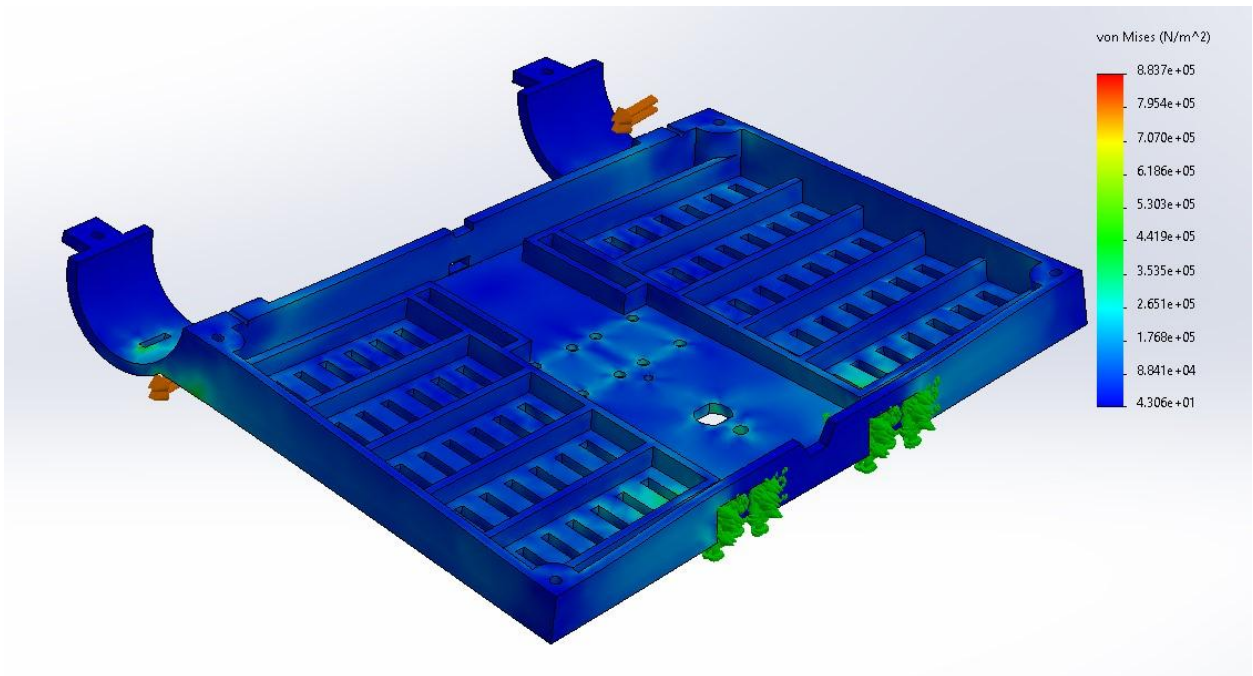


Figure: Von Mises stress of the chassis. For a yield stress of 30MPa, the chassis stress is well below failure.

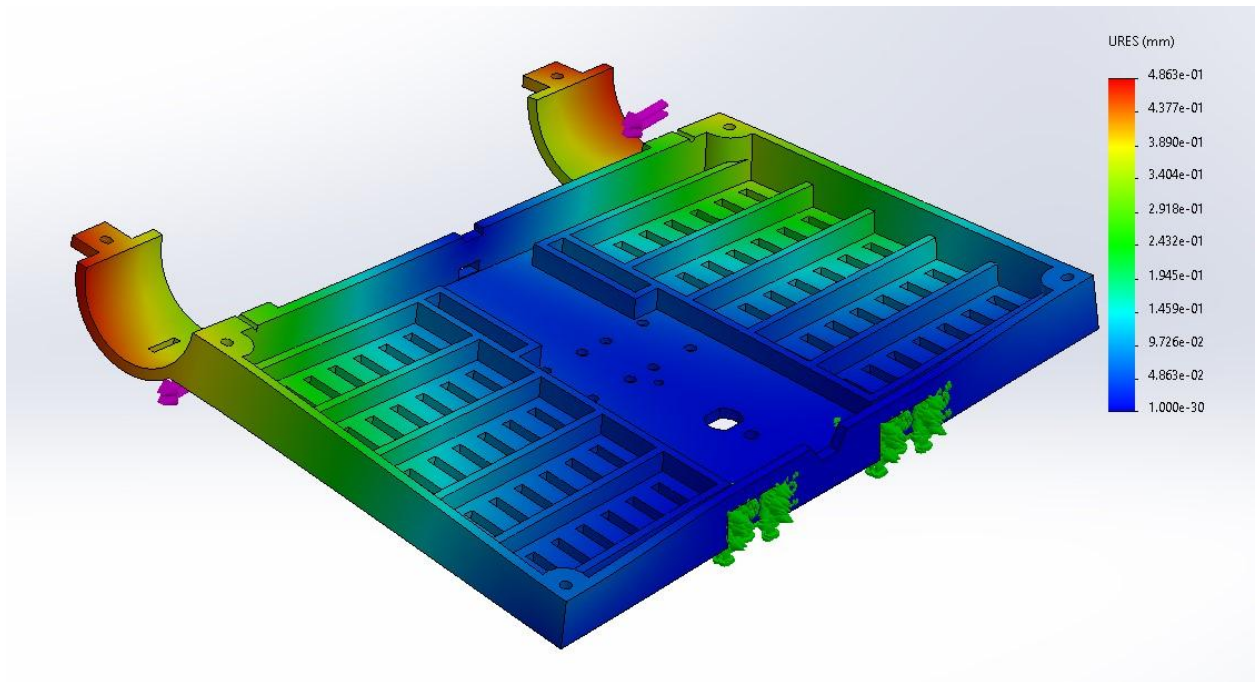


Figure: Displacement of the actuator in the range of millimeters.

Structural analysis was done on the actuator tabs and the chassis to test if the chassis can withstand the forces we are expecting from the wind and actuators. We also want to test if the actuator tabs can withstand the reaction forces it generates on the chassis. In both test cases, the maximum stress generated was much less than the 30 MPa yield stress, showing that the tabs and chassis are structurally robust. Specifically, the actuator tabs had a maximum stress of 1.497 MPa with displacement in the range of micrometers while the chassis had a maximum stress of 0.8837 MPa with a displacement of less than 1mm.

## Mounting Grip Tests

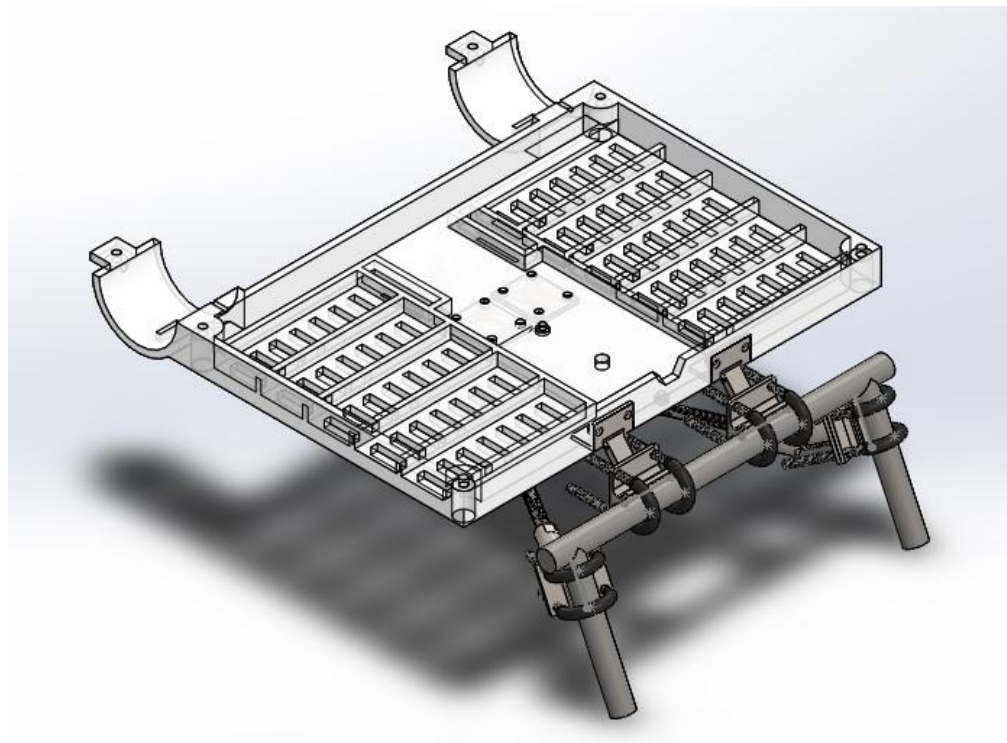


Figure: Mounting grip test setup with only critical components.

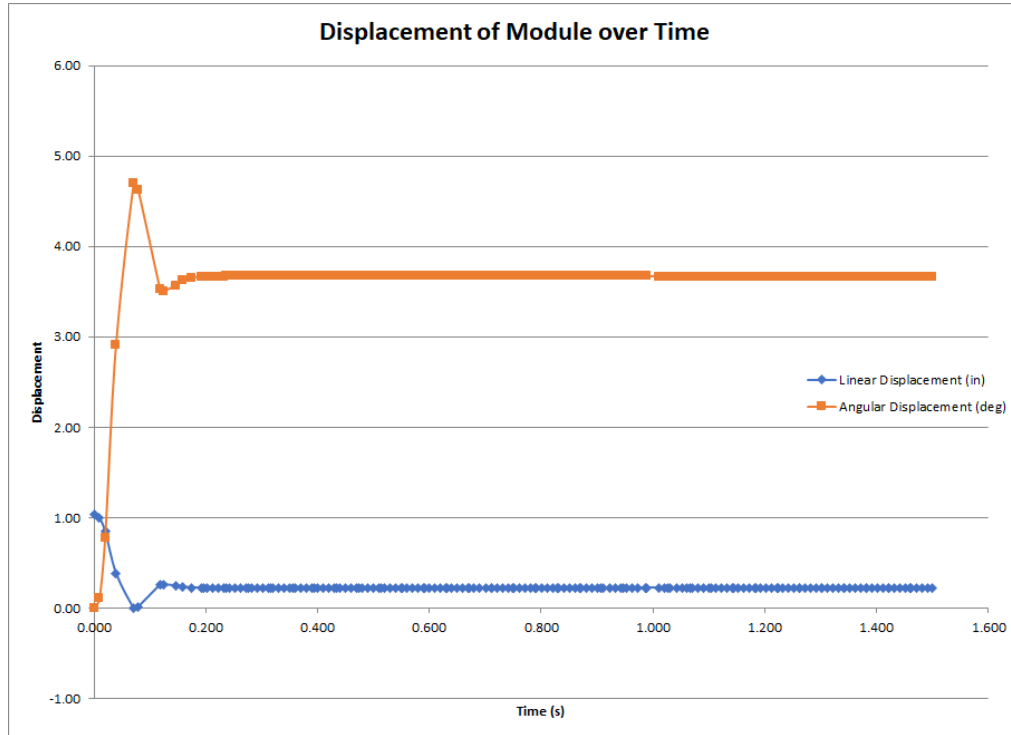


Figure: Under vertical 2G conditions, the module shows no displacement after initial adjustments.

Motion tests were simulated to determine whether there was enough friction on the mounts to transfer the thrust from the module onto the stretcher under our operating conditions. For up to 2G, the tests showed no slippage of the grips after initial adjustments in both the horizontal and vertical directions. However, the device must receive little impulsive force transfers from operators to maintain this orientation.

## Design Outcome Versus Requirements (Hieu, Jeremy, Chiraag)

For the most part, our design outcomes met our requirements; however, there were some discrepancies involved.

In all of our wind disturbance trials and system scenarios, our design was able to stabilize and track for angular velocity, keeping the value below our safety standard for maximal disturbance of 180 km/hr downwash. This was our primary goal and our benchmark for device success; the device also passed thresholds for accelerations, but failed to keep within our jerk safety standard at high disturbances and changes in direction, as most magnitudes of jerk graphs passed the  $0.9 \text{ m}/(\text{s}^3)$  threshold. Adjusting our system to keep within jerk parameters would likely involve revisions in our controller, as it primarily tracked angular velocities in its algorithm. Since magnitude of jerk is not a direct factor in patient health and simply a comfort metric, we can still consider our design as successful for its intended function.

Regarding the mechanical design, our requirements were met. However, more time to research would allow us to create a more efficient and effective design of modules. This would involve reducing weight and material in the chassis, making it more manufacturable, and more research into different mounting parts rather than custom parts. However, because our design met the requirements we imposed, we focused on simulating and developing tests to validate the functionality of our design.

Regarding the Electrical System Design, our requirements were also met. The system was designed so that there is always room for the actuators to run at maximum power without damaging any other parts and breaking the system itself. However, picking off the shelf product like battery and battery charger wasn't the optimal way for the manufacturing process. More time to research and contact with battery manufacturing companies would allow us to get a better battery system. In addition, we could also use PCB (printed circuit board) to eliminate the effort of soldering, which could potentially increase labour cost and make the manufacturing process more complicated. These methods would make it more manufacturable and potentially reduce the cost. However, these facts could not deny the fact that our product met its expected requirements.

Regarding the thermal analysis, it was determined that the temperature in non-critical components of the chassis exceeded the melting temperature of the plastic. Though a concern, the location of the melting leaves less urgency in resolving the issue. Additionally, the thermal analysis was conducted with a lot of estimates and assumptions made; thus, the only way to test the accuracy of the test is to conduct an experiment with the actual ESC's in place.

# Conclusion and Discussion (Jeremy, Chiraag)

We believe our product has the ability to be competitive in an essential market that has little competition. Its ability to be equipped to any stretcher model lends itself an immense marketable asset, and its accuracy despite thorough testing shows its robustness and design success. With these tools in mind, a couple of future considerations can be kept in mind.

## Expansion to 3 Degrees of Freedom

Currently, we simplified our system 1 Degree of freedom, which is spin about the cable axis. We focused on this for the scope of this project because spin is the main cause of patient blackout and injury. In order to account for the sway of the stretcher system, we would need to model it as a spinning mass on a pendulum. This would involve adjusting our control for linear velocities and accelerations as well as implementing state space tracking to control actuation, since we are removing many of our constraints. We would also need to model the rope and hanging stretcher in Webots, and have a more complex wind disturbance model than simplifying to external torques.

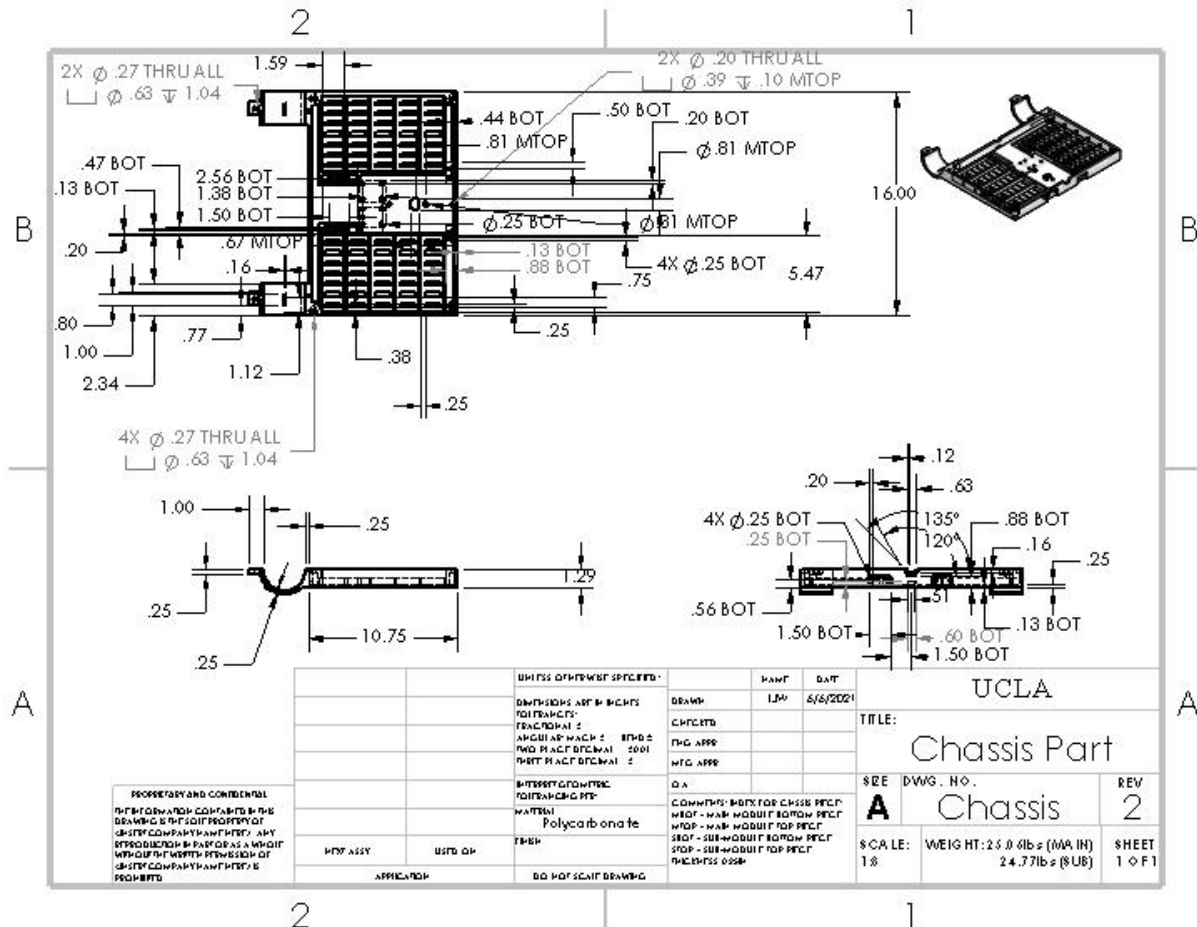
## Prototyping or Production

In the future, a major decision will be whether or not to enter prototyping or production. Prototyping would save costs as we continue to perfect our design, allowing us to conduct more research into manufacturing methods, design specifications, and market estimations. Production would also require heavy investment, but would allow us to compete earlier in a relatively open market with few competitors. This decision would lay the foundation for our future work on this project.

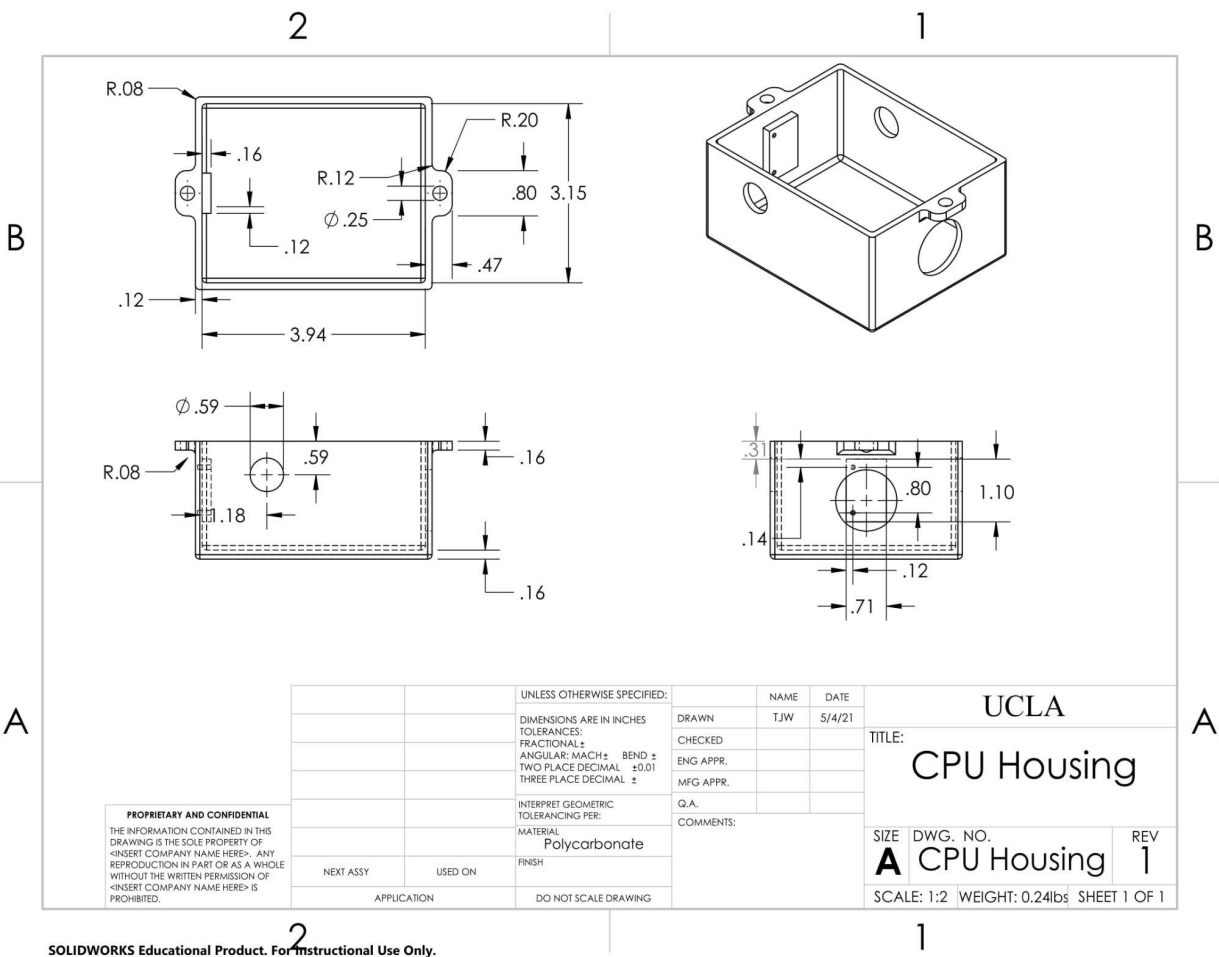
# Appendix 1 - Technical Drawings

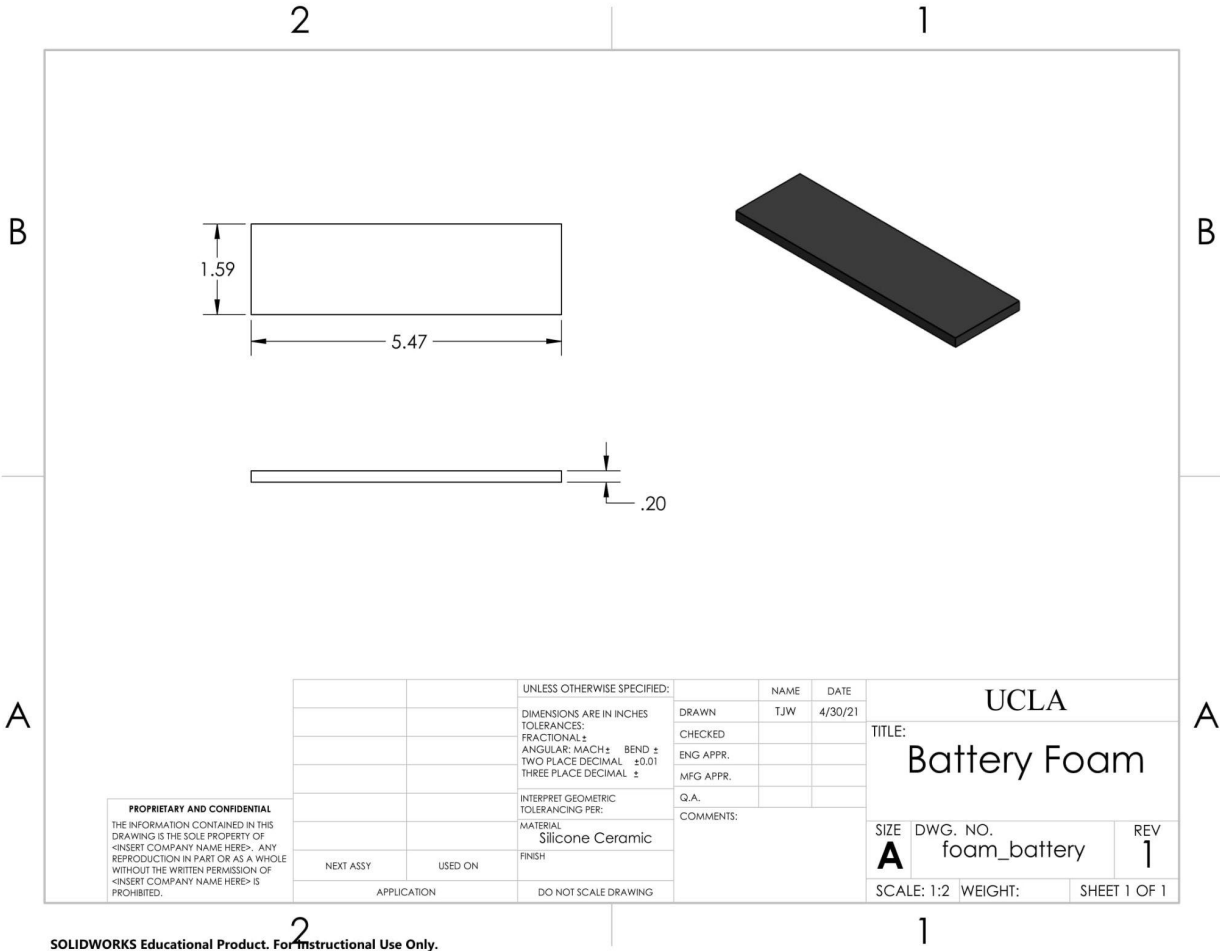
## Part Drawings

Below are the drawings for each part we created, excluding catalog parts. Assembly and subassembly drawings are in progress. Catalog parts can be found in the attached github link.<sup>50</sup>



<sup>50</sup> [https://github.com/giacomofratus/Stretcher\\_Stabilization](https://github.com/giacomofratus/Stretcher_Stabilization)



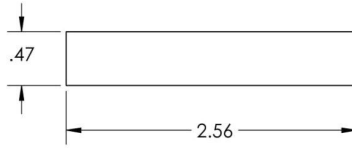


2

1

B

B



A

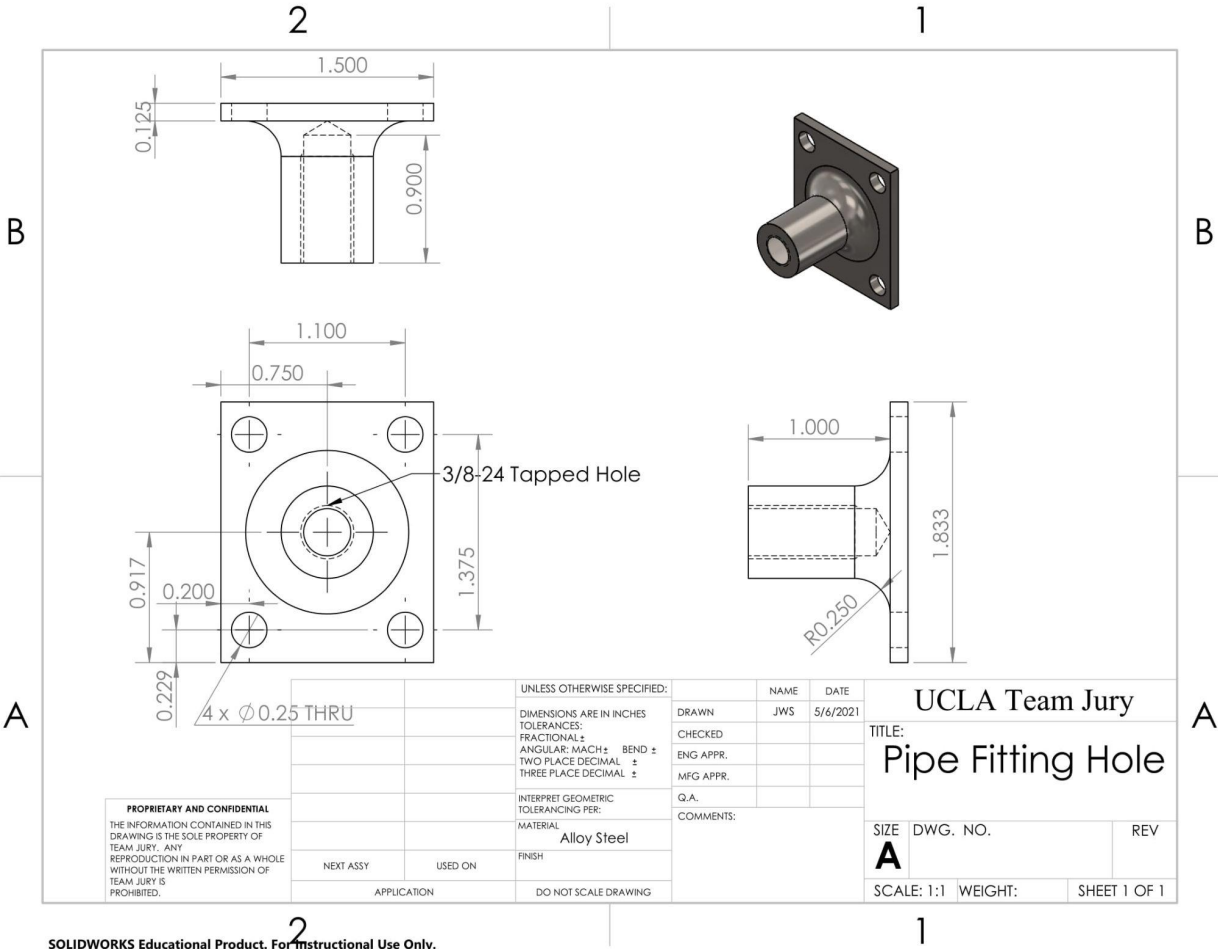
A

**PROPRIETARY AND CONFIDENTIAL**  
THE INFORMATION CONTAINED IN THIS  
DRAWING IS THE SOLE PROPERTY OF  
<INSERT COMPANY NAME HERE>. ANY  
REPRODUCTION IN PART OR AS A WHOLE  
WITHOUT THE WRITTEN PERMISSION OF  
<INSERT COMPANY NAME HERE> IS  
PROHIBITED.

		UNLESS OTHERWISE SPECIFIED:		NAME	DATE	UCLA	
		DIMENSIONS ARE IN INCHES TOLERANCES: FRACTIONAL $\pm$ ANGULAR: MACH $\pm$ BEND $\pm$ TWO PLACE DECIMAL $\pm 0.01$ THREE PLACE DECIMAL $\pm$				CHECKED	ENG APPR.
		INTERPRET GEOMETRIC TOLERANCING PER:		Q.A.	COMMENTS:	TITLE: ESC Foam	
NEXT ASSY	USED ON	MATERIAL	FINISH			SIZE	DWG. NO.
		Silicone Ceramic				A	foam_ESC
							REV 1
		APPLICATION	DO NOT SCALE DRAWING			SCALE: 1:1	WEIGHT:
							SHEET 1 OF 1

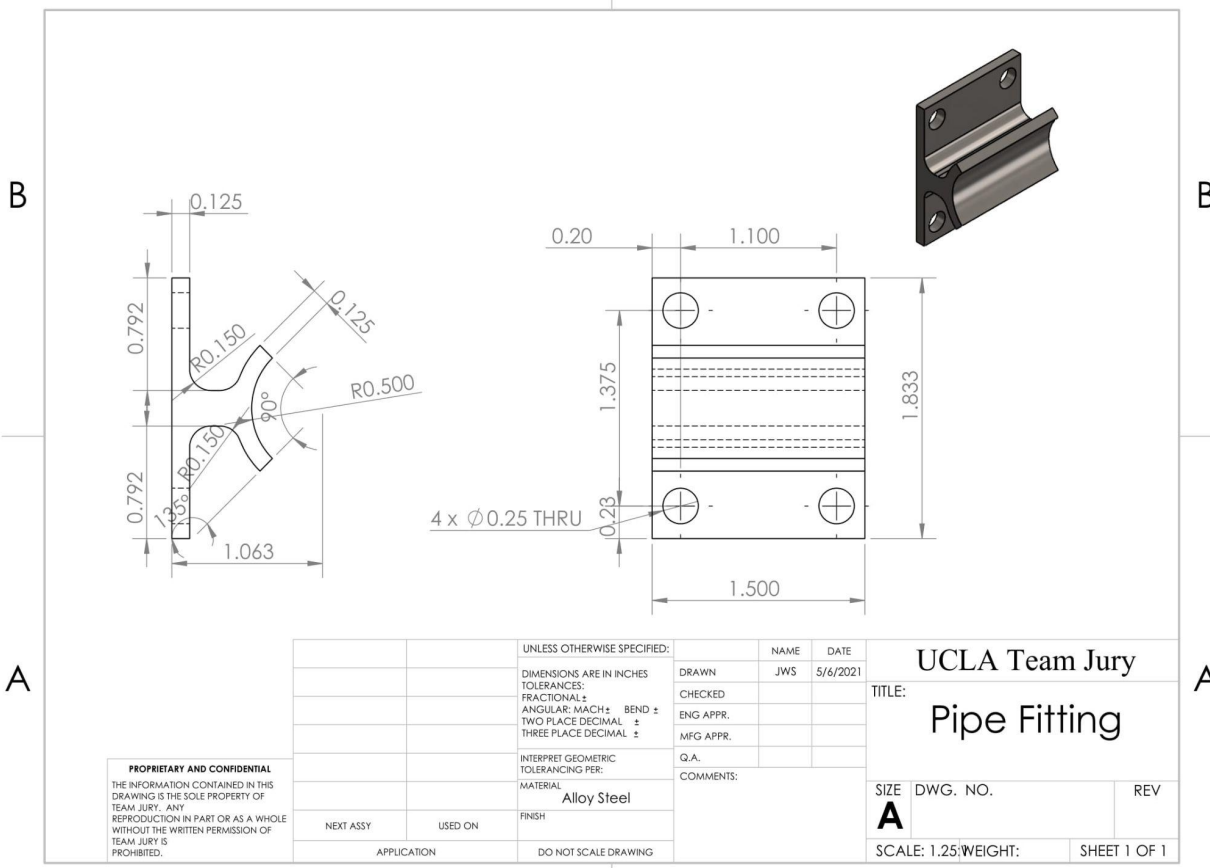
**SOLIDWORKS Educational Product. For Instructional Use Only.**

1



2

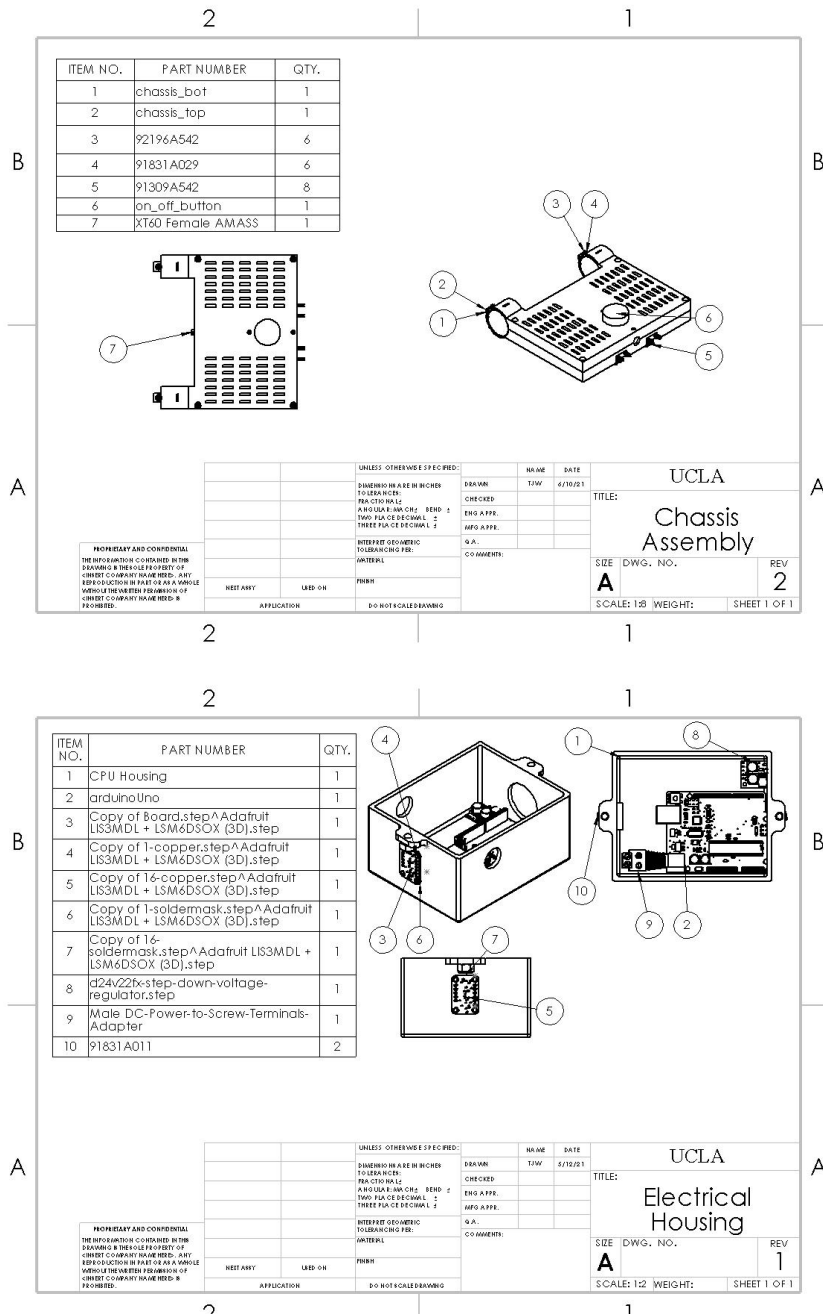
1



2

1

## Assembly Drawings



2

1

ITEM NO.	PART NUMBER	QTY.
1	Pipe Fitting Corner Mount	1
2	30555T31	2
3	92141A029	4
4	95462A029	4
5	91831A029	4

**B**

**A**

UNLESS OTHERWISE SPECIFIED:		NAME: TSW	DATE: 5/12/21
DIMENSIONS ARE IN INCHES		CHECKED:	
FEA OTHER		ENG APP:	
AND UCLACM1A.CDR: BEND: 2		MFG APP:	
TWO PLACES DECIMAL: 2			
THREE PLACES DECIMAL: 2			
INTERFERENT GEOMETRIC		QA:	
TOLERANCING PER		COMMENTS:	
MATERIAL			
NEST ANY	USED ON	FINISH	
APPLICATION		DO NOT SCALE DRAWING	

**UCLA**

**Corner Mount**

**SIZE DWG. NO. REV**

**A 1**

**SCALE: 1:2 WEIGHT: SHEET 1 OF 1**

2

1

ITEM NO.	PART NUMBER	QTY.
1	Pipe Fitting	1
2	30555T31	2

**B**

**A**

UNLESS OTHERWISE SPECIFIED:		NAME: TSW	DATE: 5/12/21
DIMENSIONS ARE IN INCHES		CHECKED:	
FEA OTHER		ENG APP:	
AND UCLACM1A.CDR: BEND: 2		MFG APP:	
TWO PLACES DECIMAL: 2			
THREE PLACES DECIMAL: 2			
INTERFERENT GEOMETRIC		QA:	
TOLERANCING PER		COMMENTS:	
MATERIAL			
NEST ANY	USED ON	FINISH	
APPLICATION		DO NOT SCALE DRAWING	

**UCLA**

**Pipe Fitting Assembly**

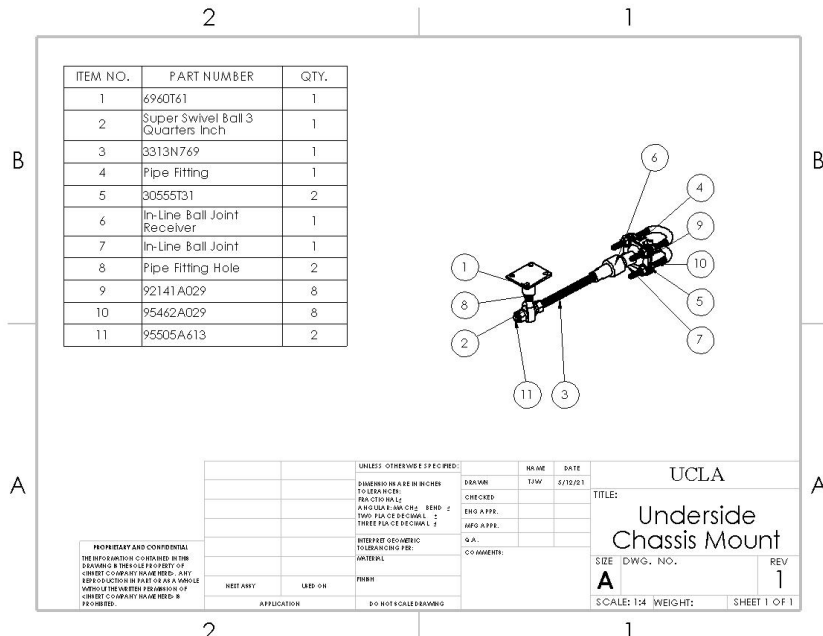
**SIZE DWG. NO. REV**

**A 1**

**SCALE: 1:2 WEIGHT: SHEET 1 OF 1**

2

1



## Appendix 2 - Bills of Materials

Category	Component	Vendor	Description	Qty.	Unit Price(\$)	Total Price(\$)
Actuators	Ducted Fans	Powerfun	70mm Ducted Fans	4	43.27	173.08
Actuators	ESC	Skywalker Hobbywing	80A ESC	4	45.99	183.96
CPU	Arduino Uno Rev3	Arduino	MCU with pin I/Os	2	23	46
Sensor	Adafruit ISM330DHCX	Adafruit	6DOF IMU	2	14.95	29.9
Power Supply	Voltage Regulator D24V22F7	Pololu	7.5V step down regulator	2	9.95	19.9
Power Supply	LiPo Battery Charger	Haisito	1-6S Lipo charger up to 22.2V and 10A	2	51.29	102.58
Power Supply	LiPo Battery	JHLIPO	Pack of 10 22.2V/6S 3500mAh 35C	2	136.9	273.8
Wiring	ESC Connector (10pcs)	HONBAY	male/female servo extension	1	6.79	6.79
Wiring	22 AWG Wires	Striveday	22 AWG Electric Wire Cable	1	15.39	15.39

Wiring	XT60 Connector (20pcs)	Assemble enthusiast	Battery-battery-ESC connectors (male/female)	1	14.99	14.99
Wiring	Adapter (Used for Arduino)	CableWholesale	DC Power Socket to 2-Pin Screw Terminal Adapter	1	0.77	0.77
Wiring	Power Wires (for Battery/ESC)	WindyNation	1 AWG Wire (5ft red, 5ft black)	1	41.91	41.91
Wiring	Power Wires (for Arduino)	BNTECHGO	12 AWG Stranded Copper Wire	1	9.48	9.48
Wiring	Communication Cable	Belden	3 20 AWG wires cable set (8ft)	1	8.64	8.64
Wiring	Cord Protector	Willbond	Cable Grip Strip 4"Width x 10'Length	1	8.85	8.85
Connector	6S balance connector	JiaYi	B6 LiPo Battery Balance Charger Plug	22	0.35	7.7
Connector	Connector between modules	Gxilee	3 Pin DIN Female/Male Solder Connectors(pack of 3)	1	11.99	11.99
Switch	On/Off Button	Partdeal	Littelfuse Cole Hersee 75920-BK Battery Disconnect Switch 300A 12V IP67 Sealed - Bulk Pkg - 75920	2	33.22	66.44
Adhesive	Plastic Adhesive	Zoro	Plastic Adhesive, 5 oz, Tube, Clear, Synthetic Resin Base	1	17.76	17.76
Fasteners	Rubber Cushioned U-Bolt 1/4"-20	McMaster	30555T31_RUBBER-CUSHIONED U-BOLT.SLDPRT	16	5.06	80.96
Fasteners	Steel Rod 3/8"-24	McMaster	3313N769_HIGH STRENGTH STEEL THREADED ROD.SLDPRT	4	10.52	42.08
Fasteners	Swivel Ball Joint Rod End 3/8-24"	McMaster	6960T610_SUPER-SWIVEL BALL JOINT ROD END.SLDPRT	4	10.68	42.72
Fasteners	Cap Screw 1/4"-20	McMaster	91309A542_LOW-STRENGTH ZINC-PLATED STEEL CAP SCREW.SLDPRT	16	0.0746	1.1936
Fasteners	Nylon Insert #10-24	McMaster	91831A011_TYPE 18-8 STAINLESS STL NYLON-INSERT LOCKNUT.SLDPRT	4	0.057	0.228
Fasteners	Nylon Insert	McMaster	91831A029_TYPE 18-8	44	0.0902	3.9688

	1/4"-20		STAINLESS STL NYLON-INSERT LOCKNUT.SLDPR			
Fasteners	Flat Washer 1/4"	McMaster	92141A029_TYPE 18-8 STAINLESS STEEL FLAT WASHER.SLDPR	48	0.0347	1.6656
Fasteners	Socket Head Screw #10-24	McMaster	92196A242_18-8 STAINLESS STEEL SOCKET HEAD SCREW.SLDPR	4	0.081	0.324
Fasteners	Socket Head Screw 1/4"-20	McMaster	92196A542_18-8 STAINLESS STEEL SOCKET HEAD SCREW.SLDPR	28	0.3214	8.9992
Fasteners	Hex Nut 1/4"-20	McMaster	95462A029_GRADE 5 STEEL HEX NUT.SLDPR	48	0.0529	2.5392
Fasteners	Hex Nut 3/8"-24	McMaster	95505A613_GRADE 5 STEEL HEX NUT.SLDPR	8	0.0552	0.4416
Fasteners	Inline Ball Joint Linkage 3/8"-24	McMaster	8412K460_HEAVY DUTY INLINE BOOTED BALL JOINT LINKAGE	4	13.47	53.88
Chassis	Main Chassis Tooling	IcoMold	PIM Chassis Tooling	1	23848	23848
Chassis	Main Chassis Part	IcoMold	Polycarbonate PIM Chassis Part	4	62.22	248.88
Attachments	CPU Housing	Protolabs	Polycarbonate 3D-printed Attachment Part	2	283.46	566.92
Attachments	Pipe Fitting Corner Mount	Protolabs	Alloy Steel Corner Mount	4	454.75	1819
Attachments	Pipe Fitting Hole	Protolabs	Alloy Steel Pipe Fitting Component	8	235.44	1883.52
Attachments	Pipe Fitting	Protolabs	Alloy Steel Mount	4	229.83	919.32
Foam	Thermal Foam	DigiKey	A17916-20 Thermal Materials	2	25.63	51.26
					<b>Total (\$):</b>	30615.83

51

51

[https://docs.google.com/spreadsheets/d/17swYE12krmb0YE4K7FG2Hg6adrQyQVdXAwm2lipHTeQ/edit?  
usp=drive\\_web&ouid=106653195278082608910](https://docs.google.com/spreadsheets/d/17swYE12krmb0YE4K7FG2Hg6adrQyQVdXAwm2lipHTeQ/edit?usp=drive_web&ouid=106653195278082608910)

## **Appendix 3 - Comprehensive & Elevator Pitch Presentation Slides**

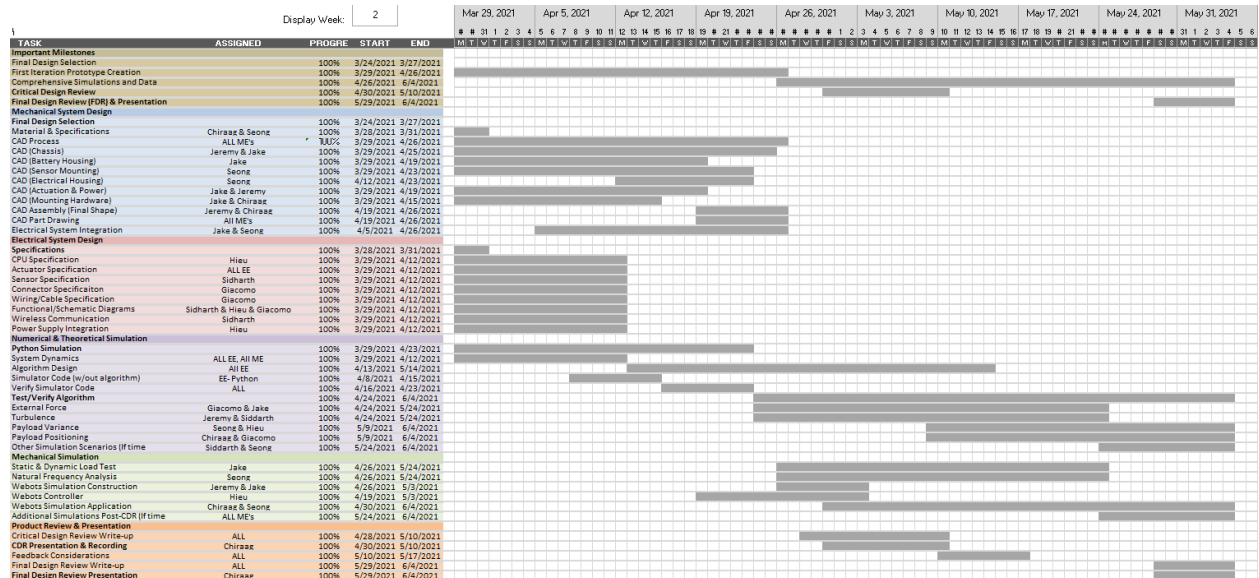
- FDR Presentation -  
[https://docs.google.com/presentation/d/1TMU2UCKGq\\_iEw3T88pav2mKTOkGCki6KuEOyvtvWVGE/edit?usp=sharing](https://docs.google.com/presentation/d/1TMU2UCKGq_iEw3T88pav2mKTOkGCki6KuEOyvtvWVGE/edit?usp=sharing)
- Sales Pitch Slides -  
[https://docs.google.com/presentation/d/18ScNQGsrKf6Ce-AaEjiptwdgRHUmL\\_z6gLK7EbL2KU/edit?usp=sharing](https://docs.google.com/presentation/d/18ScNQGsrKf6Ce-AaEjiptwdgRHUmL_z6gLK7EbL2KU/edit?usp=sharing)
- Sales Pitch Video -  
<https://drive.google.com/file/d/1V9YozkNXtoMotijGCHKE9ajsP6Boaw4O/view>
- Engineering Pitch -  
[https://docs.google.com/presentation/d/19qnLtyXKpGCLXg-NM5kQa\\_7tgytLkAUn4y-M7EefMM/edit?usp=sharing](https://docs.google.com/presentation/d/19qnLtyXKpGCLXg-NM5kQa_7tgytLkAUn4y-M7EefMM/edit?usp=sharing)
- Collaboration Task Matrix -  
[https://drive.google.com/file/d/1ckE4ik\\_-8zOrgm8VObHZWug3tYv660yr/view?usp=sharing](https://drive.google.com/file/d/1ckE4ik_-8zOrgm8VObHZWug3tYv660yr/view?usp=sharing)
- Github Link - [https://github.com/giacomofratus/Stretcher\\_Stabilization](https://github.com/giacomofratus/Stretcher_Stabilization)
- CAD Parts -  
[https://drive.google.com/drive/u/1/folders/1\\_4Vd8r\\_mHWdfonUDG8oWtA0Mbbx5RKBp](https://drive.google.com/drive/u/1/folders/1_4Vd8r_mHWdfonUDG8oWtA0Mbbx5RKBp)

## **Appendix 4 - GANTT Chart**

Following is the full visual of our GANTT Chart progress. All taskbars are greyed as we have fulfilled all planned tasks. Full link to GANNT Chart is included.<sup>52</sup>

---

<sup>52</sup><https://onedrive.live.com/view.aspx?resid=2874586556B007FF!3122&ithint=file%2cxlsx&authkey=!APBwyR9iaN0HeTk>



TASK	ASSIGNED TO	PROGRESS	START	END
<b>Important Milestones</b>				
Final Design Selection		100%	3/24/2021	3/27/2021
First Iteration Prototype Creation		100%	3/29/2021	4/26/2021
Comprehensive Simulations and Data		100%	4/26/2021	6/4/2021
<b>Critical Design Review</b>				
Final Design Review (FDR) & Presentation		100%	5/29/2021	6/4/2021
<b>Mechanical System Design</b>				
Final Design Selection		100%	3/24/2021	3/27/2021
Material & Specifications	Chiraag & Seong	100%	3/28/2021	3/31/2021
CAD Process	ALL ME's	100%	3/29/2021	4/26/2021
CAD (Chassis)	Jeremy & Jake	100%	3/29/2021	4/25/2021
CAD (Battery Housing)	Jake	100%	3/29/2021	4/19/2021
CAD (Sensor Mounting)	Seong	100%	3/29/2021	4/23/2021
CAD (Electrical Housing)	Seong	100%	4/12/2021	4/23/2021
CAD (Actuation & Power)	Jake & Jeremy	100%	3/29/2021	4/19/2021
CAD (Mounting Hardware)	Jake & Chiraag	100%	3/29/2021	4/15/2021
CAD Assembly (Final Shape)	Jeremy & Chiraag	100%	4/19/2021	4/26/2021
CAD Part Drawing	All ME's	100%	4/19/2021	4/26/2021

Electrical System Integration	Jake & Seong	100%	4/5/2021	4/26/2021
<b>Electrical System Design</b>				
Specifications		100%	3/28/2021	3/31/2021
CPU Specification	Hieu	100%	3/29/2021	4/12/2021
Actuator Specification	ALL EE	100%	3/29/2021	4/12/2021
Sensor Specification	Sidharth	100%	3/29/2021	4/12/2021
Connector Specification	Giacomo	100%	3/29/2021	4/12/2021
Wiring/Cable Specification	Giacomo	100%	3/29/2021	4/12/2021
Functional/Schematic Diagrams	Sidharth & Hieu & Giacomo	100%	3/29/2021	4/12/2021
Wireless Communication	Sidharth	100%	3/29/2021	4/12/2021
Power Supply Integration	Hieu	100%	3/29/2021	4/12/2021
<b>Numerical &amp; Theoretical Simulation</b>				
Python Simulation		100%	3/29/2021	4/23/2021
System Dynamics	ALL EE, All ME	100%	3/29/2021	4/12/2021
Algorithm Design	All EE	100%	4/13/2021	5/14/2021
Simulator Code (w/out algorithm)	EE- Python	100%	4/8/2021	4/15/2021
Verify Simulator Code	ALL	100%	4/16/2021	4/23/2021
<b>Test/Verify Algorithm</b>				
External Force	Giacomo & Jake	100%	4/24/2021	5/24/2021
Turbulence	Jeremy & Siddarth	100%	4/24/2021	5/24/2021
Payload Variance	Seong & Hieu	100%	5/9/2021	6/4/2021
Payload Positioning	Chiraag & Giacomo	100%	5/9/2021	6/4/2021
Other Simulation Scenarios (If time permits)	Siddarth & Seong	100%	5/24/2021	6/4/2021
<b>Mechanical Simulation</b>				
Static & Dynamic Load Test	Jake	100%	4/26/2021	5/24/2021
Natural Frequency Analysis	Seong	100%	4/26/2021	5/24/2021
Webots Simulation Construction	Jeremy & Jake	100%	4/26/2021	5/3/2021
Webots Controller	Hieu	100%	4/19/2021	5/3/2021
Webots Simulation Application	Chiraag & Seong	100%	4/30/2021	6/4/2021

Additional Simulations Post-CDR (If time permits)	ALL ME's	100%	5/24/2021	6/4/2021
<b>Product Review &amp; Presentation</b>				
Critical Design Review Write-up	ALL	100%	4/28/2021	5/10/2021
<b>CDR Presentation &amp; Recording</b>	Chiraag	100%	4/30/2021	5/10/2021
Feedback Considerations	ALL	100%	5/10/2021	5/17/2021
Final Design Review Write-up	ALL	100%	5/29/2021	6/4/2021
<b>Final Design Review Presentation</b>	Chiraag	100%	5/29/2021	6/4/2021

Updated Milestones Chart

7				
	Data Collection (for algorithm evaluation)	3 Preliminary Graphs and Charts		
			Run Wind Disturbance Modeling trials	Giacomo
			Run Payload Variance Environment trials	Seong
			Run Payload Positioning Modeling trials	Chiraag
			Extraneous test scenarios	Jake
	Webots Simulation	4 Complete Webots Model of System and Disturbances		
			Begin trials of Webots as per test cases	see above
	Mechanical simulation and robustness of testing	3 Webots Environment setup and Results of Load Test and Frequency Analysis		
			Complete robot setup of Webots	Chiraag
			Complete Load Tests on parts	Jake
			Complete Natural Frequency Analysis	Seong
8				
	Optimized Algorithm	2 Algorithm comparison using data analysis.		

			Evaluate algorithm on test scenarios and tune/optimize it	Hieu
	Data Collection (for new algorithm evaluation)	5 Preliminary Graphs and Charts		
			Run Wind Disturbance Modeling trials	Giacomo
			Run Payload Variance Environment trials	Seong
			Run Payload Positioning Modeling trials	Chiraag
	Analyze Data from Simulation Results	3 Code that Reads and Analyzes data	Write Analysis File For Plotting	Sidharth
			Write code compatible with algorithm	Jeremy
9				
	Finalized algorithm	2 Algorithm comparison using data analysis.		
			Evaluate algorithm on test scenarios and tune/optimize it	Hieu
	Evaluation of final algorithm	4 Progress of Completed trials		
			Run Wind Disturbance Modeling trials	Giacomo
			Run Payload Variance Environment trials	Seong
			Run Payload Positioning Modeling trials	Chiraag
			Extraneous test scenarios	Jake
	Statistical analysis of Simulation Results (in progress)	2 Partial Analysis of Output Data		
			Begin Data Analysis	Sidharth
10				
	Complete statistical analysis of Simulation Results	4 Completed Data Analysis of Test Scenario Outputs		

			Write Output	Hieu
			Plot Output	Sidharth
			Apply Statistical Analysis	Giacomo
FDR Preparation	6	Final Design Review		
			Compile Final Design Review Report	Chiraag
			Convert Solidworks Simulation results to FDR	Jake
			Convert Webots Data Analysys to FDR	Seong
			Convert CDR information to FDR	Jeremy

## Appendix 5 - Collaboration Task Matrix

	Task	Hieu Nguyen	Sidharth Subbarao	Giacomo Fratus	Chirag Hebbar	Seong Hong	Jeremy Wong	Jake Smith	Sum	Normalized Sum
Preliminary Analysis	Objective Tree Analysis						5	5	0.7	
	Transparent Box Model						15		15	2.1
	Performance Specification Analysis						2	2	0.3	
	Quality Function Deployment						8	8	1.1	
	Morphological Chart				5				5	0.7
	Weighted Objective Method			3	5				8	1.1
Design	Electrical System	12	10	12		5			39	5.6
	Mechanical System				5	15	15	20	55	7.7
	Control Algorithm	15	10	10					35	5
	Numerical Simulation Set Up	8	10	10					28	4
	Disturbance Modeling			15					15	2
	Webots Environment Set Up	15			20				35	5
Analysis	Flow Analysis						5		5	0.7
	Thermal Analysis						5		5	0.7
	Load Analysis						5	35	40	5.7
	Frequency Analysis					25			25	3.6
	System Dynamics		10	10	10	2			32	4.6
	Analytical Simulations	10	5	5					20	2.9
	Webots Simulations	10	10	5	10	5			40	5.7
	Safety Requirements		20	2		2		2	26	3.7
Report	Technical Drawings	1	1	5		2	15	5	29	4.1
	BOM	1	2	2		2	5		12	1.7
	Video – FDR Comprehensive	2	2	1	5	5	5	5	25	3.6
	Video – Sales Pitch	1	1	1	5			3	11	1.6
	Video - CDR	2	2	2	5	5	5	3	24	3.4
	Engineering Pitch (Demo Day)	1	1	1	2	2	5	2	14	2
	Demonstration (Demo Day)	1	1	2					4	0.6
	GANTT Chart	1	1	2	7	10			21	3
	CDR Report	5	5	3	5	5	5	5	33	4.7
	FDR Report	5	5	5	5	5	5	5	35	5
Management	Group	5	2	2	6	5	5		25	3.5
	Sub system	5	2	2	5	5	5		24	3.4
	Sum	100	100	100	100	100	100	100	700	100

## **Appendix 6 - Peer Review Assessment**

To be completed as a Google form.